



INVESTIGATION OF PILE SETUP (FREEZE) IN ALABAMA
Development of a Setup Prediction Method and Implementation into LRFD Driven
Pile Design

Addendum: Pile Driving Vibration Monitoring of the Future Mobile River Bridge Project

Research Project 930-839R

A Final Report Submitted by:

Eric J. Steward, Ph.D.

John Cleary, Ph.D.

Assistant Professors, Department of Civil Engineering

University of South Alabama

Mobile, AL 36688

esteward@southalabama.edu or cleary@southalabama.edu

251-460-6174

Co-Authored by Graduate Students:

Andrew Gillis

Ronald Jones

Elisa Prado

June 30, 2015



DISCLAIMER

The contents of this report reflect the views of the authors who are responsible for the facts and accuracy of the data presented herein. The contents do not necessarily reflect the official views or policies of the Alabama DOT or the University of South Alabama. This report does not constitute a standard, specification, or regulation. Comments contained in this paper related to specific testing equipment and materials should not be considered an endorsement of any commercial product or service; no such endorsement is intended or implied.

CONTENTS

CHAPTER 1 – INTRODUCTION	1
1.1 Research Objectives	1
1.2 Pile Setup	1
1.3 Field Tests Measuring Pile Capacity	2
1.4 LRFD Design Methodology of Pile Capacity	3
1.5 Scope of Work	5
CHAPTER 2–LITERATURE REVIEW	6
2.1 Driven Pile Foundations	6
2.2 Pile Set-up	6
2.2.1 Set-up in Cohesive and Mixed Soils	9
2.2.2 Set-up in Fine-Grained Granular Soils.....	9
2.3 Set-up Evaluation Using Dynamic and Static Methods	10
2.3.1 Dynamic Load Testing.....	10
2.3.2 Dynamic Testing Equipment.....	12
2.3.3 Case Method	14
2.3.4 CAPWAP® Method	16
2.3.5 iCAP® Method	19
2.3.5 Static Load Testing	22
2.4 LRFD Design of Pile Foundations	25
2.4.1 Overview of Allowable Stress Design (ASD).....	25
2.4.2 Load Resistance Factor Design (LRFD).....	25
2.4.3 Implementation of LRFD.....	27
2.4.4 Calibration by fitting ASD	29
2.4.5 Reliability Theory	30
2.4.6 Calibration by Reliability Theory	32
2.4.7 Incorporating Pile Setup into LRFD Design	35
2.5 Summary of Literature Review	36
CHAPTER 3 – ALDOT PILE DRIVING DATA ACQUISITION AND ORGANIZATION	37
3.1 ALDOT Pile Driving Practice	37
3.1.1 Hammer Requirements.....	37
3.1.2 Hammer Cushion and Striker Plate Requirements.....	37
3.1.3 Pile Cap Requirements.....	38
3.1.4 Pile Cushion Requirements.....	38
3.1.5 Set of Leads Requirements.....	38
3.1.6 Pile Driving Hammer Approval Requirements.....	39
3.1.7 Test Pile Requirements	40
3.1.8 Static Load Testing Methods	41
3.1.8 Dynamic Load Testing Methods.....	44
3.2 Test Piles Installed and Tested at the Mobile River Site	46
3.3 Acquiring and Organizing Load Test Data	49
3.3.1 PDA® and iCAP® Procedure.....	50

CHAPTER 4 – RESULTS AND DISCUSSION OF PILE LOAD TESTS AND PILE SETUP 52

4.1 Alabama Soil Conditions..... 53
4.2 Load Test Results 55
 4.2.1 Overall Load Test Results..... 57
 4.2.2 Results of the Mobile River and Montgomery Outer Loop Test Piles ... 58
 4.2.2 Load Test Results of Steel H-Piles 62
 4.2.3 Load Test Results of Concrete Piles..... 68
 4.2.4 Load Test Results Comparison of iCAP with CAPWAP and PDA..... 73

CHAPTER 5– REGIONAL CALIBRATION OF RESISTANCE FACTOR AT THE END OF THE INITIAL PILE DRIVING 81

5.1 Predicted Pile Capacity using WBUZPILE Software 81
5.2 Measure Pile Capacity from Processed Load Test Data 84
5.3 LRFD Resistance Bias Factors 86
5.4 LRFD Resistance Factor Determination..... 89
5.5 Effectiveness of Calibrated Resistance Factors 90
5.6 Discussion of Calibrated LRFD Resistance Factor Results 96

CHAPTER 6 - PRELIMINARY PROCESS TO INCORPORATE PILE SETUP INTO DEVELOPMENT OF RESISTANCE FACTOR..... 99

6.1 Process of Pile Setup Prediction..... 99
6.2 Overview of Required Design Loads at End of Driving and Beginning of Restrike 100
6.3 Pile Setup Ratio 102
6.4 Statistical Analysis of Pile Setup Ratio 104

CHAPTER 7 – OVERALL CONCLUSIONS AND RECOMMENDATIONS..... 111

7.1 Conclusions of Pile Load Testing and Pile Setup Evaluation 111
7.2 Conclusions of LRFD Resistance Factor Calibration by Reliability FOSM Method..... 113
7.3 Recommendations for Future Research 114

REFERENCES..... 116

ADDENDUM REPORT: PILE DRIVING VIBRATION MONITORING OF THE FUTURE MOBILE RIVER BRIDGE PROJECT..... 121

CHAPTER 1 – INTRODUCTION

1.1 Research Objectives

The Alabama Department of Transportation (ALDOT) often uses deep foundations consisting of driven piles, particularly in the southern half of the state, to support bridges or other highway structures. In the fiscal year 2012, a total of 22 bridges were let to contract by the ALDOT for a sum of about \$37 million (ALDOT 2012). Bullock (1999) reported that the cost of a deep foundation for some bridges can be about 30% of the overall cost and thus a reduction in cost could produce a substantial savings to the entire project and passed on to the taxpayers.

ALDOT is interested in investigating the potential of including a phenomenon called pile setup into the design procedures of driven piles to provide a more efficient and cost-effective product that provides the same level of safety. ALDOT is currently transitioning from ASD design methods to LRFD design methods, as mandated by the Federal Highway Administration (FHWA).

This funded research is tasked with three main topics of investigation. The first is to identify the pile setup potential of the driven piles installed within the soils of the state of Alabama. This task requires the organization and analysis of historical records of design and installed pile load tests. The second task is to incorporate these historical records into the calibration of statistically determined resistance factors for LRFD design methods. The third task is to install four typical driven pile types into the soil of a planned bridge location to investigate the amount of pile setup as well as the propagation of vibrations to surrounding locations during the installation of the piles. The third task was added as an addendum to the project, and the vibration report was completed and attached to the end of this report.

1.2 Pile Setup

An essential stage in the design process of driven pile foundations is to estimate the axial

resistance of driven piles. In order for foundation engineers to determine the axial resistance of driven piles with a high degree of certainty, they need an adequate understanding of and quantification of the time-dependent changes in pile axial resistance. Unfortunately, these time-dependent changes are not well-understood, and thus are usually omitted throughout the design, construction, and installation of driven pile foundations. However, when foundation engineers do include set-up in the foundation design, it is typically incorporated during static analysis. The uncertainties remain about whether or not set-up will develop at the site and quantifying set-up if it develops.

Because pile installation considerably disturbs the soil surrounding the pile, the axial resistance of driven piles typically changes with time after the end-of-the-initial-driving (EOID). Moreover, many researchers have reported that piles driven into various soil profiles, including sand, clay, and mixed soils, frequently exhibit an increase in pile axial resistance with time after installation. This phenomenon of time-dependent increase in axial resistance of driven piles is often referred to as set-up. If the amount of set-up can be identified before or during the design process, then engineers are afforded the opportunity to decrease pile cross-sectional areas, reduce pile lengths, reduce pile embedment lengths and/or decrease the number of piles supporting the structure prior to construction. As a result, pile driving contractors can potentially reduce the size of the pile driving equipment (hammers and cranes), all of which can lead to overall cost savings. However, in some soil profiles, such as dense fine sands and weak rock, driven pile axial resistance may decrease with time after installation, and the decreased amount of pile axial resistance is referred to as relaxation. For safety and stability reasons, it is important to consider the potential of pile relaxation prior to the construction of pile foundations.

1.3 Field Tests Measuring Pile Capacity

For larger projects, test piles are often installed to indicate whether or not the piles can safely carry the service loads. This is achieved by either dynamic testing or static testing, or by both. Frequently, these piles are tested at end-of-initial-driving (EOID) and at some time later to measure the effects of time on the axial resistance of piles. For High Strain Dynamic Testing, these piles are instrumented with accelerometers and strain transducers to obtain and relay

hammer-impact velocity and force signals, respectively, to a Pile Driving Analyzer system (PDA[®]). Subsequently, these signals can be further analyzed with a software program, such as iCAP[®] or CAPWAP[®], to estimate the toe, shaft, and total axial resistances of piles. When set-up is expected, the test piles are again struck with an impact-hammer at some specified time interval after the initial driving to collect data for further analysis. These restrikes are often conducted to identify the time effect on pile axial resistances and quantify the time-dependent pile axial resistance changes (Long et al. 1999, Komurka et al. 2003). Frequently, production piles are also instrumented to provide resistance data to indicate whether or not they are showing similar resistances to that of the test piles. It is also common to perform static load testing on the test piles to compare with the dynamic testing results.

The ALDOT has been collecting, analyzing, and storing dynamic and static pile testing data for decades and for two main reasons: 1) to indicate that the piles can hold the anticipated service loads, and 2) to use for research purposes. ALDOT is interested in identifying the set-up potential for soils within the state, and perhaps, one day, include set-up in the design process of driven pile foundation systems. The author has acquired the pile testing data from ALDOT's historical records between 2009 and 2014 to further analyze and organize the information in an effort to identify relationships between the time-dependent changes, particularly set-up, in driven pile axial resistance and the generalized soil surrounding the embedded pile.

1.4 LRFD Design Methodology of Pile Capacity

For decades, Allowable Stress Design (ASD) has governed the method of design for driven piles among geotechnical engineers. This method compares the actual loads acting on the piles by the structure to the capacity (or resistance) of the pile with one factor of safety. The factor of safety used in ASD is often very conservative due to the many uncertainties and specific situations related to loads and resistances of deep foundations. On the other hand, Load Resistance Factor Design (LRFD) is a design method that has begun to be the preferred for all driven pile designs. It allows for a more extensive analysis of the specific conditions of the structure. LRFD considers the material and load uncertainties based on a probabilistic approach that reflects probability of failure throughout the structure. LRFD accounts for load and material

uncertainties by implementing load and resistance factors, while ASD uncertainties in the variation of load and ultimate capacity are based in a predetermined factor of safety. LRFD resistance factors consider inevitable deviations that occur to the actual strength from the nominal value as consequence of failure.

To calculate LRFD resistance factors, calibration by reliability theory needs to be developed. By using the First Order Second Moment method, a resistance bias factor is developed that compares measured nominal resistances with predicted resistances to account for material and soil strength uncertainties that are compensated by a resistance factor. Furthermore, resistance factors can be computed by pile classification such as pile type, material, and soil type to be more precise on the computation.

To date, there are specified resistance factors for driven pile design that are recommended by the America Association of State Highway Transportation Officials (AASHTO) which were developed utilizing LRFD. The origin of these resistance factors are based on the design method utilized to test the resistance of piles after driven. Two major concerns are related with the resistance factors recommended by AASHTO. The first one is related to the change in soil geology in a specific region. The resistance factors recommended by AASHTO are not regionally specific and they are limited to the change in soil geology. Consequently, the Federal Highway Administration also recommends that resistance factors are developed for a specific region utilizing the unique soil characteristics of that specific area. The second limitation is related to the lack of incorporation of the increase of pile resistance over time (setup). Therefore, it would be more accurate to develop regional resistance factors that incorporates the uniqueness of the soil geology for a specific area and that also incorporates pile setup in its development.

The state of Alabama developed and uses a software called WBUZPILE to design the allowable embedment lengths of driven piles. A comparison between allowable design loads or predicted resistances computed by WBUZPILE and measured pile resistance data collected on the field will be analyzed and discussed. Based on this statistical analysis, resistance factors will be developed for the state of Alabama. Also, incorporating pile setup into LRFD resistance factor development could bring significant cost benefits since it decreases the conservatism in the design by the increase of capacity over time after installation. The process of LRFD resistance factors calibration by utilizing FOSM based on data obtained for driven piles installed throughout the state of Alabama is explained in this report.

1.5 Scope of Work

- Collect historical pile driving, PDA[®], and soil boring records from the Alabama Department of Transportation (ALDOT).
- Filter through PDA[®] records to find usable data collected at both the (EOID) and at some time interval after initial driving (i.e., restrike data).
- Install four different types of piles at one site to test the initial resistance and resistances at various time intervals after installation to investigate:
 - the axial resistance between each type of pile in similar site conditions,
 - the effects of time on the overall axial resistance (setup) on each pile,
 - and measure the vibration propagation of the driving process in the specific soils encountered at the site.
- Analyze all usable PDA[®] data with the iCAP[®] signal matching software and compare the PDA[®], iCAP[®], and CAPWAP[®] results.
- Identify relationships between set-up in driven pile axial resistance and the generalized soil surrounding the embedded pile.
- Prepare a database of set-up factors. Include location (coordinates), pile test records, soil boring records, and pile properties for future references.
- Utilize the ALDOT pile capacity design method to determine the design axial (predicted) capacities of each pile to use in the LRFD resistance factor calibration.
- Develop the FOSM calibrated LRFD resistance factors to be used for design.

CHAPTER 2–LITERATURE REVIEW

2.1 Driven Pile Foundations

A driven pile foundation is a particular type of deep foundation where long, slender structural elements are driven into the soil by jacking, pushing, vibrating, or impact-hammering. They are generally made of steel (pipes or H-sections), timber, or precast, prestressed concrete (PPC). According to Bradshaw et al. (2004), driven pile foundations have been a preferred deep foundation system because of their comparative low cost and ease of installation. Therefore, if it can be determined that the selected pile can be driven to the required design load and penetration depth at a practical driving resistance (blow count) without damaging the pile, then driven piles are usually selected over the other deep foundation systems that were previously mentioned.

2.2 Pile Set-up

It has been well documented that the axial resistance of driven piles can change with time after the end-of-the-initial-driving (EOID) operations are complete. The phenomenon of increased pile axial resistance with time is often referred to as *set-up*. Numerous examples in literature reveal set-up occurring in a broad range of soil profiles and for a variety of pile types and sizes (Ng. 2011, Lee et al. 2010, Bullock 1999). Budge (2009) reported that pile axial resistances can range from as small as 20% to as much as eight times the end of driving resistances due to the effects of pile set-up. Occasionally, however, piles will reduce in axial resistance after EOID due to the dissipation of negative pore-water pressure, which is often referred to as relaxation, and may occur in saturated sandy soils (Svinkin 2002).

The mechanisms that cause set-up has interested researchers and engineers for decades. Lee et al. (2010) reported that even though numerous researchers have investigated pile set-up, no theoretical basis for quantifying set-up has ensued, and no process has been made known to effectively account for set-up at both the quality-control and design stages. Consequently, the current existing methods are site specific and would involve extensive data acquisition for reasonably accurate set-up evaluation, which are not readily available. Some of the mechanisms responsible for set-up have been well-established, but these are not yet well quantified. Other mechanisms of set-up remain to be topics of debate and research.

Pile driving causes substantial disturbance, displacement, and in soils containing a considerable amount of clay, remolding of the soil surrounding the pile. Furthermore, according to Komurka et al. (2003), the soil is displaced mainly radially along the pile shaft and radially and vertically below the pile toe. Driving displacement piles compresses the neighboring soil and frequently produces a buildup of excess pore-water pressure. Komurka et al. (2003) also reported that most of the excess pore-water pressure generation and dissipation, as well as soil disturbance, occurs along the pile shaft. Consequently, set-up mainly occurs as a result of increased lateral stress and increased shear strength against the pile shaft, which are both related to the dissipation of excess pore-water pressure. Other factors, such as aging, also attribute to these increases. Therefore, most of the set-up can be attributed to an increase in shaft resistance.

Shortly after pile installation, the surrounding soil typically enters a recovery stage as the excess pore-water pressure dissipates. The time the soil takes to recover, and the magnitude of recovery often produces a change in pile axial resistance, set-up or relaxation. The change in pore-water pressure during and after pile driving can significantly affect the short-term and the long-term pile axial resistances (Das 2010). Therefore, the mechanisms responsible for set-up are different for cohesive soils (clays) and non-cohesive soils (sands) mainly because the hydraulic conductivity of clay is several orders in magnitude smaller than sands.

According to Komurka et al. (2003), set-up occurs in three phases as illustrated in Figure 2.1. During Phase 1, the dissipation of excess pore-water pressure is non-linear (not constant) with respect to the log of time for an amount of time after driving because of the large amount of disturbed soil. Furthermore, the duration of non-linear dissipation of excess pore-water pressure is a function of the pile (Material type and size) and soil properties (permeability, type, and sensitivity) with respect to the log of time. The logarithmic non-linear rate of dissipation may become linear with respect to the log of time (begin Phase 2) almost instantly after driving a pile in clean sands. However, it may take cohesive soils several days to reach Phase 2 after installation.

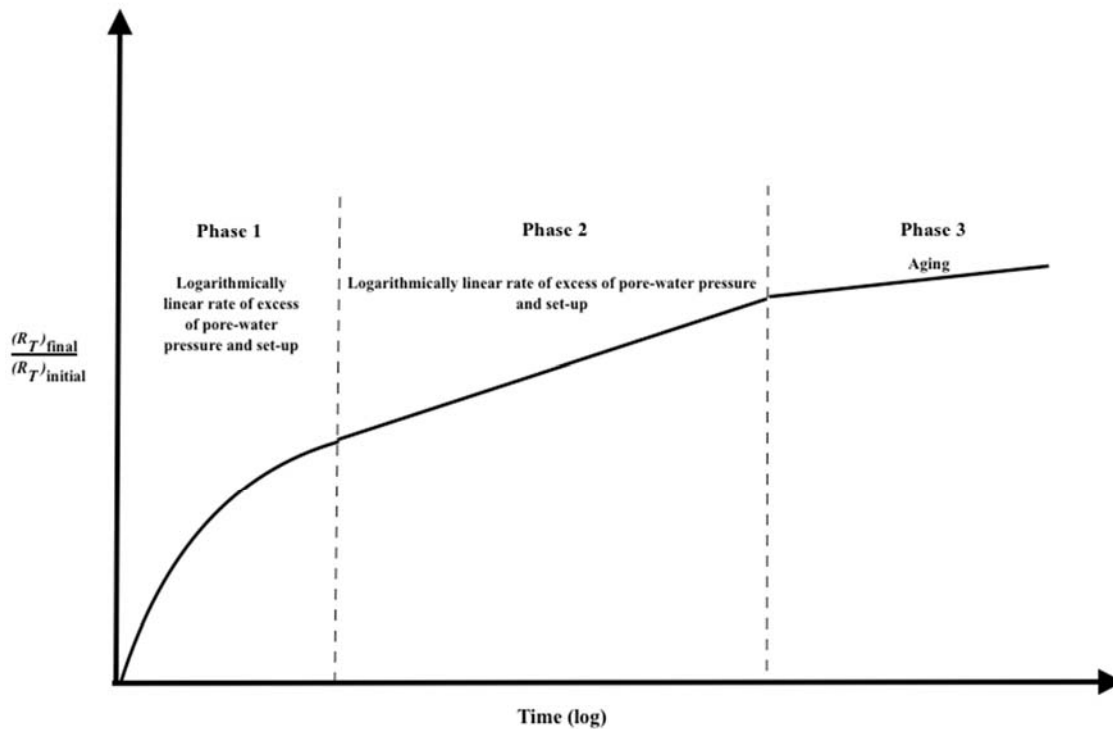


Figure 2.1 Idealized schematic of set-up phases (Komurka et al. 2003).

Komurka et al. (2003) also explained that during Phase 2, the set-up rate corresponds to the rate of dissipation, and thus for most soils, the dissipation of excess pore-water pressure is linear (constant) with respect to the log of time for an amount of time after driving. During Phase 2, the affected soil experiences an increase in shear strength, consolidates, and increases in effective horizontal and vertical stress according to the conventional consolidation theory. Furthermore, the duration of linear dissipation of excess pore-water pressure is a function of pile and soil properties with respect to the log of time. For piles driven in clean sands, the logarithmic linear rate of dissipation may immediately finish or may continue for hours. For piles driven in mixed soils, Phase 2 may last for hours, days, or weeks. For piles driven in cohesive soils, Phase 2 may last for weeks, months or even years. The less permeable the soil, and the more volume of soil displaced, the longer the duration of Phase 2 (Komurka et al. 2003). Phase 3 (often referred to as *aging*) is independent of effective stresses, and it is discussed further in the following two sections.

2.2.1 Set-up in Cohesive and Mixed Soils

According to Komurka et al. (2003), in clays or a mixture of clays and fine-grained granular soils, the excess pore-water pressure induced by pile driving may dissipate slowly. Consequently, some set-up develops during Phase 1, whereas the majority of set-up typically develops during Phase 2. For these types of soils, set-up is often reported as relatively small during Phase 3 (Komurka et al. 2003).

As piles are driven into cohesive soils, large shear and normal forces develop in the surrounding soil. These forces generate excessive pore-water pressure, which reduces the effective stresses in the soil, causing a decrease in pile axial resistance or relaxation. However, during primary consolidation of clays, the excess pore-water pressure dissipates overtime causing the effective stresses in the soil to increase, which in turn causes an increase in pile axial resistance or set-up. Basu et al. (2009) reported that the increase in effective stresses due to dissipation of excess pore-water pressure is the main cause of set-up in clays. In clayey soils, porewater pressure induced by pile driving may dissipate slowly. Das (2010) explained that excess porewater pressure usually dissipates within a few days to a few weeks, but it may take as long as a year for large pile groups. The size of the pile group and the properties of the soil significantly affect the rate of dissipation of excess pore-water pressure. According to Komurka et al. (2003), excess pore-water pressure dissipates faster for a single pile than for a pile group. In addition, Komurka et al. (2003) reported that smaller-diameter piles normally set-up faster than larger-diameter piles.

Eventually, the rate of pore-water dissipation becomes so slow that the effective stresses in the soil become constant, and thus no longer affecting the set-up rate (Komurka et al. 2003). However, during secondary compression of clays, set-up may continue to develop independent of effective stresses due to aging (Phase 3). Schmertmann (1991) explained that the aging phenomenon in cohesive soils is a combination of secondary compression, thixotropy, clay dispersion and particle interference. Set-up due to aging is often reported much smaller when compared to set-up during primary consolidation. In terms of percentages, soft clays have been discovered to set-up more than stiff clays (Komurka et al. 2003).

2.2.2 Set-up in Fine-Grained Granular Soils

According to Komurka et al. (2003), the excess pore-water pressure induced by driving

may dissipate very fast in fine-grained granular soils (fine sands or silts), oftentimes while driving. Therefore, in these types of soils, some set-up may develop during Phase 2; however, the majority of set-up occurs during aging (Phase 3) (Komurka et al. 2003). Dissipation of the excessive pore pressure could be used to explain short-term pile axial resistance increases (Seed and Reese 1955, Vesic 1977). However, cases have been reported where shaft resistance of piles driven in sandy soils increased and continued to increase over a long period of time. This increase is likely due to soil reconsolidation and creep effect (Chow et al. 1998, Komurka et al. 2011).

Lee et al. (2010) reported that a portion of the set-up in fine-grained granular soils may be produced from a creep-induced breakdown of both the arching mechanism and the driving-induced skin friction surrounding the pile. Increases in the radial effective stress often occur because of the breakdown of the arching mechanisms surrounding the pile. Aging occurs after the excess porewater pressure has totally dissipated. The aging process has been ascribed to time-dependent changes in soil properties at constant effective stresses (Komurka et al. 2003). Some researchers (such as Budge 2009, Lee et al. 2010, and Komurka et al. 2003) reported that arching may also play a role in pile set-up, but it has not been significantly explored. For axial loaded piles, arching means that the working load is not only transferred along the pile shaft with simple shear, but also by compression, specifically near the pile toe (Lee et al. 2010).

2.3 Set-up Evaluation Using Dynamic and Static Methods

In order to measure set-up, a minimum of two field measurements of a pile's axial resistance are required. According to Komurka et al. (2003), the manner in which, and the times at which, such field measurements are performed are very important to the value of the information acquired and to the conclusions that may be drawn from this information. According to Komurka et al. (2003), the first measurement of a pile's axial resistance is best obtained as close to the EOID process as possible, and the second measurement should be postponed as long as possible. The most common field methods used for measuring a pile's axial resistance are dynamic load testing and static load testing.

2.3.1 Dynamic Load Testing

The modern dynamic testing and evaluation methods were made possible through

research conducted during the 1960's and 1970's at the Case Western Reserve University in Cleveland, Ohio. These methods (PDA[®] and CAPWAP[®]), which are based on the wave propagation theory, became commercially available in 1972 (Hannigan et al. 2006). There have been many improvements in the software and hardware since 1972 (Hannigan et al. 2006). Today, the Pile Driving Analyzer and CAPWAP[®] are routinely used on deep foundation projects around the world.

Dynamic testing acquires data during driving, and are therefore unique in that the pile axial resistance can be evaluated immediately at the end-of-initial-driving (EIOD). Restriking a pile or several piles at some later time after EIOD and comparing the pile axial resistance at the EIOD with the pile axial resistance at each restrike can be beneficial in measuring set-up.

High Strain Dynamic Testing is a method of testing pile foundations, which requires a Pile Driving Analyzer (PDA[®]) to collect information from the stress and velocity waves generated by the impact of a hammer on a pile head. The PDA[®] software uses the Case Method, which is a closed-form solution, to determine estimates of the shaft and toe resistances. The Case Method uses an assumed soil damping value, which is based on soil type at the pile toe (Hannigan et al. 2006). In addition, many codes and standards require additional analysis for more-accurate results. These resistance estimates can be improved by using signal matching software such as CAPWAP[®], which uses a soil-pile interaction model that can adjust for layering of the soils for a more-accurate estimate of resistances (Preim, et. al. 1989). However, the CAPWAP[®] analysis requires skilled personnel to operate and the analysis can take a considerable amount of time to complete.

There is a new, automatic signal matching software called iCAP[®] that can be used in the field or some time later for quick determination of resistances using the signal matching method similar to CAPWAP[®] (Likins et al. 2012). The data collected during the end-of-the-initial-driving (EIOD) and at the beginning of the restrikes (BOR) by the PDA[®] can be analyzed using iCAP[®], and then these results can be compared to identify changes in pile axial resistances. Research has shown that iCAP[®] resistance results match very well with the full CAPWAP[®] analysis for various types of piles and soils encountered (Likins et al. 2012). The High Strain Dynamic Testing equipment and software mentioned is developed and manufactured by Pile Dynamics, Inc.

According to Hannigan et al. (2006), dynamic pile test methods use measurements of

acceleration and strain taken close to the pile head (within two to three pile diameters below the pile head) as the pile is struck with a hammer. These dynamic measurements can be used to estimate pile installation stresses, assess the effectiveness of the pile driving process, approximate static pile capacity, and gauge pile integrity. The Case Method and CAPWAP[®] are two methods that have been developed for analyzing dynamic measurement data (Hannigan et al. 2006).

According to Hannigan et al. (2006), to mobilize all available soil resistances (shaft and toe) during restrikes or EOID, a penetration resistance of less than approximately ten blows per inch is usually required. Dynamic load testing typically underestimates soil resistances when more than approximately ten blows per inch are required. For mobilization, the toe resistance typically requires more movement than the shaft resistance (Hannigan et al. 2006).

2.3.2 Dynamic Testing Equipment

A standard dynamic load testing system consists of a minimum of two accelerometers and two strain transducers bolted on opposite sides of the pile and at a distance of approximately 2 to 3 diameters below the pile head (Hannigan et al. 2006). As the pile is driven, the accelerometers and strain transducers relay acceleration and strain signals to the PDA[®] via a wireless transmitter or cable. Figure 2.2 shows a Pile Driving Analyzer model PAX. Figure 2.3 shows an accelerometer and a strain transducer bolted on one side of a precast, prestressed concrete (PPC) pile.

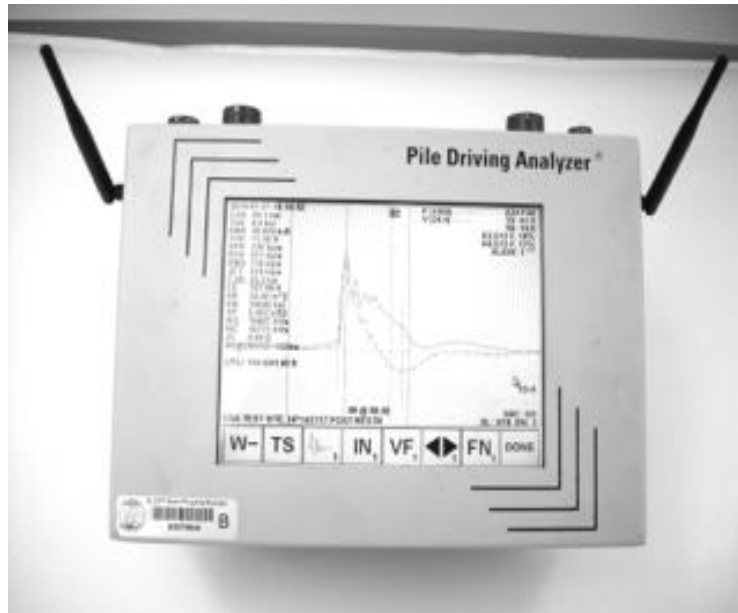


Figure 2.2. Pile Driving Analyzer—Model PAX (Property of ALDOT).

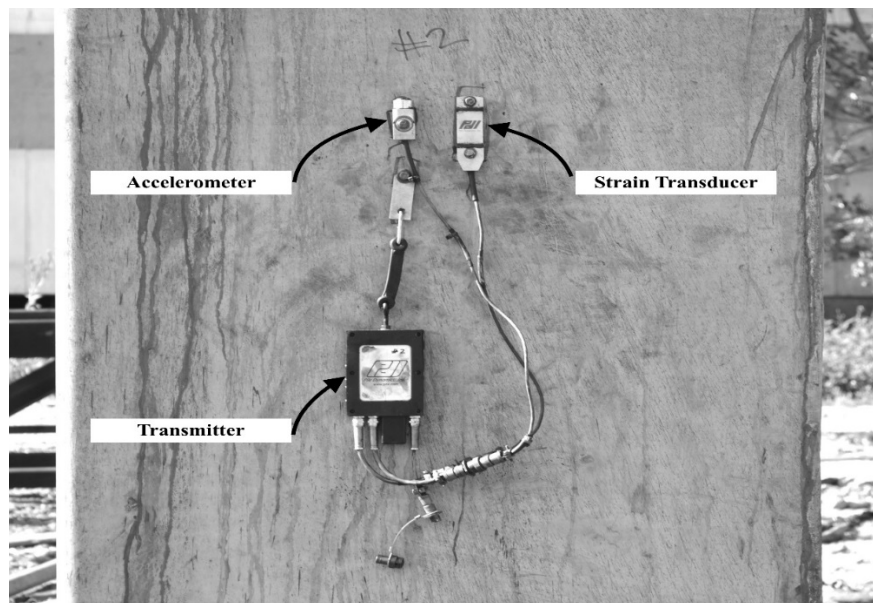


Figure 2.3. Accelerometer and strain transducer bolted to an ALDOT 36”x36” PPC test pile.

Immediately following the hammer’s impact, a compression wave is generated and travels down the shaft. After time L/c (where c is the wave speed and L is the pile length), the

compression wave arrives at the toe and an upward tension wave is generated and travels back to the pile head. The strain transducers relay the strain and the accelerometers relay the acceleration of these waves to the PDA[®]. The PDA[®] collects the data and the internal software converts the acceleration and strain signals to velocity and force as a function of time using Equation 2.1 and 2.2 respectively (Hannigan et al. 2006).

$$v(t) = \int_0^T a(t) dt \quad (2.1)$$

$$F(t) = EA\varepsilon(t) \quad (2.2)$$

where $v(t)$ is velocity at time, t , $a(t)$ is acceleration at time, t , T is the default maximum limit which is 0.2028 second, $F(t)$ is force at time, t , E is the pile elastic modulus, A is the pile cross-sectional area at the gauge location, $\varepsilon(t)$ is strain at time, t .

2.3.3 Case Method

The Case Method includes several closed form equations (Case Method equations) that were developed through research conducted at the Case Western Reserve University in Cleveland, Ohio. The Case Method equations are used for estimating total pile axial resistance, driving stresses, hammer energy, and pile integrity (Hannigan et al. 2006).

According to Hannigan et al. (2006), as the pile is being struck with an impact-hammer, the Pile Driving Analyzer (PDA[®]) uses the Case Method capacity equations (Equations 2.3 and 2.4) for determining the total pile axial resistance for each blow. Furthermore, the Case Method capacity results are estimated in real time from the measured velocity and force records for each hammer blow.

Assuming the pile has a constant cross section and the pile is linearly elastic, the total dynamic and static soil resistance acting on a pile during the impact of a single blow may be expressed with the Case Method equation (Equation 2.3). Rausche et al. (1985) reported a thorough derivation of the Case Method.

$$\text{RLT} = \left(\frac{F_{t_1} + F_{t_2}}{2} \right) + \left(\frac{V_{t_1} - V_{t_2}}{2} \right) \left(\frac{EA}{c} \right) \quad (2.3)$$

where: RLT = total soil resistance (static plus dynamic resistances),

F_{t_1} = force measured at time of initial impact,

F_{t_2} = force measured at time of reflection of initial impact from the toe,

V_{t_1} = velocity measured at time of initial impact,

V_{t_2} = velocity measured at time of reflection of initial impact from the toe,

E = pile modulus of elasticity,

A = pile cross-sectional area at the gage location,

t_1 = time of initial impact,

t_2 = time of reflection of initial impact from the pile toe ($t_1 + 2L/c$),

c = wave speed of the pile material,

L = pile length.

Furthermore, to estimate the total axial resistances of the pile, the damping (dynamic resistance) should be subtracted from the preceding (Equation 2.3), and can be expressed with the Case-Goble static resistance (RSP) equation (PDA Manual 2001):

$$\text{RSP} = \text{RLT} - J_c \left(V(t_1) \frac{EA}{c} + F(t_1) - \text{RLT} \right) \quad (2.4)$$

where J_c is the dimensionless Case damping factor, which is based on soil type at the pile toe (Hannigan et al. 2006). According to Hannigan et al. (2006), the Case-Goble static resistance (RSP) is best used to evaluate the axial resistance of piles with large shaft resistances and of small displacement piles.

Table 2.1. Recommended Case damping factors (J_c) (PDA manual 2001)

Soil Type at Pile Toe	Case Damping Ranges
Clean Sands	0.10 to 0.15
Silty Sands	0.15 to 0.25
Silts	0.25 to 0.40
Silty Clays	0.40 to 0.70
Clays	0.70 or higher

The recommended J_c values given by the PDA[®] Manual 2001 are illustrated in Table 2.1. The damping factors (J_c) shown in Table 2.1 are empirical values that describes the dynamic soil resistances. According to Hannigan et al. (2006), the recommended (J_c) values shown in Table 2.1 may offer suitable initial pile axial resistance estimates; however, site specific (J_c) values should be developed based upon CAPWAP[®] analysis and static load testing.

2.3.4 CAPWAP[®] Method

The Case Pile Wave Analysis Program (CAPWAP[®]) is a software program that uses PDA[®] records of velocity and force measurements for a given hammer blow to evaluate the distribution of soil resistance at the pile toe and along the shaft. The CAPWAP[®] Method is an iterative process that is typically performed until the best matching signal between the measured and calculated forces are obtained.

According to Rausche et al. (2010), the main purpose of CAPWAP[®] is the determination of static and dynamic soil resistance parameters of the Smith-type soil-pile model. The authors further explained that due to certain limitations of the original Smith model, several modifications were made to it for more reliable signal matching results. Therefore, the CAPWAP[®] model is a modified version of the original Smith model.

The CAPWAP[®] software estimates the dynamic soil properties (damping and quake), total axial resistances, the driving stresses throughout the pile, and the relative soil resistance distribution. Hannigan et al. (2006) reported that the CAPWAP[®] analysis program performs these estimates by using the dynamic measurement data together with the wave equation type

soil and pile modeling. The CAPWAP[®] Method uses measured velocity and force records (PDA[®] data) from one hammer blow that is typically selected from the beginning of a restrike or near the end of initial driving because these blows typically represent the pile axial resistance at the time of dynamic testing.

As depicted in Figure 2.4, the CAPWAP[®] model is divided into soil and pile models (Ng 2011). The soil is modeled by dashpots (dynamic resistance) and the pile is modeled by elasto-plastic springs (static resistance). CAPWAP[®] uses the acceleration and force data from the PDA[®] to quantify pile motion and pile force (Hannigan et al. 2006).

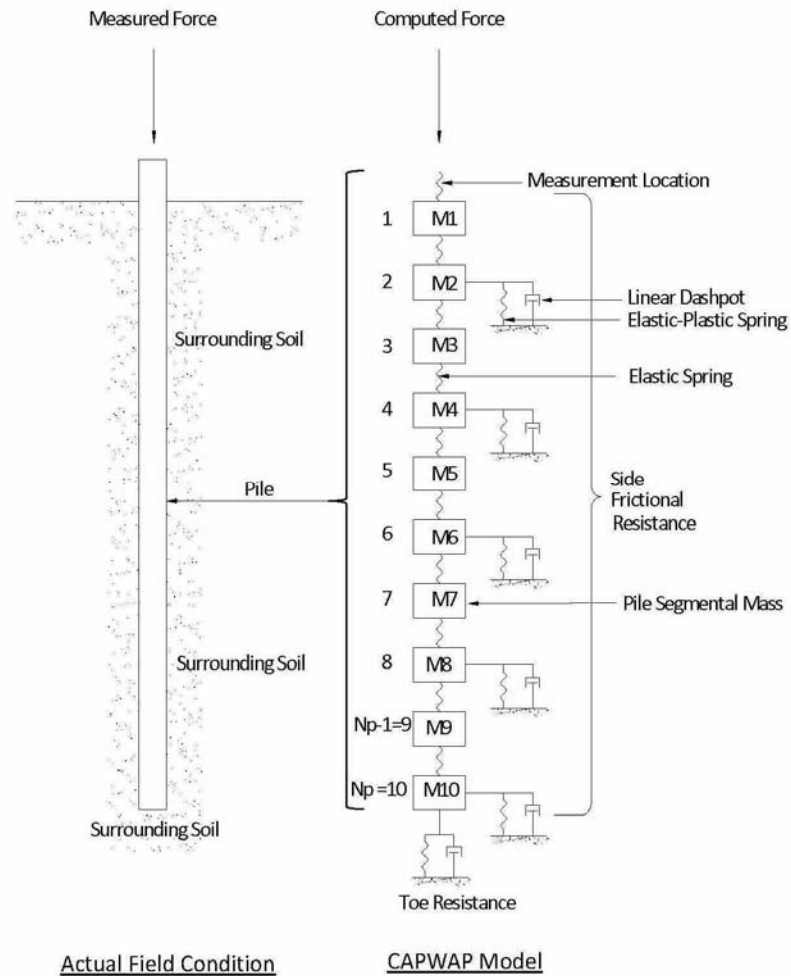


Figure 2.4. Schematic of CAPWAP[®] analysis method (Ng 2011).

First, the CAPWAP[®] operator enters reasonable estimates of damping and quake as well

as a total pile axial resistance with an initial soil resistance distribution into the program (Rausche et al. 2010). Next, the pile model is set in motion by measured acceleration. Subsequently, CAPWAP[®] computes the equilibrium pile force head, which can be compared to the PDA[®] measured force. Through trial and error the soil model is refined until no further agreement can be achieved between the computed and measure pile head forces (Hannigan et al. 2006). The signal matching process has been simplified with automatic search procedures, and the resistance distribution and total axial resistance estimates can be automatically improved by seeking the lowest match quality (MQ), or “Best Match” (Rausche et al. 2010). The match quality is a value to aid in determining if the signal match was appropriate based on the properties provided as well as the soil damping values. Higher match quality values indicate that less confidence can be placed in the CAPWAP[®] results. The Match quality values between 1 and 4 are usually considered acceptable, where 1 is a perfect match. Several iterations are usually required before the best matching signal between the measured and calculated forces is obtained. The CAPWAP[®] iteration matching process is illustrated in Figure 2.5.

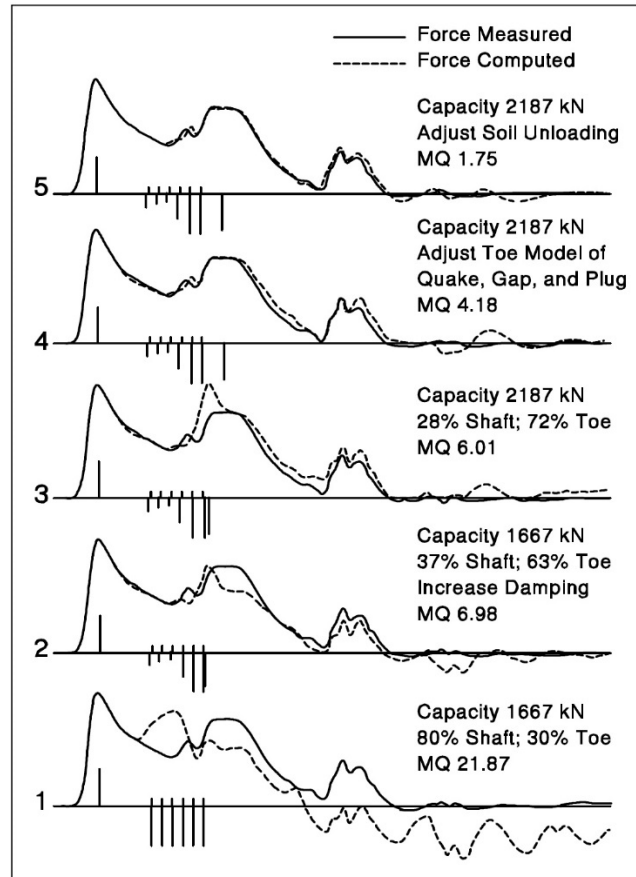


Figure 2.5. CAPWAP® iteration signal matching process (Hannigan et al. 2006).

2.3.5 iCAP® Method

There is a new, automatic signal matching software called iCAP® (which is installed onto the PDA® unit) that can be used in the field or some time later for quick evaluation of pile axial resistance. The iCAP® automatic signal matching procedure was created using the basic CAPWAP® soil and pile model, but does not require nearly as much user intervention as the CAPWAP® Method (Likins et al. 2012). The iCAP® operator is allowed to select certain controls for qualifying data quality, but all other aspects of the iCAP® procedure is completely automatic. Furthermore, the iCAP® procedure provides results independent of an assumed damping factor. The data collected during the end-of-the-initial-driving (EOID) and at the beginning of the restrikes (BOR) by the PDA® software can be analyzed using the iCAP® software, and then these results can be compared to identify changes in pile axial resistances, and thus aid in estimating set-up.

The measured velocity and force data (PDA[®] data) can be transferred directly to the iCAP[®] software, and a continuous model of the pile is created. To perform the wave propagation computations, the iCAP[®] analysis uses the method of characteristics (which is a method for solving partial differential equations) (Likins et al. 2012). The wave propagation computations are made by using the dynamic measurement data together with the wave equation type soil and pile modeling (similar to the basic CAPWAP[®] model) to provide results for total, shaft, and toe resistances for a driven pile. The iCAP[®] software generates a soil model with 2 meter segments along the shaft, which matches the general data resolution, and an additional soil component at the pile toe (Likins et al. 2012). An initial total pile axial resistance is selected, either from the Case Method equation (which is provided by the PDA[®]) or from the previous solution, and the resistance distribution at the pile toe and along the pile shaft is evaluated from the velocity and force preceding the initial return of the input wave after reflecting from the toe of the pile (Likins et al. 2012).

The iCAP[®] software can perform either the Quick or the Full signal matching. If a blow is analyzed with the Quick iCAP[®] signal matching option, then a soil model is developed based on the preceding signal matching result from the preceding blow. However, if a blow is analyzed with the Full iCAP[®] signal matching option, then a completely fresh soil model is developed (Likins et al. 2012).

The iCAP[®] operations are quite simple for the user. When the iCAP[®] user navigates the screen and selects the iCAP[®] tab, a window will appear from which the user selects the “Use iCAP[®]” box. At which point, a second window will appear on the screen offering several interactive boxes that the user can check (select) or define numerically, such as Quick iCAP[®], Full iCAP[®], and several iCAP[®] qualifiers. There are six iCAP[®] qualifiers that will assess if there is a problem with the data, and there are four qualifiers that are limits (such as minimum energy and penetration) that the user can define. After selecting the qualifiers and defining the limits, the user selects either the quick iCAP[®] or the Full iCAP[®] option.

Once the iCAP[®] analysis has been started, the automatic signal matching procedure begins as shown in Figure 2.6. The force and velocity records are automatically transferred from the PDA[®] software to the iCAP[®] software.

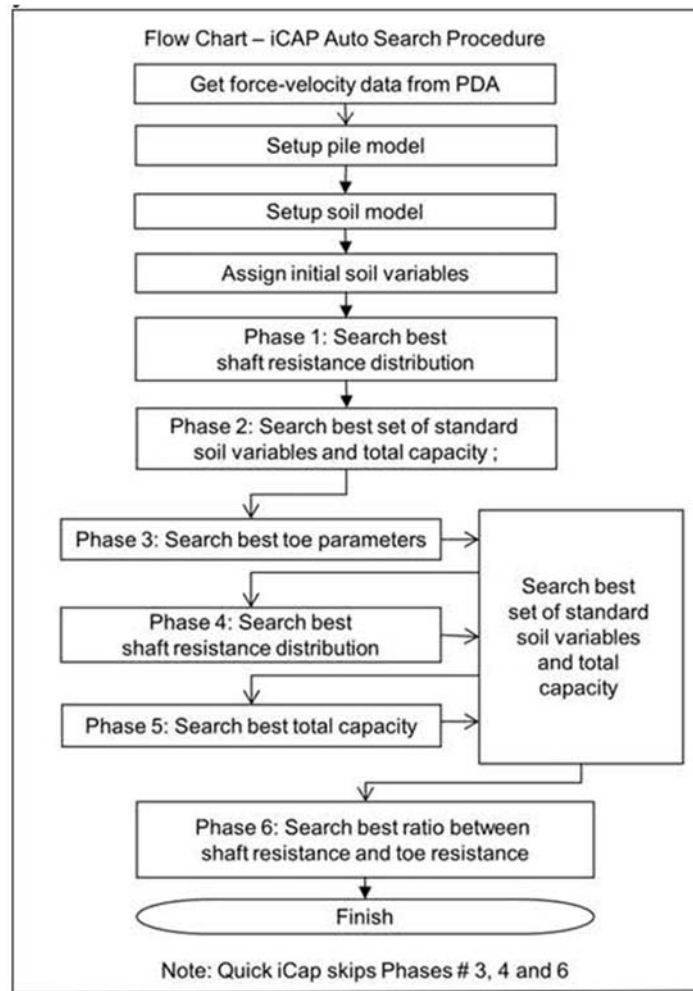


Figure 2.6. iCAP[®] auto search flowchart (Likins et al. 2012).

The iCAP[®] software uses the PDA[®] records to automatically create both a pile and a soil model. In addition, the iCAP[®] software will also assign initial soil variables so that Phase 1 of the iCAP[®] auto search procedure can begin. During phase 1, the iCAP[®] software automatically searches for the best shaft resistance. During Phase 2, the iCAP[®] software automatically searches for the best soil variables and the best total axial resistance of the pile. If the user has selected Quick iCAP[®] analysis, Phases 3, 4, and 6 are skipped. During Phase 3, the iCAP[®] software automatically searches for the best toe parameters. During Phase 4, the iCAP[®] software again automatically searches for the best shaft resistance. During Phase 5, the iCAP[®] software again automatically searches for best total axial resistance of the pile. During Phase 6 (which is the final stage), the iCAP[®] software automatically searches for the best ratio between shaft and toe resistances (Likins et al. 2012). Similar to the CAPWAP[®] Method, match quality (MQ) values

between 1 and 4 are usually considered acceptable, where 1 is a perfect match.

2.3.5 Static Load Testing

A static loading test includes the direct measurements of pile head displacement that occurs during an applied load. According to Hannigan et al. (2006), the static load test is the most accurate approach of estimating pile axial resistance. Axial tension, axial compression, and lateral load tests are the conventional types of static load tests performed on piles.

Static load tests should be conducted on test piles strategically located at the most critical area of the site, such as where the bearing stratum is weakest or deepest. Static loading tests require a substantial amount of effort, time, and money to set up. Engineers are sometimes reluctant to recommend static loading tests because of cost concerns or possible time delays in construction or design (Hannigan et al. 2006).

Compressive load tests (also referred to as top-loaded static loading test) are the most common type of static load testing performed on piles (see Figure 2.7). They can provide an abundance of information for construction and design of pile foundations. However, they cannot be used to account for negative shaft resistance, long-term settlement, or to represent pile group action. Furthermore, they provide very little information on pile damage and driving stresses (Hannigan et al. 2006).

Because static loading tests generally require several days to assemble, they are considered impractical to evaluate initial pile axial resistance. However, static load testing can be useful for evaluating pile axial resistance at various times after initial driving, and thus can be useful for assessing set-up (if tested to failure).

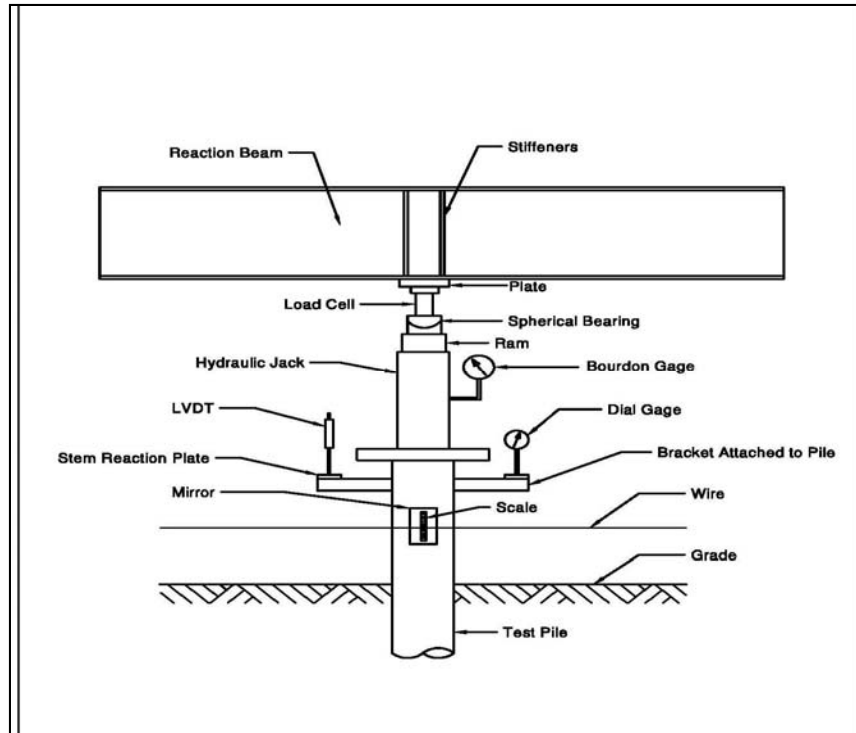


Figure 2.7. Typical axial compressive test system (Hannigan et al. 2006).

Compressive loads are typically applied by hydraulically jacking against a beam that is held in place by an anchorage system or by jacking against a weighted platform. To supply tension resistance, the anchorage system may be arranged with reaction piles or cable anchors placed into the ground. A calibrated load cell should be the main means of measuring the load applied to the pile. Also, a calibrated pressure gauge should be used to record the jack load (Hannigan et al. 2006). A typical system for applying a load in an axial compressive test is illustrated in Figure 2.7 (Hannigan et al. 2006).

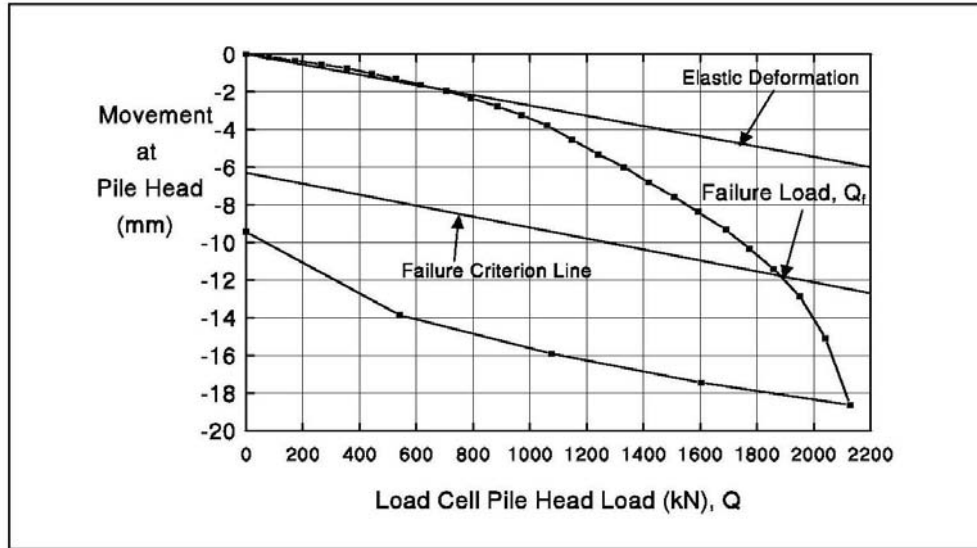


Figure 2.8. Example of typical pile load-movement curve (Hannigan et al. 2006).

For a compression test, the test pile can be loaded from the pile head at a continuous, constant rate, or it can be loaded incrementally using some predetermined sequence. During the test, measurements of time, load, and movement at the pile head and at several points along the shaft are recorded. These recorded measurements are used to plot a load-movement curve. An example of a load-movement curve is illustrated in Figure 2.8. Load-movement curves are used to interpret the test results, and are ultimately used to determine the movement at failure and the total pile axial resistance (Hannigan et al. 2006). The intersection of the load-movement curve and the failure criterion line yields the failure load (total pile axial resistance) as illustrated in Figure 2.8.

There are various methods of defining failure load from static testing. However, many codes and standards recommend compression test results be evaluated using the Davisson (1972) failure criterion. The Davisson failure load is defined as the load corresponding to a movement that surpasses the elastic pile compression by a value of 0.15 inches plus a factor of $D/120$, where D is pile diameter, the Davisson failure criterion can be expressed as:

$$S_f = \frac{PL}{AE} + 0.15 + \frac{D}{120} \quad (2.5)$$

where S_f is settlement at failure (inches), P is the applied test load, L is pile length, A is pile cross-sectional area, E is pile elastic modulus, and D is pile diameter.

2.4 LRFD Design of Pile Foundations

2.4.1 Overview of Allowable Stress Design (ASD)

ASD is a design method that has been used for decades in the geotechnical engineering community. The basic concept in this method is that the elements designed do not exceed the summation of forces applied in the structure. Uncertainties in the variation of applied loads and ultimate capacity are incorporated in a factor of safety, F.S. Equation 2.6 shows the relationship used when utilizing ASD method:

$$\frac{R_n}{FS} \geq \sum Q_i \quad (2.6)$$

where R_n is the nominal resistance; and $\sum Q_i$ is the sum of the load effects (dead, live and environmental loads) applied on a pile (Withiam et al, 1998). According to Paikowsky et al. (2004), ASD does not account for specific resistance and load uncertainties in the design; instead, a factor of safety is used which is generally dependent on experience and engineering judgment. By utilizing ASD, uncertainties are relegated to a single safety factor which can lead to conservatism. Consequently, a more rational approach is needed to account for specific geotechnical conditions and load uncertainties in driven pile design.

2.4.2 Load Resistance Factor Design (LRFD)

As stated, the ASD method is considered to have multiple limitations on specific situations. The LRFD method is a more rational approach in which applicable failure and serviceability conditions can be evaluated considering the uncertainties associated with loads and material resistance (Paikowsky et al, 2004). Specified uncertainties are accounted and analyzed by a statistical analysis based on their average performance in order to avoid conservatism. These uncertainties are incorporated into the design method by load and resistance factors, instead of using a single factor of safety as with ASD. A limit state is a condition beyond which a structural component, such as a foundation or other bridge component, ceases to fulfill the

function for which it is designed (Withiam et al, 1998). Equation 2.7 can be used to represent the limit state design for utilizing LRFD method,

$$\phi R_n \geq \sum \gamma_i Q_i \quad (2.7)$$

where ϕ is a statically based resistance factor; R_n is the nominal resistance; γ_i is the statistically based load factor; and Q_i is the load effect. The limit state condition is represented by equation 2.8, and failure by equation 2.9,

$$\phi R_n = \sum \gamma_i Q_i \quad (2.8)$$

$$\phi R_n < \sum \gamma_i Q_i \quad (2.9)$$

The uncertainties associated with resistances and loads can be defined through the distribution of their Probability Density Functions (PDFs). Figure 2.9 shows the probabilistic curves used in LRFD by assuming load (Q) and resistance (R) PDFs as independent random variables. The overlap area in Figure 2.9 shows the failure region, which is considered as a statistically acceptable safety margin that defines an acceptable risk of failure (Withiam et al, 1998). The function between load and resistance to represent a safety margin assuming the independency in random variables is given as $g(R,L)$. Once an acceptable risk of failure is determined, the resistance and load factors are defined by the uncertainties that need to be consider in order to avoid failure utilizing LRFD.

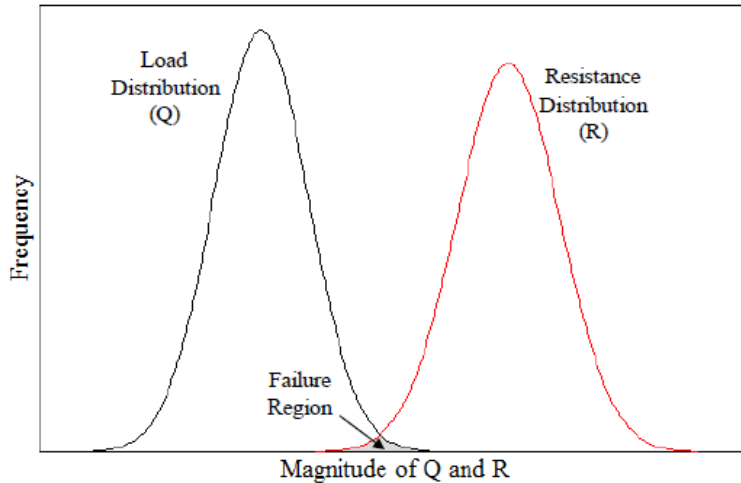


Figure 2.9. LRFD failure criterion between the PDFs of load and resistance (Withiam et al, 1998)

2.4.3 Implementation of LRFD

Significant efforts have been directed towards development and application of LRFD approach in geotechnical engineering. The AASHTO Standard Specifications for Highway Bridges has provided national requirements for the design of highway bridge superstructures for decades. Barker et al (1991) suggested that resistance factors could be calibrated based on a fitted factor of safety of the ASD approach. This approach was utilized in the AASHTO Standard Specifications (1995). However, it was concluded by Nowak (1999), that resistance factors calibrated (or computed) by fitting ASD did not provide sufficient level of reliability. Instead it was recommended that reliability theory be used to calibrate resistance factors, and that calibration by fitted ASD could be used as a benchmark to compare both methods. In June 2000, the FHWA declared in a policy memorandum the requirement of superstructures, substructures and bridge foundations built after October 1, 2007 to follow the AASHTO LRFD Bridge Design Specification (FHWA, 2000). Consequently, new research was conducted resulting on two major reports by Paikowsky, et al (2004) and Allen, Nowak & Bathurst (2005). These reports developed general use resistance factors based on reliability theory which are implemented in the 2012 AASHTO-LRFD Bridge Design Specifications.

In the past few decades there has been an increase in the application of LRFD concepts on the design of deep foundations. Some of the major research that has been conducted implementing LRFD principles includes Rahman et al (2002), Paikowsky et al (2004), McVay et al (2000), Allen et al (2005), among others. One of the most influential research on calibration of resistance factor by reliability of theory was conducted by Paikowsky et al (2004). This research compiled a large amount of data in order to develop the reliability based method of LRFD. It concluded that a regional resistance factor needs to be developed that accounted for variability of site conditions, quality of soil parameter estimations, construction quality control and previous site or construction experience in order to achieve safety (Paikowsky et al., 2004).

However, despite the FHWA deadline, not all State Departments of Transportations (DOTs) have adopted the LRFD regional calibration in their foundation designs. Some of the DOTs are still transitioning from ASD to LRFD. The resistance factors suggested in the 2012 AASHTO LRFD Specifications are known for providing conservatism in their design when applied to a localized region due to variability of the regional geology (AbdelSalam et al., 2012). For this reason, AASHTO has permitted state Departments of Transportation (DOTs) to develop regional resistance factors based on local practices and geology to minimize this unnecessary conservatism.

Various state DOTs have implemented the calibration for LRFD resistance factors. AbdelSalam et al (2009) conducted a survey that asked how the implementation of AASHTO LRFD bridge foundation design was being used in each state; 52% of the respondents to the survey were fully implementing LRFD, 33% were in a transition from ASD to LRFD, and 15% were still using ASD with FS of 2 and 2.5. Some of the states that have fully implemented LRFD had developed regional resistance factors for use within their states including Florida (McVay, 2000), Iowa (AbdelSalam et al. 2009), Oregon (Smith et al. 2011), Missouri (Luna, 2014), Louisiana (Yoon, Ching, & Melton 2008), Illinois (Long, Hendrix & Baratta, 2009a), and Wisconsin (Long, Hendrix & Jaromin, 2009b).

The Alabama Department of Transportation (ALDOT) is in transition from ASD to LRFD because it takes large amount of data to develop the specifications required in LRFD. Currently, ALDOT is interested in computing a resistance factor for driven piles installed within the state. Developing a resistance factor within the state of Alabama could allow a reduction of costs on the design and installation of driven piles throughout the state. ALDOT is currently

utilizing LRFD by incorporating resistance factors calibrated by fitting the F.S of the ASD method. However, resistance factor calibration by reliability theory is desired. It is important to understand both method of developing resistance factors using LRFD.

2.4.4 Calibration by fitting ASD

Calibration by fitting ASD was first proposed by Barker et al. (1991). This calibration method is used when the data required for statistical analysis to determine the probability of failure is not available. Calibration by fitting ASD can be used as a benchmark of a degree of safety to the calibration using reliability theory. A resistance factor using fitting to ASD can be determined using the following equation:

$$\phi = \frac{\gamma_{DL}\left(\frac{DL}{LL}\right) + \gamma_{LL}}{\left(\frac{DL}{LL} + 1\right)FS} \quad (2.10)$$

where ϕ is a resistance factor, γ_{DL} and γ_{LL} are the dead and live load factor, and DL/LL is the dead to live load ratio. AASHTO Specifications (2012) recommends a 1.25 and 1.75 for dead load factor and live load factor (AASHTO, 2012). Paikoswky et al. (2004) suggested the DL/LL should be within 2.0 to 2.5; while Allen et al. (2005) considered DL/LL ratio of 3.0 to be consistent with previous work done by Barker et al. (1991). However, Alabama Department of Transportation (ALDOT) recommends a safety of factor of 2 and DL/LL ratio of 2 for driven piles designs (Ashour, Helal & Ardala, 2012). Currently, ALDOT utilizes a resistance factor of 0.71 calibrated by fitting ASD for driven piles design. Calibration by fitting ASD is a method to develop either a safety of factor or a resistance factor by back calculating one of the parameter when the other is known. It is desired to develop regional resistance factors using reliability theory calibration that can be utilized by ALDOT for pile designs in order to completely transition from ASD to LRFD. By utilizing new resistance factors calibrated by reliability theory, conservatism could be avoided and potential cost benefits could be achieved.

2.4.5 Reliability Theory

The purpose of the reliability theory is to utilize data to conduct statistical analysis that presents a more rational approach when calibrating a resistance factor since it accounts for resistance and load uncertainties. Utilizing reliability theory limits the probability of failure (P_f) of structures; in other words, the probability that the loads will not exceed the resistances. Designing a structure that ensures 100% safety is not only unrealistic, but very expensive. Consequently, an acceptable level of risk or probability of failure (P_f) must be determined. By utilizing a probability of failure in the implementation of LRFD, the structure is design to provide a margin of 95% of confidence. The safety of any given structural element can be translated as the probability that load, Q , will exceed a resistance, R . Equation 2.11 shows this relationship as,

$$p_f = P(R < Q) \quad (2.11)$$

The probability of failure can be expressed in terms of a reliability index, β . The reliability index is the measure of safety associated with the probability that pile resistance is less than the loads applied (Paikowsky et al. 2004). In other words, the reliability index represents how reliable the system is to avoid failure. From figure 2.9, a single curve that combines both probability density curves (load and resistance) can be developed resulting in figure 2.10, in order to obtain the reliability index.

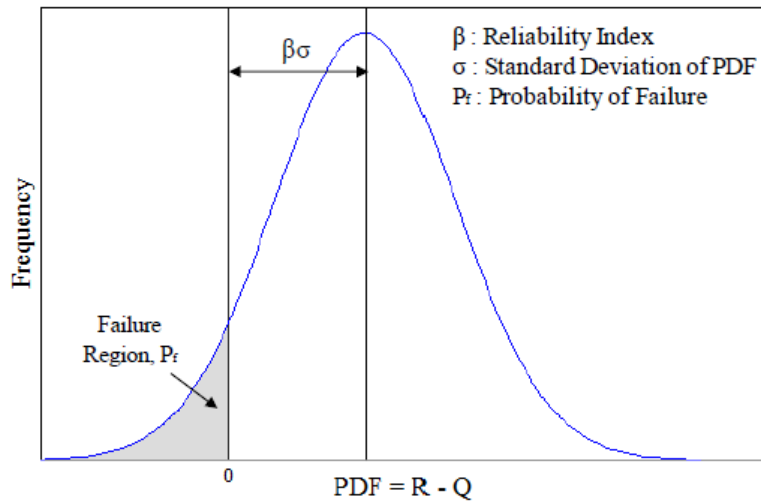


Figure 2.10 Probability of failure and reliability index (Withiam et al. 1998)

The reliability index can be developed when a large amount of data is available and analyzes the possible occurrences of failure among the design based on statistics. Since LRFD is distinguished by applying statistical principles to develop resistance and load factors, statistical parameters are utilized such as mean, standard deviation and coefficient of variation (COV). The mean value of a set of data, μ , is also known as the average of the data set and it is represented by equation 2.12. The standard deviation, σ , is a measure of dispersion of the data in the same units as the data; it is defined by equation 2.13. And lastly, the coefficient of variation, COV, is a dimensionless measure of the variability and dispersion of the data. COV can also be computed by dividing the standard deviation by the mean value as presented in equation 2.14. These parameters are fundamental in the LRFD resistance factor calibration by reliability methods,

$$\mu = \frac{\sum \mu_i}{N} \quad , \quad (2.12)$$

$$\sigma = \sqrt{\frac{\sum (\mu - \mu_i)^2}{N-1}} \quad , \quad (2.13)$$

$$COV = \frac{\sigma}{\mu} \quad , \quad (2.14)$$

where N is the number of cases. The mean value and standard deviation of the random variables, resistance and loads, are used to develop the PDFs curves based on a given database. From figure 2.10 it can also be observed that the reliability index can be expressed as,

$$\beta = \frac{\mu_R - \mu_Q}{\sqrt{\sigma_R^2 + \sigma_Q^2}} \quad (2.15)$$

where μ_R and μ_Q are the mean of resistance and load, and σ_R and σ_Q are the standard deviations. According to Withiam et al. (1998), if $g(R, L) = R/Q - 1$ and the distribution shape of the data is lognormal, the reliability index can be calculated as,

$$\beta = LN \frac{[\mu_R / \mu_Q \sqrt{(1+COV_Q^2)/(1+COV_R^2)}]}{\sqrt{LN[(1+COV_Q^2)(1+COV_R^2)]}} \quad (2.16)$$

Furthermore, Rosenblueth & Esteva (1972) developed a relationship between probability of failure and reliability index that follows lognormally distributed values of R and Q, which is stated by equation 2.17,

$$p_f = 460^{(-4.3\beta)} \text{ if } 2 < \beta < 6. \quad (2.17)$$

According to Barker et al. (1991), the reliability index ranges from 2.0 to 2.5. Furthermore, Zhang, Tang & Ng (2001) showed that reliability target index for pile groups would be smaller than for single piles (β_{group} from 2.0 to 2.5, and for β_{single} 3.0). Based on extensive analysis using reliability methods with database, Paikowsky et al. (2004) recommended for redundant piles (defined as five or more piles per pile cap) a probability of failure of $P_f=1\%$, corresponding to a target reliability index of $\beta=2.33$. For non-redundant piles, defined as four or fewer piles per pile cap, the recommended probability of failure of $P_f=0.1\%$, corresponding to a target reliability index of $\beta=3.0$. The probability of failure and reliability index need both to be defined and included in the calibration of resistance factors using reliability theory.

2.4.6 Calibration by Reliability Theory

LRFD allows conducting calibration by reliability theory by using statistical analysis to develop resistance factors. Calibration is the process of assigning numbers to resistance or load factors based on data collected from field testing. The two most common methods used to calibrate LRFD resistance factors are the First Order Reliability Method (FORM) and the First Order Second Moment (FOSM) method.

FORM can be used to assess the reliability of a pile with respect to a specified limit state and provides means for calculating partial safety factors for resistance and loads against a target reliability index, β , (Paikoswky et al., 2004). FORM requires only first and second moment information on resistances and loads, and an assumption of a distribution shape on the data set. A mean value and standard deviation of the variables are obtained at limit state and at failure state. A resistance factor is computed by dividing the mean of the resistance at the serviceability state and failure state and then accounting for the reliability index. Paikowsky et al. (2004) calculates resistance and loads factors using FORM. Three major historical databases were utilized accounting for 804 piles, which were classified by variables such as type of pile (drilled shaft or driven pile) and method used to analyze pile resistance, such as static analysis or dynamic analysis. The process followed was to compute the statistical parameters (mean and standard deviation) of resistance and loads for a given reliability index, β . Several resistance factors were developed depending on the type of pile and load test method used to analyze the ultimate resistance of the pile. Paikowsky et al. (2004) chose FORM as a reliability theory method in order to compare it to the AASHTO (2001) specifications which utilized FOSM; and, concludes that the difference between the two methods for resistance factors varies in less than 10% since both methods are similar. Consequently, Paikowsky et al. (2004) concluded that using FOSM for resistance factor calibration is more acceptable as it is slightly more conservative. Therefore, FOSM will be used in this study.

FOSM assumes a lognormal distribution shape for the random variables of pile resistance and loads. It also assumes that both variables are statistically independent, such that events related to each other are self-governing. Resistance and load mean values are calculated at the design point and failure point in FORM, as opposed to FOSM which compares the resistance and loads variable with predicted and measured resistance values by a bias factor, λ_R .

The resistance bias factor, λ_R , is defined as the ratio of measured nominal resistance and predicted axial capacity. The bias factor is utilized to account for sources of errors within the collected set of data when comparing a measured resistance collected in the field with a predicted value. It is an important parameter used to correct the discrepancy between designed and measured values. The ratio of predicted axial capacity to measured axial capacity is used as the measure for a method's ability to predict capacity. Consequently, if the bias factor is less than one, the method over-predicted capacity.

In order to successfully design driven piles, load tests are utilized as part of verification. Two types of pile load test are commonly used: static load test (SLT) and dynamic load test (DLT). Static load test can be defined as an analytical procedure that accounts for soil strength and compressibility properties to evaluate the pile load bearing capacity and its effectiveness based on pile-load movement relationship. SLTs are typically conducted during early stages of a project as part of the foundation design process to confirm or refine design parameters and assumptions, and/or as a visual pile proof-test to determine the ultimate capacity of the pile. Head monitoring of deformation are recorded while increments of loads are applied to the pile head until failure. SLTs are typically considered the definitive answer regarding pile load bearing capacity (Fellenius, 1980).

Dynamic Load Tests (DLT) are utilized to determine the ultimate pile capacity during initial installation, or sometime later using the blow of the hammer to the pile head. DLTs are also used to inspect pile integrity, hammer efficiency and evaluate pile driving stresses, which are beneficial to avoid material damaging on the pile while driving. DLTs consist in recorded measurements of strain and acceleration created by the impact at the top of the pile which translates into wave responses that are received by high definition technology in order to measure the resistances produced on a pile. Utilizing DLTs, driven piles can be monitored over several intervals of time after installation. Typically, DLTs are administered immediately at the end of driving (EOD), and at Beginning of Restrike (BOR) which is a specified interval of time after EOD. During the BOR, the pile must be treated and monitored in the same manner as it was at EOD. According to AASHTO (2012), there are specifications for the time after EOD to produce a restrike. This depends mainly in the type of soil surrounding the pile. The state of Alabama conducts DLTs at time intervals based on engineering judgment, but typically from 3 to 7 days after EOD.

The information provided by pile load tests is essential for determining resistance factors utilizing LRFD. Load test data provide the measured nominal resistance utilized to compute resistance bias factors when compared to predicted capacity. To calibrate LRFD resistance factor using FOSM, the following equation is used:

$$\varphi = \frac{\lambda_R(\gamma_{QD}\frac{QD}{QL} + \gamma_{QL}) \sqrt{\frac{1 + COV_{QD}^2 + COV_{QL}^2}{1 + COV_R^2}}}{(\lambda_{QD}\frac{QD}{QL} + \lambda_{QL}) \exp\left\{\beta_T \sqrt{\ln\frac{1 + COV_R^2}{1 + COV_{QD}^2 + COV_{QL}^2}}\right\}} \quad (2.18)$$

where COV_R , COV_{QD} , COV_{QL} are the coefficients of variation of resistance, dead load and live load respectively; λ_R , λ_{QD} , λ_{QL} are bias factors for resistance, dead and live loads; QD/QL is the dead to live ratio; and γ_{QD} , γ_{QL} are the dead and live load factors.

FOSM is a straightforward method that can compute a resistance factor utilizing a methodology that includes statistical parameters for resistance and loads. Resistance uncertainties are incorporated into resistance statistical parameters by utilizing design methods and load test data. Furthermore, for load uncertainties, Paikowsky et al (2004) recommends to use the following dead and live loads parameters for superstructures:

$$\begin{aligned}\gamma_L &= 1.75 & \lambda_{QL} &= 1.15 & COV_{QL} &= 0.2 \\ \gamma_D &= 1.25 & \lambda_{QD} &= 1.05 & COV_{QD} &= 0.1\end{aligned}$$

By obtaining the appropriate amount of test data and design values and utilizing the FOSM equation, regional resistance factors can be developed which account for resistance and load uncertainties within the state of Alabama.

2.4.7 Incorporating Pile Setup into LRFD Design

It can be observed that there has been an extensive effort to apply LRFD method to substructure designs. An important aspect that has not been mentioned is utilizing the increase in capacity over time. Even though research has been developed for calibration of LRFD resistance factors by utilizing reliability theory, there is a lack of work of implementing pile setup into calibration. Benefits of this action could include reducing length of pile, varying cross-section of pile and choice in using heavy or light driving equipment. All these benefits translate into decreased costs. Yang & Liang (2007) conducted research to incorporate long-term set-up into LRFD resistance factors for driven piles in sand. It was concluded that a resistance factor of 0.4 can be taken for a bridge span length less than 60 meters, and 0.5 for a bridge span length greater than 60m by incorporating pile setup. Ng, Suleiman & Sritharan (2010) investigated the impact of including pile set-up in the resistance factor. Ng et al. (2010) developed a setup parameter factor based on the best fitted line for six different piles with dynamic load test data collected at exact intervals of time in cohesive soils. Verma (2010) incorporated pile setup in LRFD resistance factor calibration in the gray delta clay of Louisiana by utilizing a setup parameter

factor specifically for the state of Louisiana and two different methods for prediction of capacity accounting for setup. Verma (2010) developed resistance factors by utilizing FOSM equation and compared different methods of axial capacity prediction with dynamic load test data with pile setup capacity predictions.

To incorporate pile setup in LRFD, resistance factors must be developed that accounts for the increase in resistance after end of driving (EOD). Resistance factors that are currently recommended by 2012 AASHTO Bridge Specification are based on pile testing methods using load testing. A more useful resistance factor can be developed which not only accounts for the increase in resistance over time; but also the uncertainties in the soil type of a desired region.

2.5 Summary of Literature Review

The benefits of developing a regional resistance factor calibrated for the state of Alabama are very significant. It does not only decrease cost in driven piles, but it allows more accuracy. Consequently, the objective of this research is to develop a LRFD resistance factors by utilizing First Order Second Moment in Alabama soils. Completing this task will allow the state to move forward on the transition from ASD to LRFD methods to design deep foundations. However, in order to complete this tasks, a significant amount of design data and pile load test data must be acquired and analyzed. The remainder of this report explains the aspects of the Pile Setup potential in Alabama soils and the development of the LRFD resistance factors for pile foundation design.

CHAPTER 3 – ALDOT PILE DRIVING DATA ACQUISITION AND ORGANIZATION

The Alabama Department of Transportation has been testing driven piles for decades to ensure the piles are achieving the minimum capacity to properly support the loads of the structure. Historical pile load testing data is required to a) analyze the setup in Alabama soils and b) use the measured capacities of piles to calibrate the LRFD resistance factors. ALDOT has provided PDA data files along with the appropriate driving and testing logs for test piles installed within the previous 5 years (2009 – 2014). Pile test data prior to 2009 was not located or utilized due to a change in PDA equipment. Since the majority of the dynamic load test data only included one restrike test within 7 days of the initial installation, there was a need to provide restrike analysis at further times from the initial drive as well as analyze the increase in capacity of the piles throughout an extended period of time. To acquire additional setup information, and to investigate the vibration propagation during pile driving, four piles that differ in size and material were installed at a state owned site near a future project location along the Mobile River in downtown Mobile, AL. This chapter discusses the pile driving process, the acquisition of the pile load test data, and the data processing and analysis of the pile load test data acquired.

3.1 ALDOT Pile Driving Practice

The information presented regarding the current ALDOT pile driving practice was obtained from the Alabama Department of Transportation Standard Specifications for Highway Construction of 2012. For additional details, the reader is referred to the latest ALDOT standard specifications.

3.1.1 Hammer Requirements

Diesel, air, steam, and hydraulic hammers are acceptable for driven pile installation, except diesel hammers are not acceptable for driving prestressed concrete pile 20 inches (510 mm) or larger unless approved by the Engineer. In addition, gravity hammers are not acceptable unless approved by the Engineer.

3.1.2 Hammer Cushion and Striker Plate Requirements

When hammer cushions are required by the hammer manufacturer, the ALDOT also

requires them during impact pile driving. In addition, each hammer cushion must be constructed in accordance with the hammer manufacture's recommendations with appropriate material and thickness to help prevent damage to the pile and hammer and to aid in assuring uniform driving performance. Before pile driving begins at each structure and after each 100 hours of pile driving, the hammer cushion should be inspected in the presence of an Engineer. Furthermore, each hammer cushion must be replaced as soon as they have been reduced to less than 75 percent of the original thickness. As recommended by the hammer manufacture, the top of the hammer cushion requires a striker plate to ensure uniform hammer cushion compression.

3.1.3 Pile Cap Requirements

Piles driven with impact-hammers require a proper pile drive head (also referred to as pile cap or helmet) to distribute the hammer blow to the head of the pile. The pile cap should fit around the pile head in such a way as to maintain suitable hammer-pile alignment while prohibiting the transfer of torsional forces during pile driving.

3.1.4 Pile Cushion Requirements

Before driving a concrete pile, the pile head must be protected with a wooden pile cushion. The thickness of pile cushion should not be less than four inches (100 mm). A new wooden pile cushion must be provide for each driven pile. The pile cushion must be replaced if during driving, the pile cushion burns to the point that flames are visible or is compressed to less than one-half the original thickness. The dimensions of the pile cushion should equal or exceed the pile head's cross-sectional area, and must suitably fit the pile cap's dimensions.

3.1.5 Set of Leads Requirements

Driven piles must be maintained in alignment and position with leads during driving. To ensure concentric hammer impacts for each blow, the leads should be constructed in a way that allows freedom of hammer movement while maintaining hammer-pile alignment. Leads must be swinging or fixed type. Swinging leads must be equipped with a pile gate. To maintain position and alignment, the pile must be constrained with a template (structural frame) or the lead must be

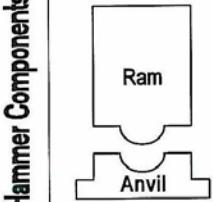
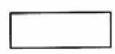
sufficiently embedded into the ground. The pile must not extend beyond the leads.

3.1.6 Pile Driving Hammer Approval Requirements

The pile driving hammer must be capable of driving the selected pile to the required pile toe elevation with a blowcount of less than refusal, which is defined as 240 blows per foot (300 mm).

Pile driving contractors must submit a completed Pile and Driving Equipment Data Form (Form C-14) to the ALDOT for evaluation and approval. An example of a completed Form C-14 is illustrated in Figure 3.1.

The ALDOT will perform all analysis with a Wave Equation Analysis Program (WEAP) for each pile driving hammer submitted for evaluation. In the event that a WEAP analysis cannot be performed, dynamic load testing must be performed to verify whether or not the pile driving hammer is capable of successfully installing the selected piles. If the pile driving hammer is approved, the ALDOT specifies the hammer stroke and blow count required to achieve the minimum pile axial resistance, which is equal to twice the design load, along with the count/bearing capacity graph.

FORM C-14 ALABAMA DEPARTMENT OF TRANSPORTATION Revised 08-07-95 PILE AND DRIVING EQUIPMENT DATA FORM		
Project Number USA Test Pile & Vibration	County Mobile	Division 9th
Pile Driving Contractor or Subcontractor Jordan Pile Driving Inc.	Bridge Identification Number N/A	
Details of access method to pile top for dynamic testing are: <input type="checkbox"/> Attached <input checked="" type="checkbox"/> Not Applicable		
Hammer Components 	Hammer	Manufacturer: <u>Delmag</u> Model: <u>D-62-22</u> Type: <u>S.A. Diesel</u> Serial No.: <u>238</u> Rated Energy: <u>165,000</u> (ft.-lbs.) at <u>11.3</u> (ft.) Length of Stroke Modifications: <u>Adjustable Fuel Pump</u> Pump Setting 1 <u>78,960</u> ft. lbs. Pump Setting 2 <u>109,725</u> ft. lbs. Pump Setting 3 <u>136,950</u> ft. lbs. Pump Setting 4 <u>165,000</u> ft. lbs.
		Capblock (Hammer Cushion) 
	Pile Cap <div style="border: 1px solid black; padding: 2px; display: inline-block;"> Helmet <input checked="" type="checkbox"/> Bonnet Anvil Block Drivehead </div>	Weight : <u>10,000</u> (lbs.) Note: Should include weight of striker plate.
	Pile Cushion	Cushion Material: <u>Plywood</u> Thickness: <u>10</u> (in.) Area: <u>576</u> (in. ²) Modulus of Elasticity - E : <u>45</u> KSI (P.S.I.) Coefficient of Restitution - e : <u>0.5</u>
	Pile	Pile Type: <u>36" x 36" & 24" x 24" Prestressed Concrete Test Pile</u> Length (in Leads): <u>89' & 81'</u> (ft.) Weight / Ft: <u>936 & 510</u> (lbs./ft.) Wall Thickness: <u>NA</u> (in.) Taper: <u>NA</u> Cross Sectional Area: <u>489 & 898</u> (in. ²) Design Pile Capacity: _____ (Tons) Description of Splice: <u>N/A</u> Tip Treatment Description: <u>N/A</u>

Note: If mandrel is used to drive this pile, attach separate manufacturer's detail sheet(s) including weight and dimensions.

Submitted By: _____ Date: _____
 Davis Daniel

Figure 3.1. ALDOT pile driving equipment data form (Form C-14).

3.1.7 Test Pile Requirements

A test pile must be driven in the designated location and to the minimum pile toe elevation. Test piles should be driven to a hammer blow count specified on the blow count/bearing graph. The blow count/bearing graph should be used as an estimate of the test

pile's total axial resistance. This graph uses hammer stroke and the required minimum pile axial resistance, which is equal to twice the design load, to obtain the required blow count for the test pile.

Static load testing must be performed to indicate the minimum pile axial resistance. Once the required minimum pile toe elevation and blow count is reached (i.e., once EIOD is reached), the test pile's total axial resistance must be confirmed (after a minimum 36 hour wait for steel piles and a minimum 7 day wait for concrete piles) with static load testing. Static load testing indicates a failure if the pile axial resistance determined from static load testing is not greater than or equal to the required minimum pile axial resistance, which is twice the design load.

Dynamic load testing may be used to supplement static load testing. Furthermore, all dynamic load testing must be correlated by at least one static loading test. The correlation should also include a dynamic restrike within 48 hours after completion of static load testing using the approved pile driving system. Pile hammers should be warmed up before dynamic load testing begins by applying a minimum of 20 blows to a neighboring pile. During restrikes, the test pile should be struck by the hammer until the pile penetrates the soil an additional three inches (75 mm) or for 50 blows, whichever comes first. However, the restrike may be ended after 20 blows if the pile movement is less than one-quarter inch (6 mm).

3.1.8 Static Load Testing Methods

Static load testing should be used to evaluate the axial resistance of individual piles or groups of piles. Static load testing should be used after the test pile has met the bearing capacity estimate based on hammer stroke and blow count from the provided bearing curves and has been driven to the minimum pile toe elevation.

The test must be performed using the Quick Load Method as defined by ASTM D 1143, Standard Test for Piles Under Static Axial Compressive Load. The Engineer must evaluate the safe allowable load from the load versus settlement curve produced by incremental loading based on the Davisson's failure criterion.

Once the required minimum pile toe elevation and blow count is reached (i.e., once EIOD is reached), the test pile's total axial resistance must be confirmed (after a minimum 36 hour wait for steel piles and a minimum 7 day wait for concrete piles) with static load testing.

The static load testing equipment must have a capacity of 300 percent the design load or 1000 tons (8900 kN), whichever is less. Incremental loads of 10% of the design load should be

applied to the pile head at 2.5 minute intervals until the load-frame capacity has been reached or continuous jacking is required to sustain the incremental load. The settlement data, time, and load must be recorded on Form C-15B immediately before and after each applied load increment. Figure 3.2 shows a completed Form C-15B. As soon as the maximum load has been applied and the jacking has stopped, readings must be taken and recorded. Additional readings should be taken and record after 2.5 minutes and 5 minutes. If no additional readings are required, then the load should be removed in four equal parts with rebound and time readings taken and recorded at each unloading increment. Readings must be taken and recorded immediately after each load removal allowing 2.5 minutes between increments. After removing the total load, rebound and time readings must be taken and recorded. Additional rebound and time readings must be taken and recorded after 2.5 minutes and at 5 minutes.

The load test data must be plotted as applied load in kips (abscissa) versus settlement in inches (ordinate, positive down). Total pile axial resistance must be evaluated based on the Davisson's failure criterion as illustrated in Equation 8. The elastic modulus for steel piles should always be assumed as 29,000 ksi.

ALABAMA DEPARTMENT OF TRANSPORTATION PILE LOADING RECORD - QUICK LOAD TEST				
FORM C-15B Revised 07-15-94				
Project Number USA Test Pile & Vibration		County MOBILE		Division NINTH
Station, Bent No. & Lane			Bridge Identification Number	
Contractor Jordan Pile Driving, Inc		Inspector Jenifer Butler		
Date 3-Jan-14	Pile Number		Length of Pile (Feet)	
Size and Type of Pile Steel HP 12x53	Calculated Elastic Modulus of Pile (E) (ksi)		Measured Elastic Modulus of Pile (E) (ksi) 30000	
Dist. From Settlement Gage To Pile Tip (Feet) 64.71	Elevation of Ground Line at Pile		Pile Tip Elevation	
Design Load (Tons) 70				
Elapsed Time (Minutes :	Increment Of Load (Tons)	Total Accumulated Load (Tons)	Settlement Before Loading Increment (Inches)	Settlement After Loading Increment (Inches)
0:00	0	0	0.0000	0.0000
2:30	7	7	0.0000	0.0000
5:00	7	14	0.0000	0.0000
7:30	7	21	0.0000	0.0000
10:00	7	28	0.0000	0.0000
12:30	7	35	0.0000	0.0000
15:00	7	42	0.0000	0.0000
17:30	7	49	0.0313	0.0313
20:00	7	56	0.0313	0.0313
22:30	7	63	0.0313	0.0625
25:00	7	70	0.0625	0.0938
27:30	7	77	0.1250	0.1250
30:00	7	84	0.1563	0.1875
32:30	7	91	0.2813	0.2813
35:00	7	98	0.3750	0.4063
37:30	7	105	0.5000	0.5313
40:00	7	111	1.0000	1.0000
42:30	0	111	1.0000	1.0000
45:00	-27.75	83.25	0.9688	0.9688
47:30	-27.75	55.5	0.9063	0.9063
50:00	-27.75	27.75	0.8125	0.8125
52:30	-27.75	0	0.6875	0.6563
55:00	0	0	0.6563	0.6563
57:30				
60:00				
62:30				
65:00				
Pile Loading Record Continued On Sheet No. 2 of 2				

Figure 3.2. ALDOT Quick Load Test Record (Form C-15B).

3.1.8 Dynamic Load Testing Methods

Dynamic Load Testing should be used to indicate whether or not the test pile or production pile is being overstressed during driving and to estimate pile axial resistance.

The test must be performed as defined by AASHTO T 298, Standard Method of Test for High-Strain Dynamic Testing of Piles. In general, the dynamic load testing system consists of a minimum of two accelerometers and two strain transducers bolted on opposite sides of the pile and at a distance of approximately 2 to 3 diameters below the pile head (or at a convenient location during dynamic restrikes).

Figure 3.3 shows an example of a completed Form C-15A, which is a form used by ALDOT personnel to record dynamic load testing field measurements such as blows per foot of pile penetration, pile penetration depth, height of hammer fall, and energy delivered to the pile head.

ALABAMA DEPARTMENT OF TRANSPORTATION				
TEST PILE RECORD				
FORM C-15A REVISED 08-07-95				
Project Number USA Test Pile & Vibration		County MOBILE		Division NINTH
Bridge: Station _____ to Station _____			Bridge Identification Number N/A	
Road Between _____ and _____				Lane (if applicable)
Contractor Jordan Pile Driving, Inc.		Inspector Jen Butler		
Date 8/21/13	Bent No. & Lane		Pile No.	Kind of Soil sand
Kind of Pile Steel		Size of Pile HP 12x53		Total Length (ft)
Elev. Ground Line at Pile		Final Elev. At Top of Pile		Tip Elevation
Hammer Make APE		Hammer Model D30-42		Hammer Kind Open
Hammer Type Diesel		Hammer Action Single Action		Rated Energy (ft.-lbs.) 74,419
Weight of Hammer (lbs.) 6,615		Design Load (from plans) (tons) 70		
Hammer Cushion: Material Aluminum & Micarta Alternating		Thickness (in.) 4	Area (sq. in.) 398	
Pile Cushion (Before Driving): Material N/A		Thickness (in.)	Area (sq. in.)	
Pile Cushion (After Driving): Material N/A		Thickness (in.)	Area (sq. in.)	
Pile Cap Weight (lbs.) 1,704				
Height Of Fall (feet)	Energy Delivered To Pile (E) (ft.-lbs.)	Blows Per Foot Of Penetration (N)	Total Penetration (feet)	Bearing (tons)
5.7	37,706	5	43	
5.73	37,904	4	44	
5.71	37,772	5	45	
6.05	40,021	5	46	
6.02	39,822	5	47	
5.62	37,176	5	48	
5.69	37,639	6	49	
5.96	39,425	5	50	
5.96	39,425	6	51	
5	33,075	7	52	
4.8	31,752	8	53	
4.6	30,429	11	54	
4.6	30,429	11	55	
6.2	41,013	10	56	
5.95	39,359	10	57	
6	39,690	9	58	
6.02	39,822	10	59	
6	39,690	10	60	
6.14	40,616	10	61	
6.08	40,219	11	62	
6.57	43,461	12	63	
5.63	37,242	11	64	
6.07	40,153	12	65	

Figure 3.3. ALDOT Dynamic Load Testing Record (Form C-15A).

3.2 Test Piles Installed and Tested at the Mobile River Site

The study includes the installation of four piles at a state owned site along the Mobile River in downtown Mobile, Alabama. This site was chosen because it lies along a potential alignment of a future bridge. The information gained from installing and testing piles at this location will provide more than testing data to add to this study. Installing various types of piles at this location can also provide assistance with design and construction planning when the State begins the bidding and design phases. There will be two different steel H piles and two different square precast, prestressed concrete piles installed. The details of the site and installation process are discussed.

The project site is located on the west bank of the Mobile River, just south of the Alabama Cruise Terminal, as seen in figure 3.4.

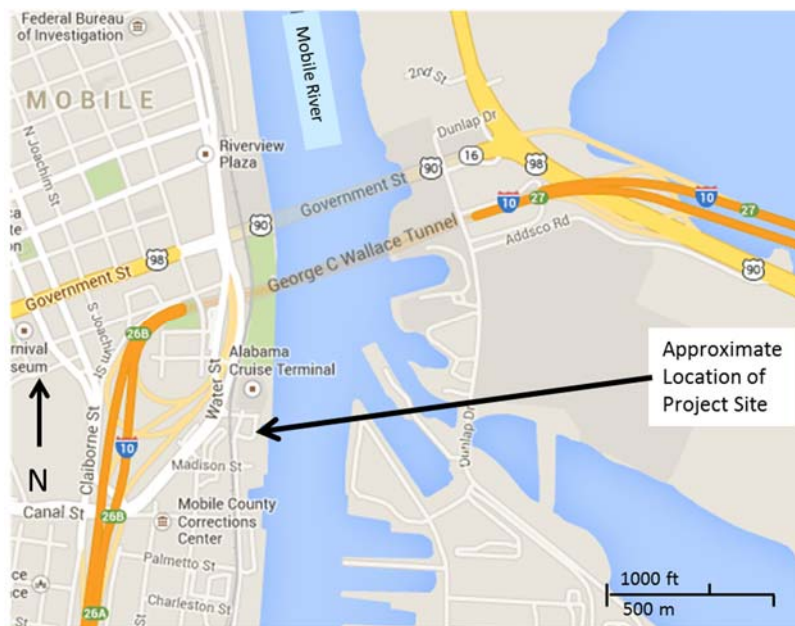


Figure 3.4: Location of project site, Mobile, AL (Google 2013)

Two soil investigations were performed at the site. The first was a Standard Penetration Test (SPT) drilled and tested to 115 feet below the ground surface, performed by an ALDOT drilling crew. The second soil investigation was a Seismic Cone Penetration Test (SCPT) with soundings to 100 feet below the ground surface, as conducted by Southern Earth Sciences.

Detailed soil results are found in the Appendix of the Addendum report detailing the vibration study. The soil profile at the site consists primarily of sandy soils to a depth of 90 feet below the ground surface with a clay layer located at an approximate depth of 90 to 110 feet. Table 3.1 contains a summary of the soil layers that were defined by a standard penetration test (SPT) conducted at the project site, and figure 3.5 provides a visual display of the pile type and depths with the encountered soils.

Table 3.1: Soil profile at site location

Depth (ft.)	Basic Material	Average Blow Count	Consistency
0-23.5	Sand	12	Loose to Medium
23.5-89.5	Sand	31	Medium to Dense
89.5-108.5	Clay	28	Stiff to Very Stiff
108.5-115	Sand	27	Medium

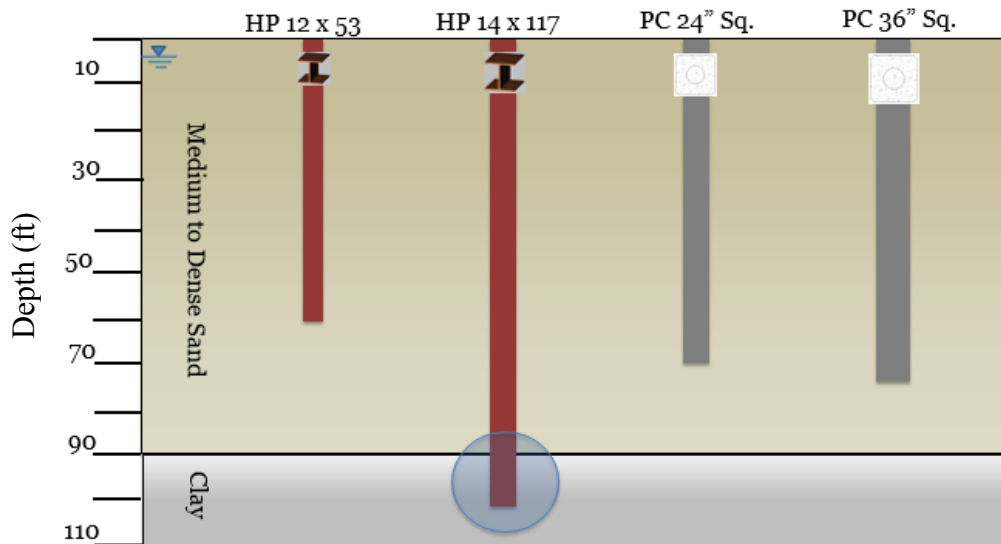


Figure 3.5: Pile type and depth of soils encountered

Figure.6 contains a plan view of the project site. The dashed line in the figure represents the approximate property boundary. Note that the pile locations are approximate and the drawing is not to scale.

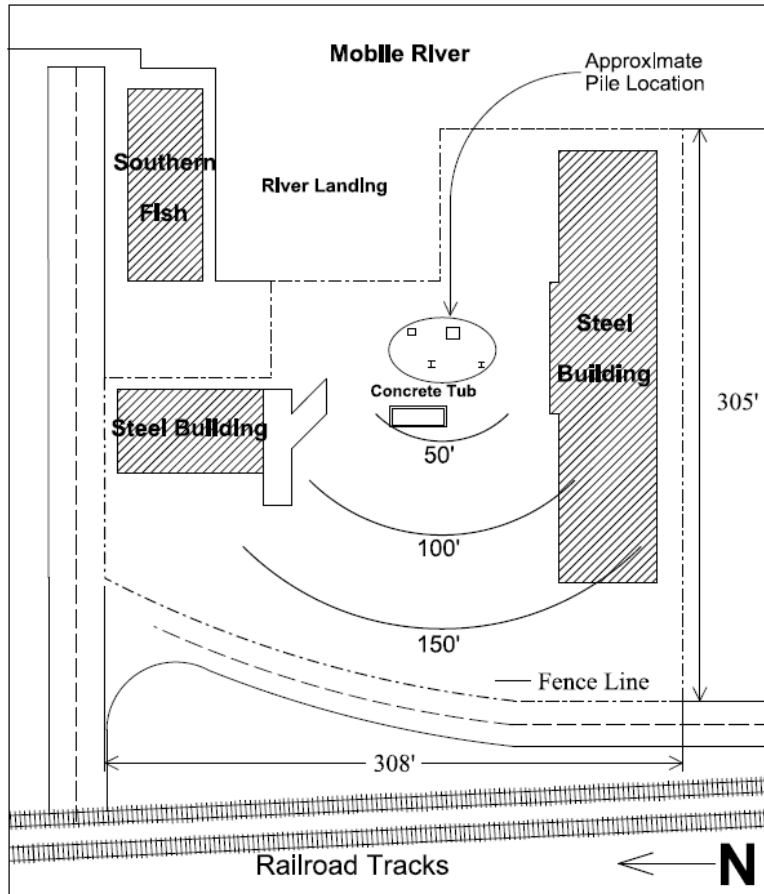


Figure 3.6: Plan view of Mobile River Project Site and Approximate Location of Piles

The piles were installed using typical techniques including pile jetting or vibration followed by driving with a diesel hammer. The concrete piles were jetted to a depth of approximately 30 feet and driven to the final elevation using a Delmag Model D-62-22 diesel hammer. A vibratory driver was used to drive the steel HP 14 to 55 feet and the HP 12 to 15 feet. The steel piles were then driven to the final elevation using an APE Model D30-42 diesel hammer. Figure 3.7 provides an image of the four test piles after installation.

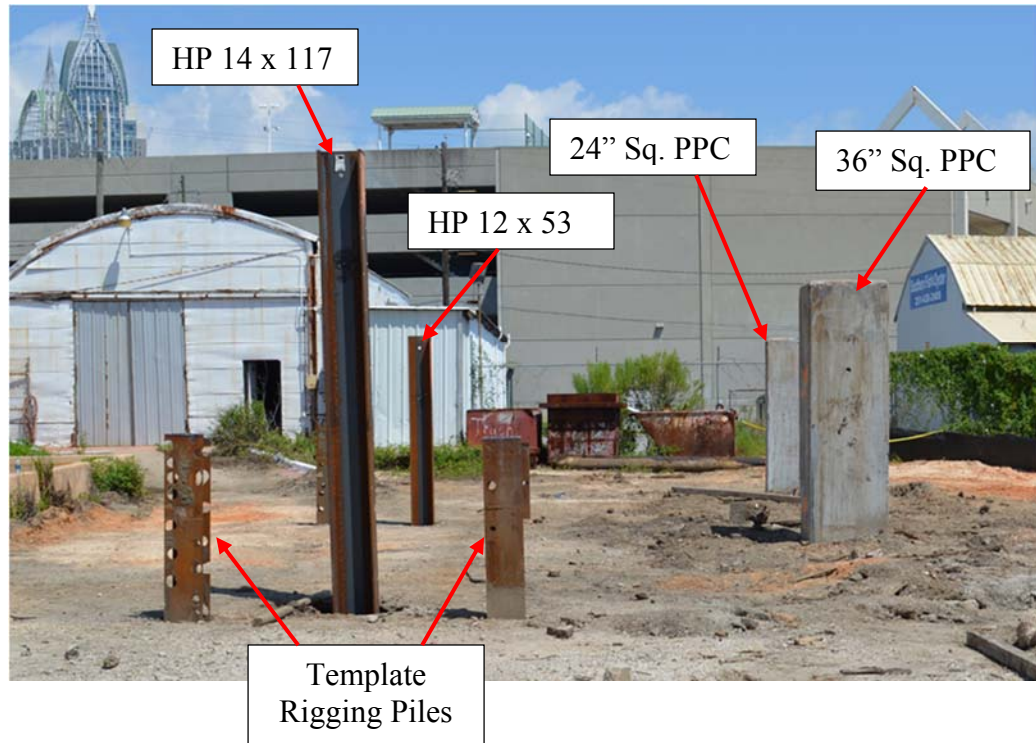


Figure 3.7. Image of four test piles after installation (provided by author)

3.3 Acquiring and Organizing Load Test Data

The Alabama Department of Transportation provided the PDA[®] load testing data of test piles performed in the state between 2009 and 2014. The PDA[®] data were archived in the current format of PDA[®] (W01 files). Along with the PDA[®] data, the inspector driving logs and reports containing site characteristics were collected for each project.

The near-surface soils (up to 150 feet (46 m) in depth) in the State of Alabama can be categorized by five types. The northeast 1/3 of the state consists of Limestone uplift, Appalachian Plateau, and Piedmont Plateau, which consist of a hard layer of bedrock close to the surface. The foundation elements in these areas typically do not include driven piles with set-up potential as they are toe-bearing piles typically driven to refusal. The remaining areas in the state consists of either interbedded layers of sand and clay that typically show set-up effects or silty sands that occasionally exhibit relaxation. The typical foundation design of highway structures in these areas is driven pile foundations. The standard types of piles used by ALDOT for bridge construction are steel H-piles or square precast, prestressed concrete (PPC) piles.

3.3.1 PDA[®] and iCAP[®] Procedure

The wave force and velocity information along with the driving logs from the site inspector was provided for further evaluation. The properties of each test pile were determined using the driving logs or wave analysis. Information about the pile driving equipment, which is recorded on Form C-14 (see Figure 3.1), along with certain pile properties were entered into the PDA[®] software.

The following properties were determined and entered in the PDA[®], and were ultimately utilized during iCAP[®] analysis. Pertinent data that was determined for analysis were the following: AR is pile cross-sectional area at sensor location, LE is length from sensor location to pile toe, EM is pile elastic modulus (steel $EM = 30,000$ ksi and concrete EM was computed using Eq. 3.1), SP is pile specific weight density (steel $SP = 0.492$ kips/ft³ and concrete $SP = 0.150$ kips/ft³), and WS is wave speed. For steel, WS was computed using Equation 3.1. For concrete, the WS was estimated with the PDA[®], which estimates the computed wave speed (WC). The WC can be calculated by first investigating the Wave Down (WD) and Wave UP (WU) screen display and then moving the second dashed rise time marker to the beginning of the wave up valley at $2L/c$ (PDA[®] Manual 2001).

$$EM = \rho c^2 = \frac{SP}{g} (WS)^2 \quad (3.1)$$

Equation 3.1 was used to determine the elastic modulus (EM) for concrete piles or the wave speed (WS) for steel piles; where, ρ is mass density, c is wave speed, and g is gravitational constant (32.2 ft/sec²).

Field measurements for the pile embedment depth and displacement, which are recorded on Form C-15A (see Figure 3.3), were entered into the iCAP[®] software. After entering the pile properties into the PDA[®] software, the iCAP[®] qualifiers were selected and defined. Lastly, signal matching was performed on each test pile using the iCAP[®] software. Full iCAP[®] analysis was performed on a representative blow at or near EOID. For restrrike analysis, each of the early blows was investigated, and typically the blows selected for iCAP[®] analysis ranged from blow 2 to blow 5. Choosing which blow to analyze was based on two criteria. The first criterion was to

select the earliest blow with enough energy to fully mobilize the pile's axial resistance. The second criterion was based on a parameter provided by the iCAP[®] software called match quality. The match quality is a value to aid in determining if the signal match was appropriate based on the properties provided as well as the soil damping values. Higher match quality values indicate that less confidence can be placed in the iCAP[®] results. The match quality values for all blows used in the analysis were between 1 and 5, where 1 indicates a perfect match. If an analyzed blow produced a match quality larger than five, then another blow was selected.

The PDA data was also analyzed by the manufacturer of the iCAP[®] and CAPWAP[®] signal matching software, GRL Engineers, Inc., using the full CAPWAP[®] software due to an initial discrepancy in analysis when results were compared to the Static Load Tests and iCAP[®] results. This discrepancy appeared to be a result of a small initial dataset and was found to be insignificant when the larger dataset was analyzed and compared, as will be reported in the next chapter. The results from the CAPWAP[®] analysis was compared to the original PDA data and the iCAP[®] analysis performed in this study to validate the accuracy of results.

CHAPTER 4 – RESULTS AND DISCUSSION OF PILE LOAD TESTS AND PILE SETUP

A total of 23 test piles (steel H-piles and square PPC piles) were analyzed for this portion of the project. Five of these test piles (USA test piles) were installed specifically for research purposes. Four test piles were installed near the Mobile River (HP 12x53, HP14x117, PPC 24"x24", and PPC 36"x36") and the fifth test pile (HP14x102) was installed in Montgomery, AL at the Montgomery Outer Loop Project. The coordinates of all 23 test piles were entered into the ArcGIS software to create a map to display the test pile locations. As can be seen in Figure 4.1, the density of test piles is much larger in the southern region of Alabama due to the large number of projects in this area during recent years and due to less frequent testing in the northern 1/3 region of the state because of the subsurface conditions.

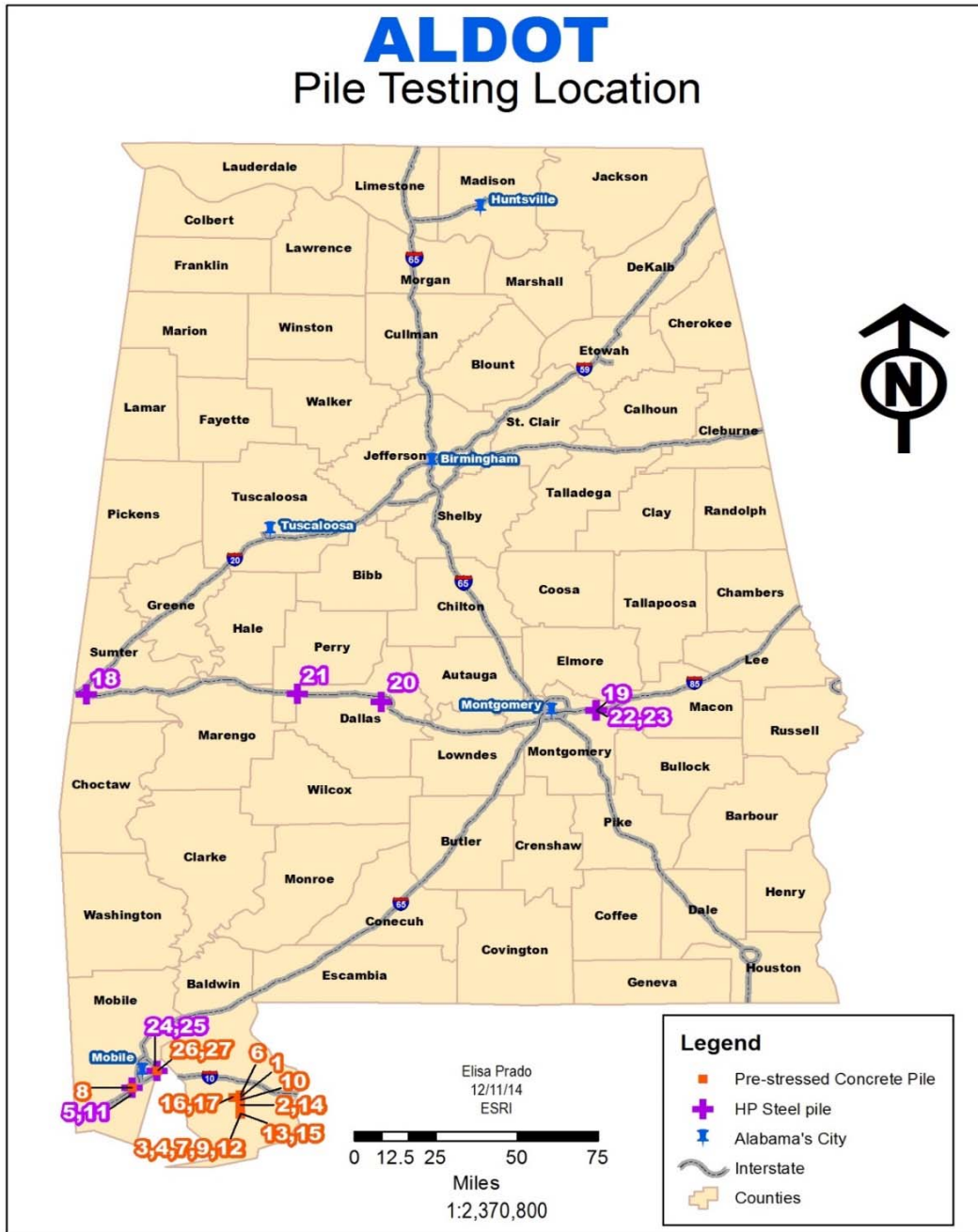


Figure 4.1 ALDOT Pile testing location throughout the state of Alabama (ArcMap 10 Software)

4.1 Alabama Soil Conditions

A geographical map of the state of Alabama is shown in figure 4.2 (Mitchel & Cameron, 2008). According to Mitchell (2008), the central part of the state is defined as the Blackland Prairies region, dominated by dark to orange clayey soils. The southern part of the state is

defined by the Coastal plain region and dominated by sandy soils. The northern part of the state is defined as the limestone valleys, Appalachian Plateau, and Piedmont plateau which mainly consist of limestone, rock and sand stones (Mitchel & Cameron, 2008).

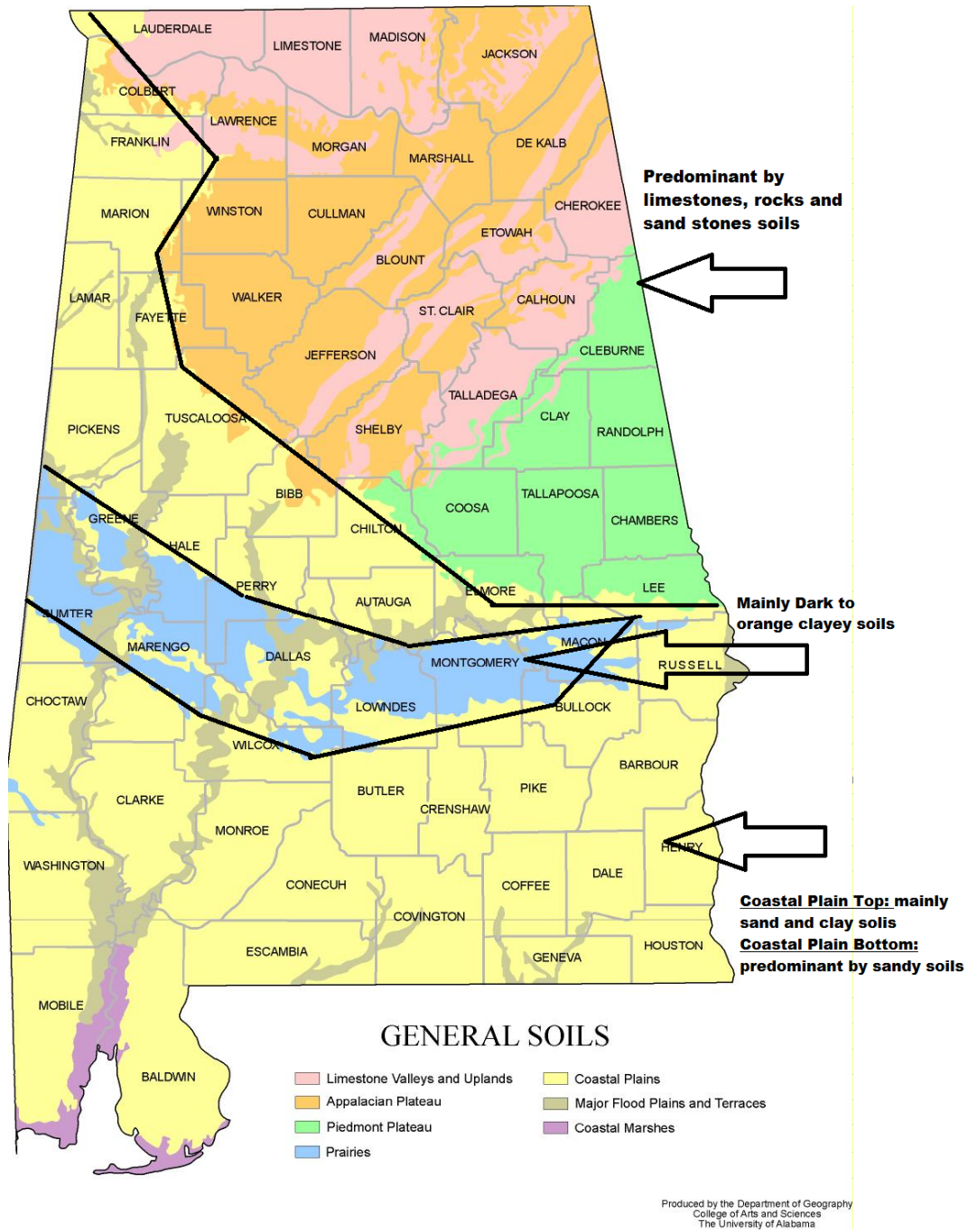


Figure 4.2 Geographical map for the state of Alabama (Mitchell & Cameron, 2008)

4.2 Load Test Results

The total pile axial resistance (R_u) results used in this paper were estimated with three dynamic analysis methods: 1) the iCAP[®] Method, 2) the CAPWAP[®] Method, and 3) the PDA[®] Method (also called the Case Method). It must be noted that the PDA[®] data were independently and blindly (i.e., without looking at the other dynamic analysis results) analyzed using all three dynamic analysis methods. The author of this paper analyzed the PDA[®] data with the iCAP[®] software, and thus provided the total pile axial resistance (R_u) estimates using the iCAP[®] Method. A single PDA[®] operator from the ALDOT provided the total pile axial resistance (R_u) estimates using the PDA[®] Method (or Case Method). GRL Engineers, Inc. provided the total pile axial resistance (R_u) estimates using the CAPWAP[®] Method. Table 4.1 shows the total pile axial resistance (R_u) estimates from each dynamic analysis method at the end-of-initial-driving (EOID) and at the beginning of each restrike (BOR).

Table 4.1. Dynamic load testing results for ALDOT test piles

Pile #	Time	Pile Type	L (ft)	GRL	USA	ALDOT	Time	Time	Time	Days from EOID	Soil Type	USA Pile ID
				CAPWAP	iCAP	PDA	Effect	Effect	Effect			
				Ru (kips)	Ru (kips)	Ru (kips)	iCAP Rr/Ro	CAPWAP Rr/Ro	PDA Rr/Ro			
1	EOID	HP 10x42	53.5	150	129	204					Clay	12
	BOR1			180	182	259	1.41	1.2	1.27	3		
2	Set-check	HP 14x73	52	375	332	378					Clay Fill	23
	BOR1			306	256	398	0.77	0.82	1.05	6		
3	EOID	HP 14x73	42	377	384	450					Selma Chalk	22
	BOR1			636	704	695	1.83	1.69	1.54	7		
4	EOID	HP 14x73	55	304	328	375					Clay Fill	24
	BOR1			335	391	457	1.19	1.1	1.22	7		
5	EOID	HP 12x53	35	170	175	255					Dense Sand	19
	BOR1			161	152	254	0.87	0.95	1	18		
6	EOID	HP 14x102	19.8	158	131	252					Clayey Sand	20
	BOR1			185	156	256	1.18	1.17	1.02	7		
	BOR2			182	183	310	1.39	1.15	1.23	14		
	BOR3			174	200	366	1.52	1.1	1.45	21		
7	EOID	HP 10x42	47	149	150	204					Dense Sand	6
	BOR1			173	168	218	1.12	1.16	1.07	6		
8	EOID	HP 12x53	62	Faulty Data at EOID							Medium Sand	26
	BOR1			199	153	294	1.52					
	BOR2			233	232	336	1.52	1.17	1.14	7		
	BOR3			224	240	450	1.57	1.13	1.53	30		
	SLT			SLT = 212 kips			1.39	1.07	0.72	135		
	BOR4			321	222	370	1.45	1.61	1.26	153		
9	EOID	HP 14x117	102	368	469	400	3.07	1.85	1.36	439	Medium Sand	27
	BOR1			192	156	191	2.04	1.33	2.98	2		
	BOR2			255	318	570	1.49	1.25	2.28	7		
	BOR3			240	232	435	3.01	1.65	2.38	30		
	SLT			SLT = 560 kips			3.59	2.92	2.93	146		
	BOR4			365	592	505	3.8	1.9	2.64	153		
10	EOID	PPC 20x20	65	612	593	560	3.8	3.19	2.88	439	Firm Silty Sand	15
	BOR1			530	429	485	1.07	1.02	1.21	1		
11	EOID	PPC 20x20	61.5	542	460	587	1.07	1.02	1.21	1	Firm Silty Sand	4
	BOR1			357	312	424	0.9	0.65	1.13	7		
12	EOID	PPC 16x16	50	205	204	269					Medium Silty Sand	7
	BOR1			245	276	518	1.36	1.2	1.93	7		
13	EOID	PPC 20x20	65	450	429	617					Clay with Dense Sand	11
	BOR1			464	438	633	1.02	1.03	1.03	9		
14	EOID	PPC 14x14	46	131	147	158					Sandy Clay	17
	BOR1			267	177	377	1.21	2.04	2.39	9		
15	EOID	PPC 14x14	65	54	87	115					Clay	18
	BOR1			161	151	232	1.74	2.98	2.02	1		
16	EOID	PPC 20x20	75	220	277	284	3.18	4.07	2.47	10	Firm Silty Sand	16
	BOR1			273	265	380	0.93	1.11	1.22	13		
17	EOID	PPC 16x16	55	150	127	187					Loose Silty Sand	10
	BOR1			210	142	335	1.12	1.4	1.79	14		
18	EOID	PPC 20x20	55	320	337	378					Firm Silty Sand	8
	BOR1			344	304	407	0.9	1.08	1.08	14		
19	EOID	PPC 20x20	66	202	222	342					Sandy Clay	13
	BOR1			460	339	447	1.52	2.28	1.31	83		
20	EOID	PPC 20x20	68	208	214	269					Loose Silty Sand	14
	BOR1			278	298	382	1.39	1.34	1.42	9		
21	EOID	PPC 20x20	78	310	319	545	1.49	1.49	2.03	139	Loose Silty Sand	5
	BOR1			181	152	156	1.73	1.78	2.4	8		
22	EOID	PPC 24x24	73.6	491	316	774	2.07	2.71	4.96	147	Medium sand	28
	BOR1			648	565	784	1.15	0.98	1.02	3		
	BOR2			634	650	797	1.14	1.08	1.25	7		
	BOR3			700	642	977	1.4	1.21	1.25	31		
	SLT			SLT = 1050 kips			1.86	1.62	1.34	120		
	BOR4			1015	946	941	1.68	1.57	1.1	154		
23	EOID	PPC 36x36	79.6	784	934	930	1.65	1.21	1.2	440	Medium sand	29
	BOR1			912	839	892	1.13	1.05	1.72	3		
	BOR2			961	952	1538	1.18	1.07	1.63	7		
	BOR3			975	989	1453	1.22	1.04	1.63	32		
	BOR4			949	1023	1011	1.38	1.16	1.13	155		
BOR5	1059	1158	1548	2.16	1.25	1.74	441					

4.2.1 Overall Load Test Results

The time effects presented in Table 4.1 show the ratio of the total pile axial resistance at the beginning of the restrike (BOR) to the total pile axial resistance at the EOID. For example, the time effect values listed under the column labeled “Time Effect CAPWAP[®] R_r/R_o” in Table 4.1 are the ratio of the total pile axial resistance at the BOR (R_r) as estimated by the CAPWAP[®] Method to the total pile axial resistance at the EOID (R_o) as estimated by the CAPWAP[®] Method. If this ratio is greater than 1.00, then the results indicate that set-up had developed. On the other hand, if this ratio is less than 1.00, then results reveal that relaxation had developed. Figures 4.3 and 4.4 provide a visual display of the time effects of the piles separated by the type of pile.

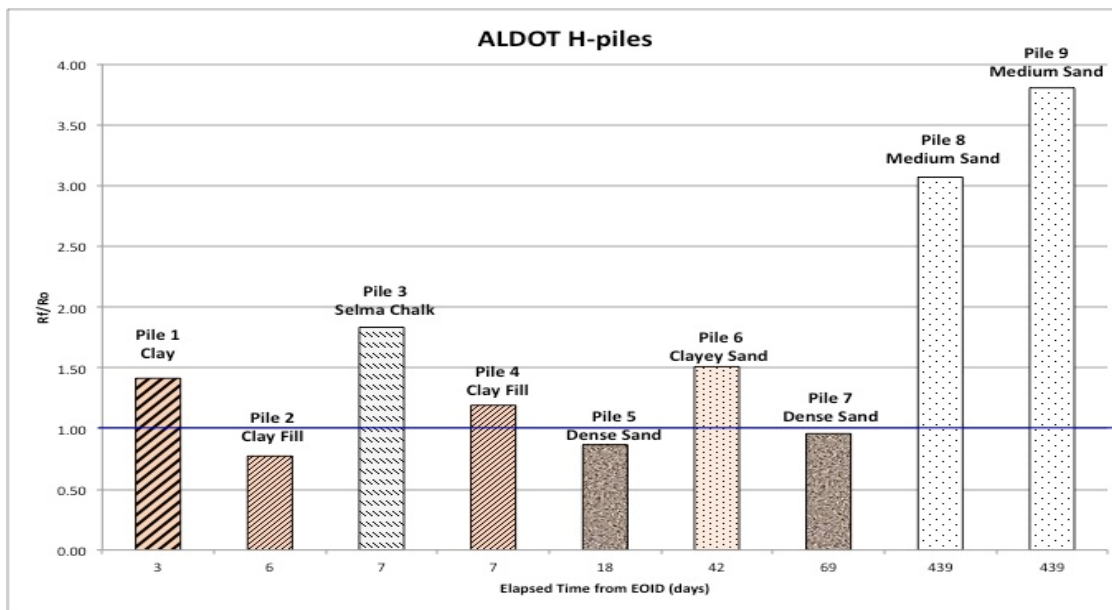


Figure 4.3. Time effect of ALDOT H-pile to the elapsed time between EOID and final restrike according to the total resistance results from the iCAP[®] Method.

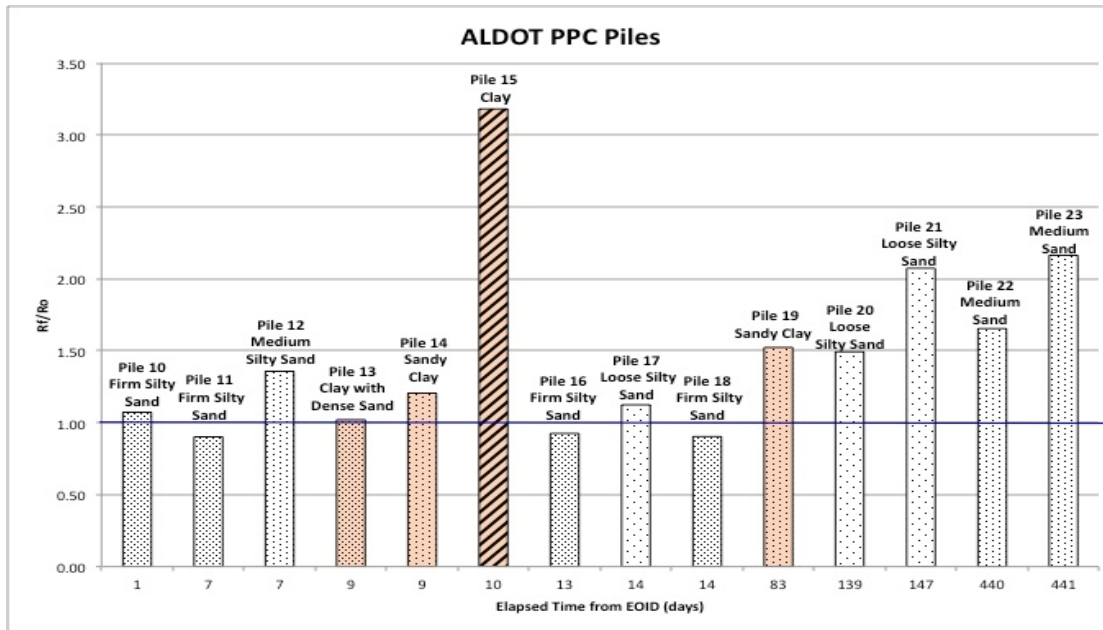


Figure 4.4. Time effect of ALDOT PPC pile to the elapsed time between EOID and final restrike according to the total resistance results from the iCAP® Method.

4.2.2 Results of the Mobile River and Montgomery Outer Loop Test Piles

It must be noted that the PDA® data at EOID for the ALDOT HP12x53 test pile (USA test pile near the Mobile River) are invalid because the PDA® did not receive strain signals. As a result, the total pile resistance (Ro) estimates at the EOID were replaced by the first restrike estimates (BOR1).

Figure 4.5 illustrates the time effect (Rr/Ro) with the time interval after EIOD of the restrike for the ALDOT HP12x53 test pile (USA Mobile River Project). For example, the iCAP® data series (as shown in Figure 4.5) expresses the ratio of the restrike total pile resistance (Rr) estimates using the iCAP® software to the EOID total pile resistance (Ro) estimates using the iCAP® software. In addition, both the CAPWAP® and PDA® data series (as shown in Figure 4.5) are also expressed in a similar fashion. Thus, the time effect comparisons as estimated with each dynamic analysis method are plotted in Figure 4.5.

Because the ALDOT HP12x53, HP 14x117 and PPC 24”x24” test piles achieved the Davisson failure criterion during the static loading test (SLT), ratios of the Davisson Capacity to the EOID total pile resistance (Ro) estimates are also illustrated in Figures 4.5 to 4.7. For

example, the SLT/(iCAP-Ro) data series (as shown in Figure 4.5) expresses the ratio of the Davisson Capacity to the total pile resistance (Ro) estimates at the EIOD using the iCAP[®] software. In addition, both the SLT/(CAPWAP-Ro) and SLT/(PDA-Ro) data series (as shown in Figure 4.5) are also expressed in a similar fashion. If the ratio is larger than 1.00, then the results indicate that set-up has developed. On the other hand, if the ratio is less than 1.00, the results reveal that relaxation has developed. Figures 4.6 to 4.9 show similar relationships and comparisons for the other USA test piles.

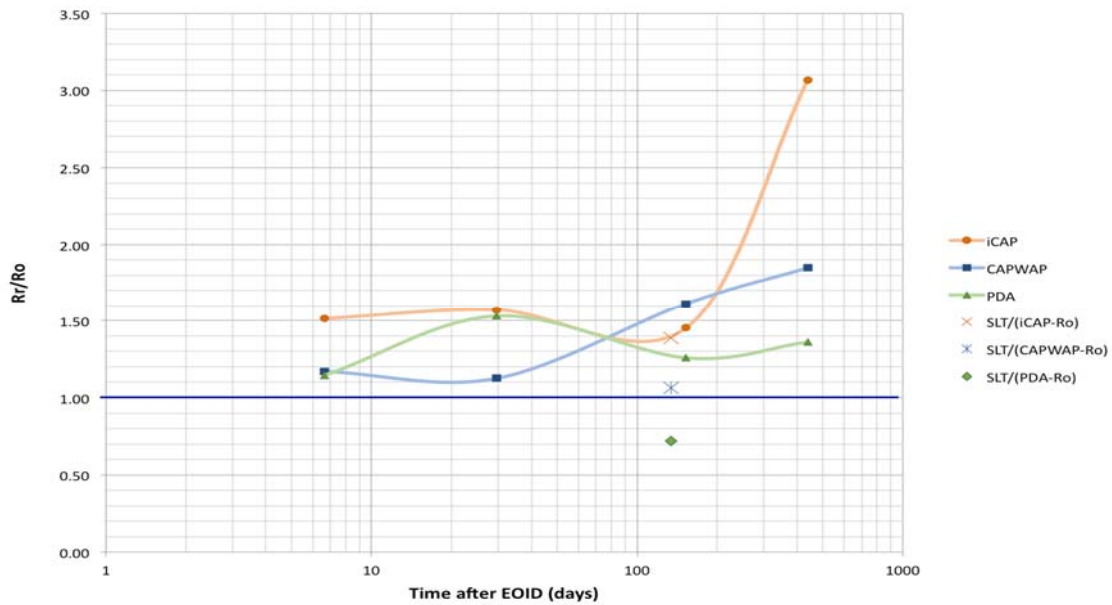


Figure 4.5. Time effect comparison for the ALDOT 12x53 H-pile (Mobile River).

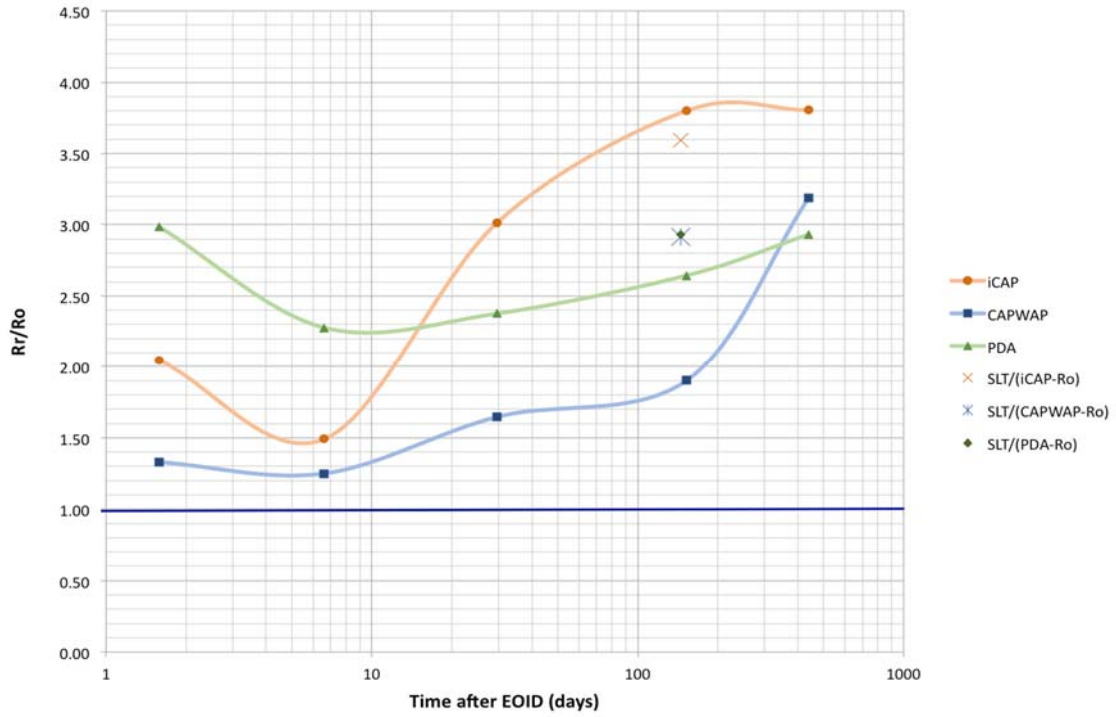


Figure 4.6. Time effect comparison for the ALDOT 14x117 H-pile (Mobile River).

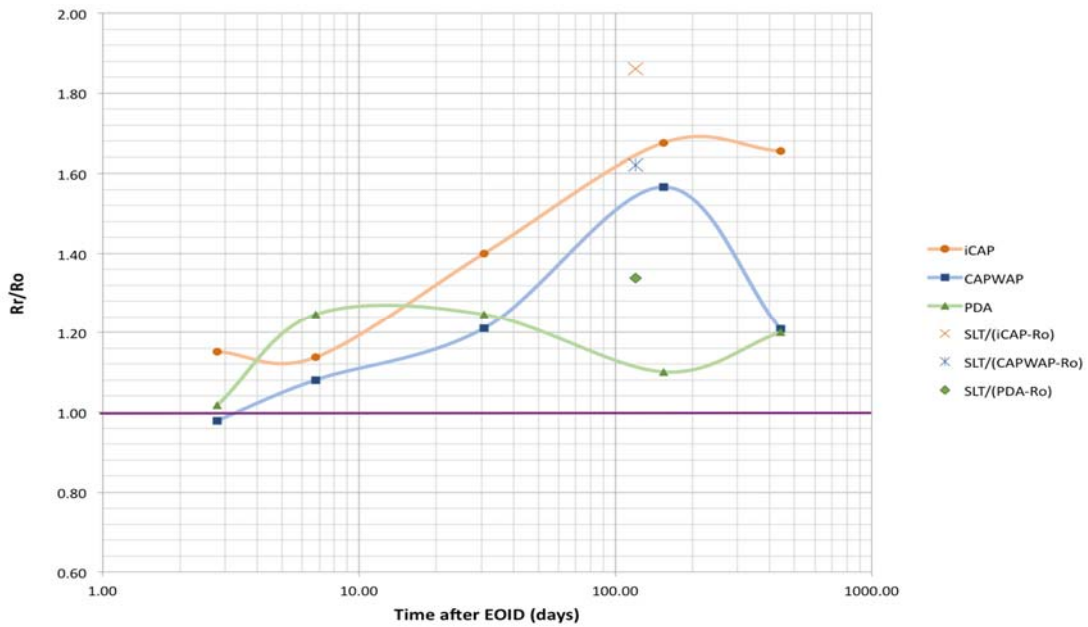


Figure 4.7. Time effect comparison for the ALDOT 24"x24" PPC pile (Mobile River).

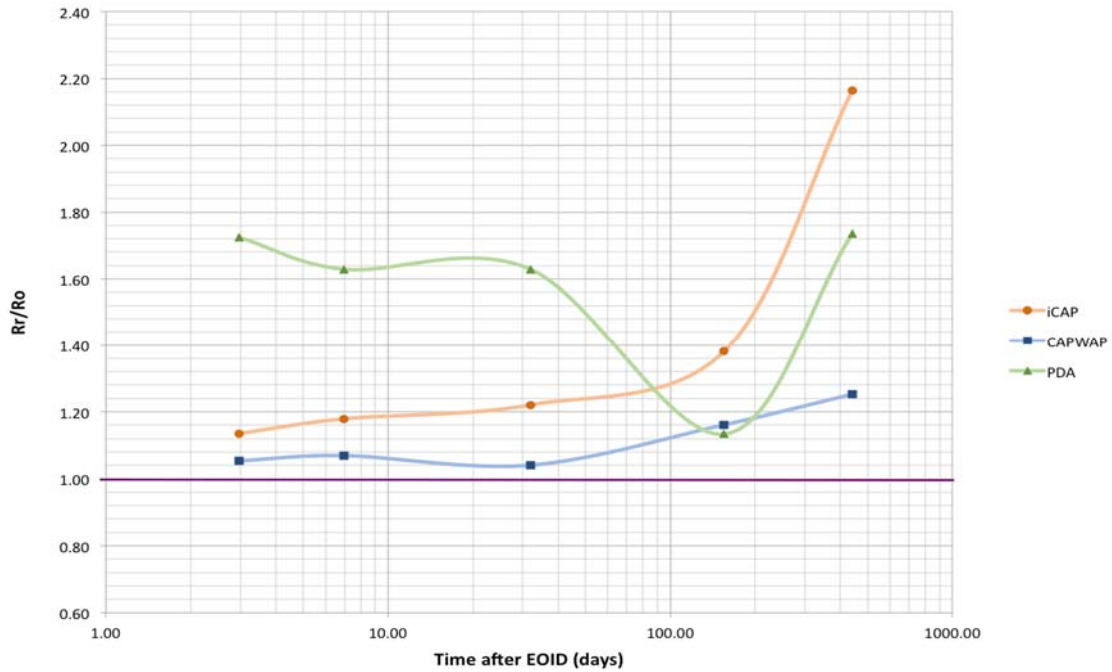


Figure 4.8. Time effect comparison for the ALDOT 36”x36” PPC pile (Mobile River).

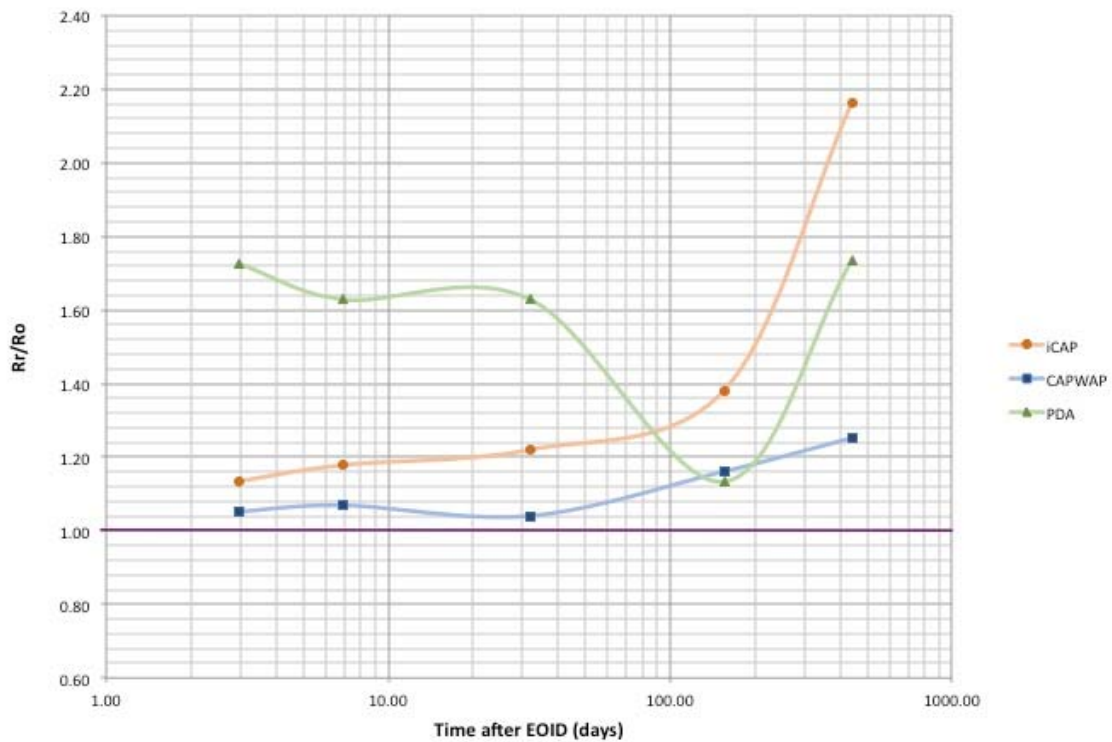


Figure 4.9. Time effect comparison for the ALDOT 14x102 H-pile (Montgomery Outer Loop).

4.2.2 Load Test Results of Steel H-Piles

The number of cases, the average (mean) time effect (R_u / R_o), the standard deviation (Std. Dev.), and coefficient of variation (COV) are shown in Figures 4.10 to 4.27. Figures 4.10, 4.11, and 4.12 illustrate the time effect of the ALDOT H-piles using total pile resistance estimates (iCAP[®], CAPWAP[®], and PDA[®], respectively), including the time effect on total pile resistance at each restrike (R_r). For example, the time effects on total pile resistance at BOR1 to BOR5 for Pile 8 (see Table 4.1) are all included in Figures 4.10 to 4.12.

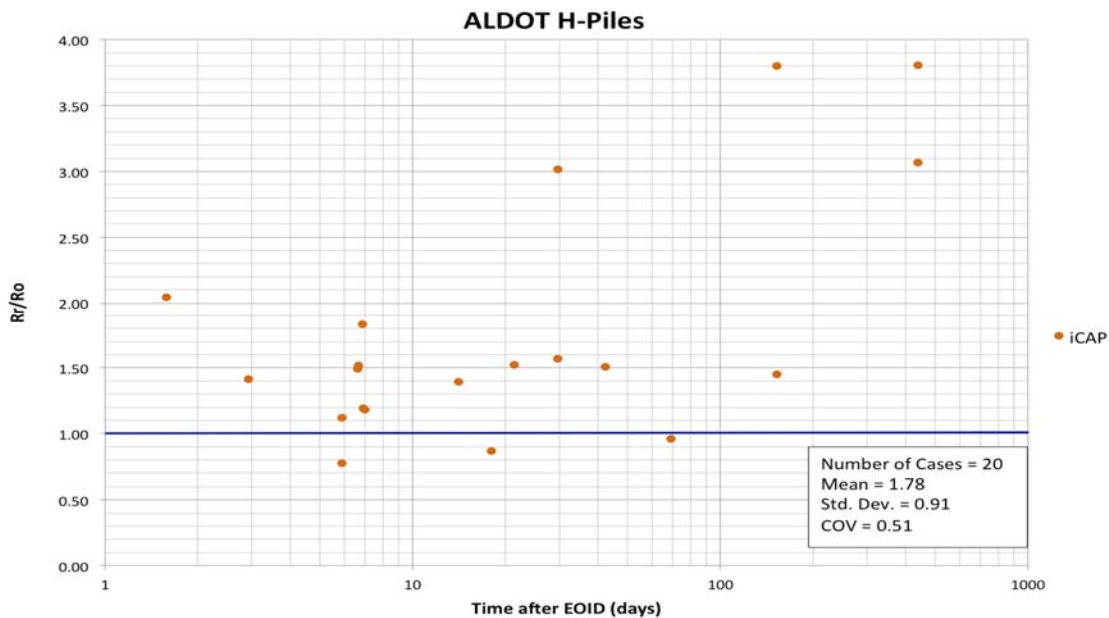


Figure 4.10. Time effect of ALDOT H-piles using iCAP[®] total pile resistance estimates, including the time effect on total pile resistance at each restrike (R_r).

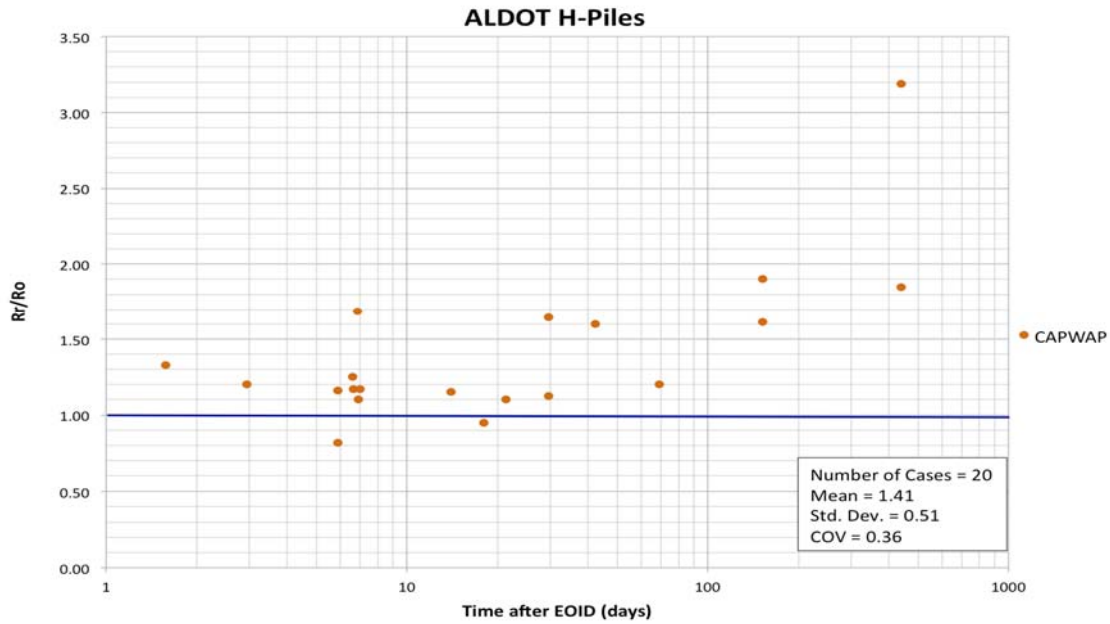


Figure 4.11. Time effect of ALDOT H-piles using CAPWAP® total pile resistance estimates, including the time effect on total pile resistance at each restrike (Rr).

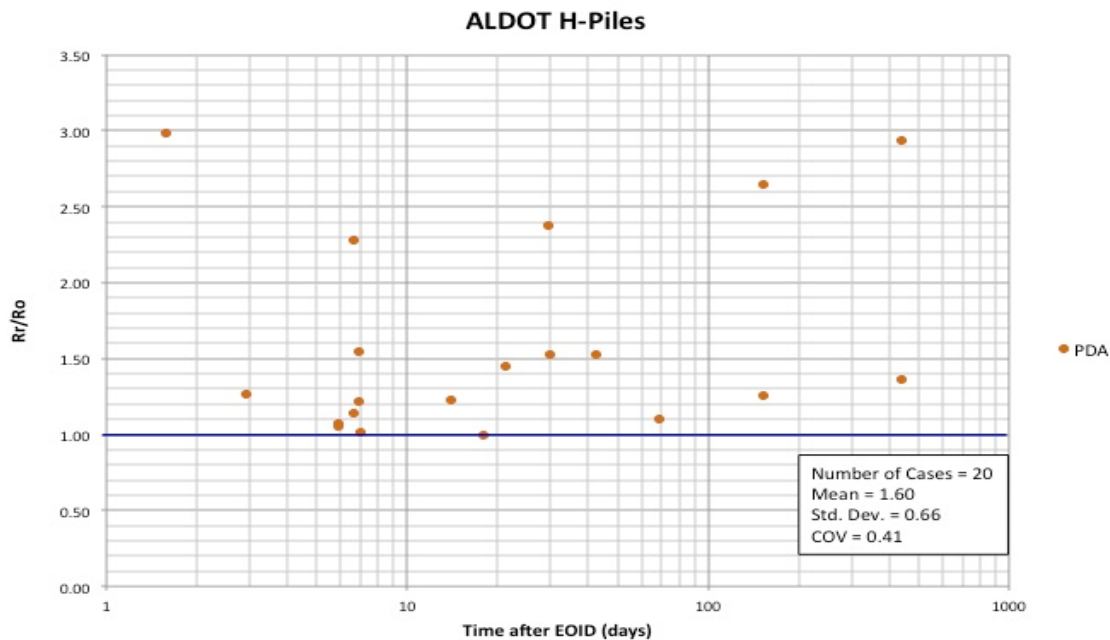


Figure 4.12. Time effect of ALDOT H-piles using PDA® total pile resistance estimates, including the time effect on total pile resistance at each restrike (Rr).

Figures 4.13, 4.14, and 4.15 show the time effect of the ALDOT H-piles using total pile resistance estimates (iCAP[®], CAPWAP[®], and PDA[®], respectively), including only the time effect on total pile resistance at final restrikes (Rf).

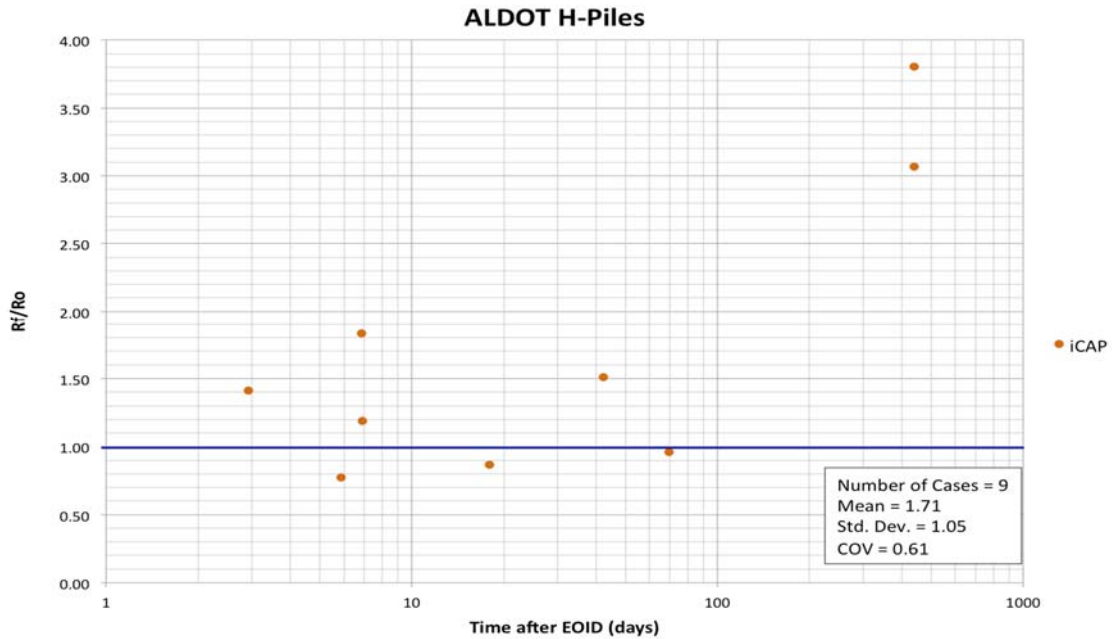


Figure 4.13. Time effect of ALDOT H-piles using iCAP[®] total pile resistance estimates, including only the time effect on total pile resistance at final restrikes (Rf).

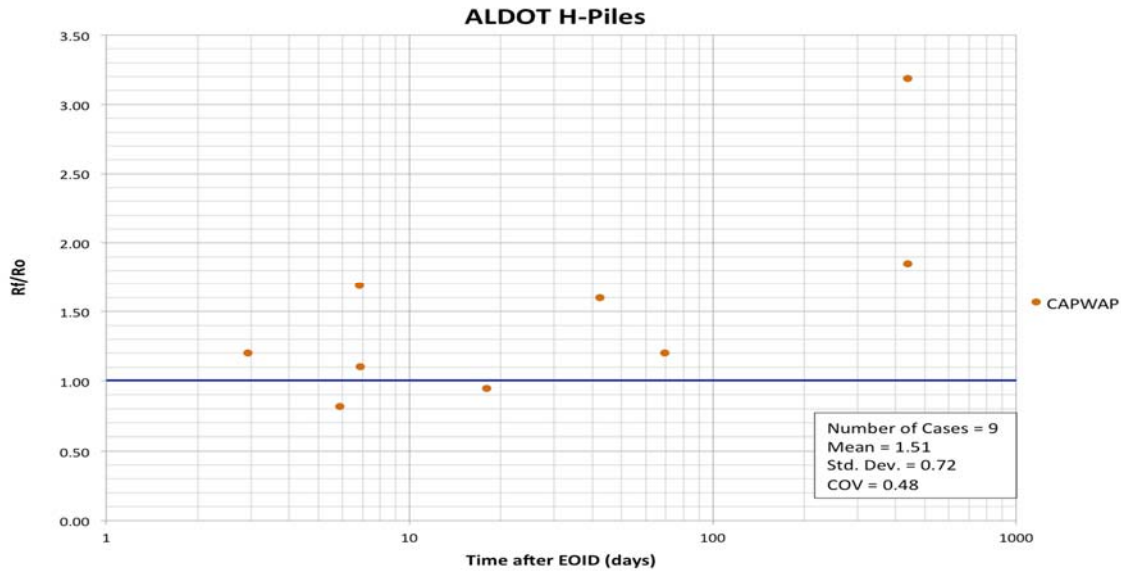


Figure 4.141. Time effect of ALDOT H-piles using CAPWAP[®] total pile resistance estimates, including only the time effect on total pile resistance at final restrikes (Rf).

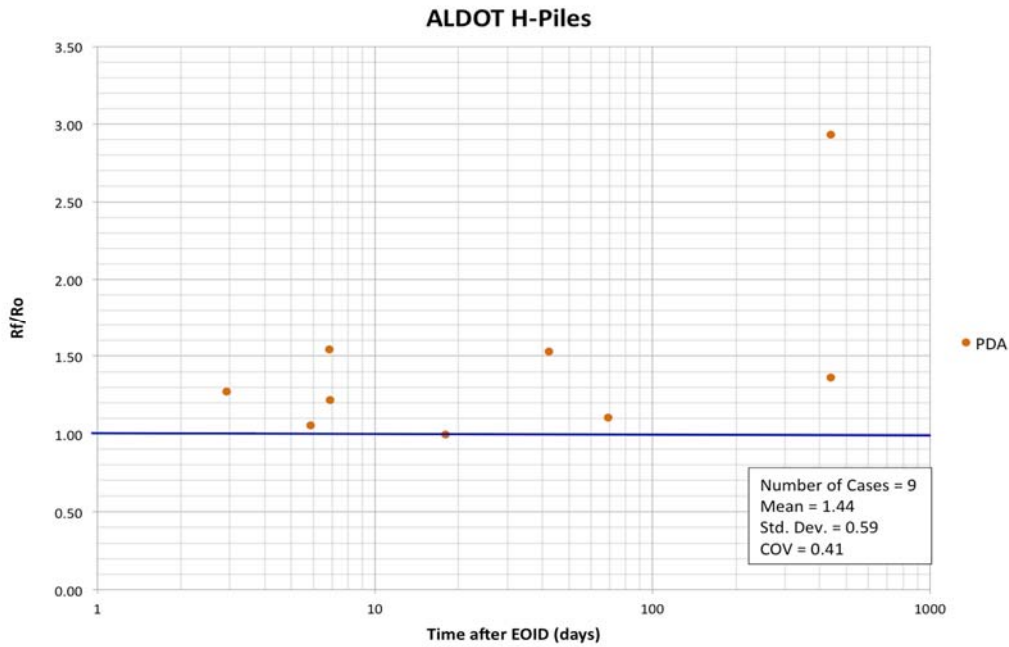


Figure 4.152. Time effect of ALDOT H-piles using PDA[®] total pile resistance estimates, including only the time effect on total pile resistance at final restrikes (Rf).

Figures 4.16, 4.17, and 4.18 show the time effect of the ALDOT H-piles using total pile resistance estimates (iCAP[®], CAPWAP[®], and PDA[®], respectively), including only the time effect on total pile resistance at BOR1 (R1).

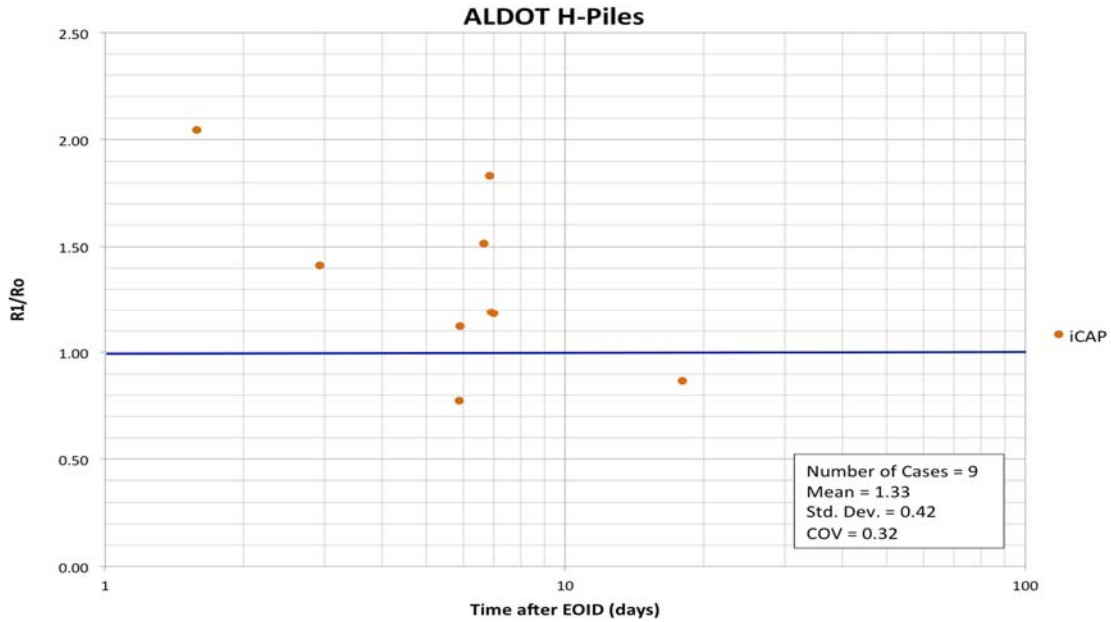


Figure 4.16. Time effect of ALDOT H-piles using iCAP[®] total pile resistance estimates, including only the time effect on total pile resistance at BOR1 (R1).

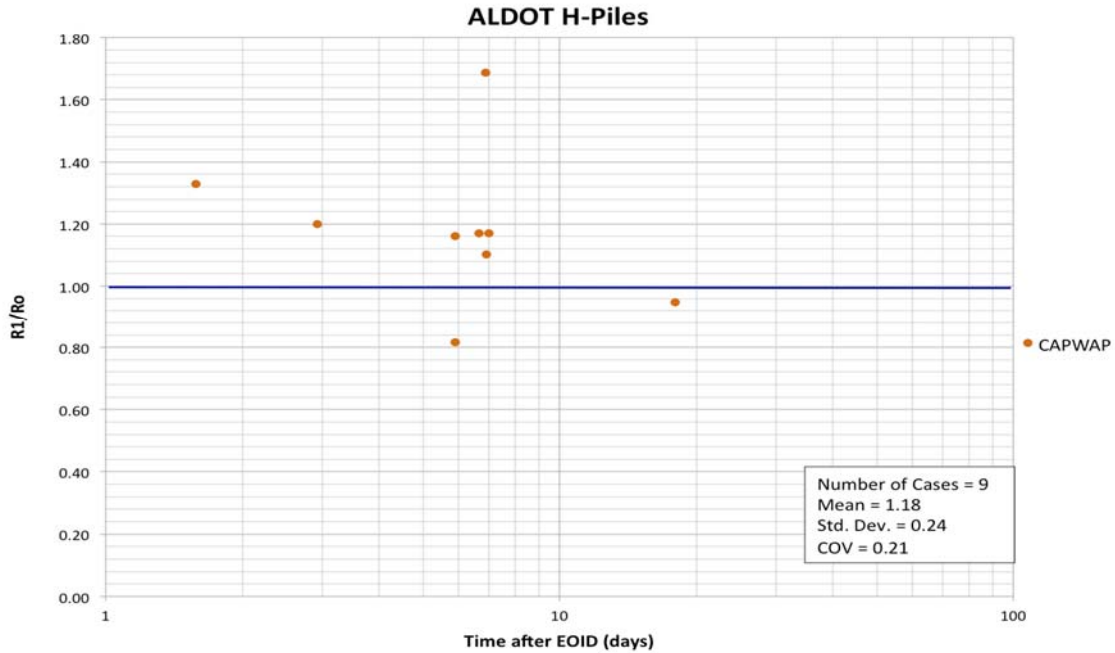


Figure 4.17. Time effect of ALDOT H-piles using CAPWAP[®] total pile resistance estimates, including only the time effect on total pile resistance at BOR1 (R1).

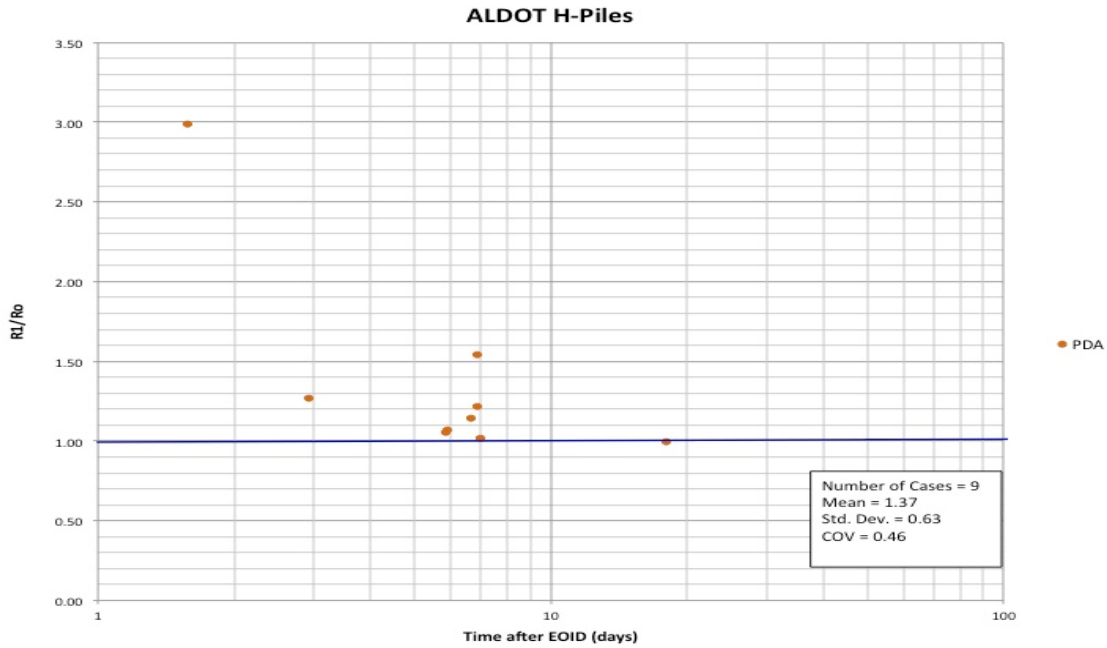


Figure 4.18. Time effect of ALDOT H-piles using PDA[®] total pile resistance estimates, including only the time effect on total pile resistance at BOR1 (R1).

4.2.3 Load Test Results of Concrete Piles

Figures 4.19, 4.20, and 4.21 illustrate the time effect of the ALDOT PPC piles using total pile resistance estimates (iCAP[®], CAPWAP[®], and PDA[®], respectively), including the time effect on total pile resistance at each restrike (Rr).

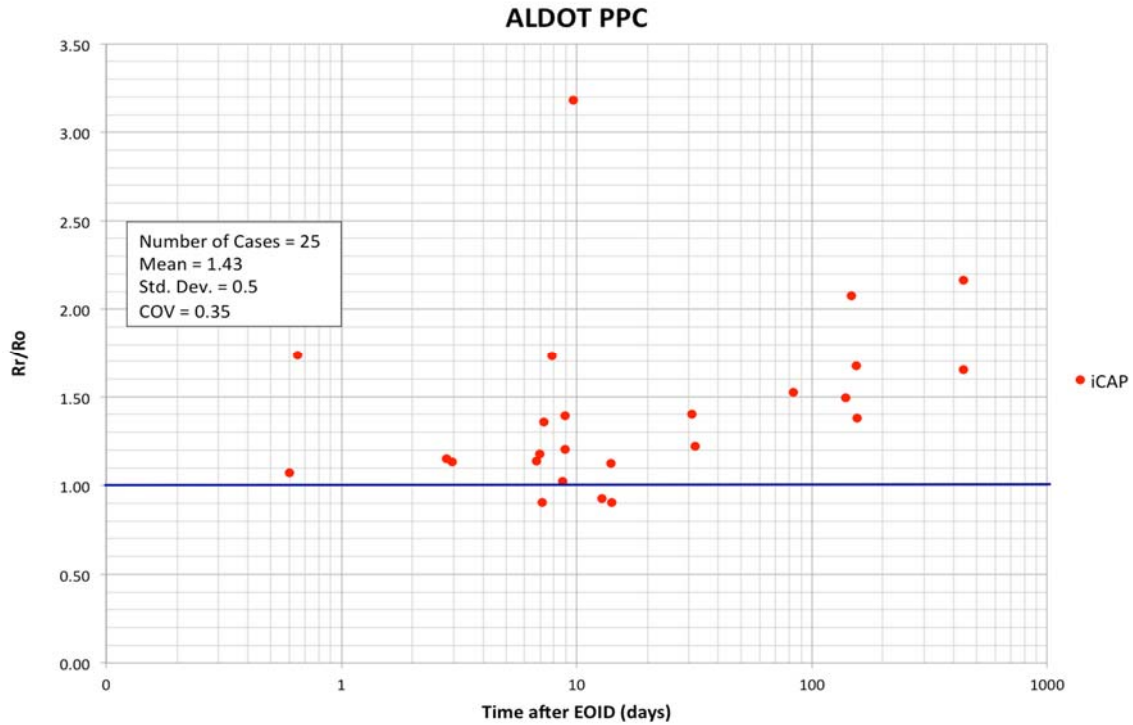


Figure 4.19. Time effect of ALDOT PPC piles using iCAP[®] total pile resistance estimates, including the time effect on total pile resistance at each restrike (Rr).

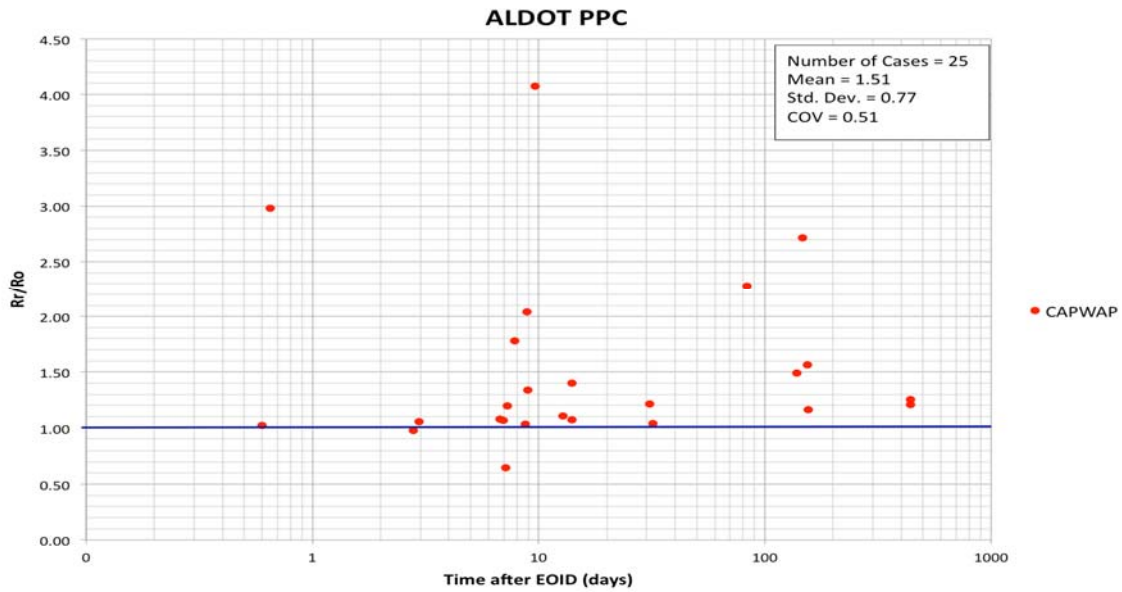


Figure 4.20. Time effect of ALDOT PPC piles using CAPWAP[®] total pile resistance estimates, including the time effect on total pile resistance at each restrrike (Rr).

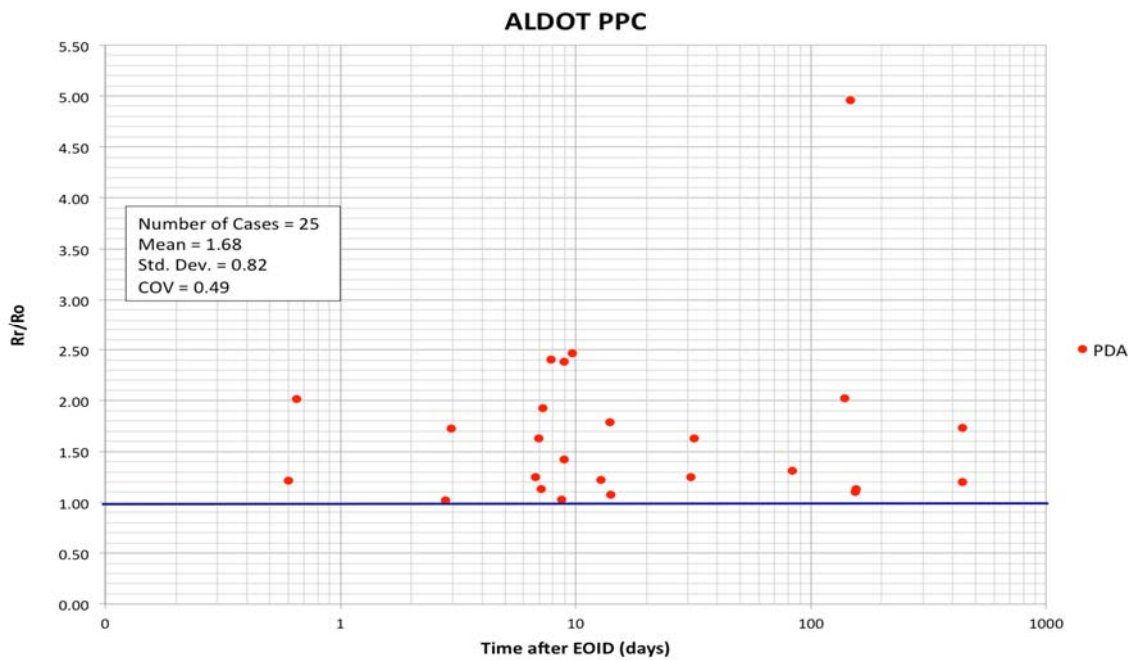


Figure 4.21. Time effect of ALDOT PPC piles using PDA[®] total pile resistance estimates, including the time effect on total pile resistance at each restrrike (Rr).

Figures 4.22, 4.23, and 4.24 show the time effect of the ALDOT PPC piles using total pile resistance estimates (iCAP[®], CAPWAP[®], and PDA[®], respectively), including only the time effect on total pile resistance at final restrikes (Rf).

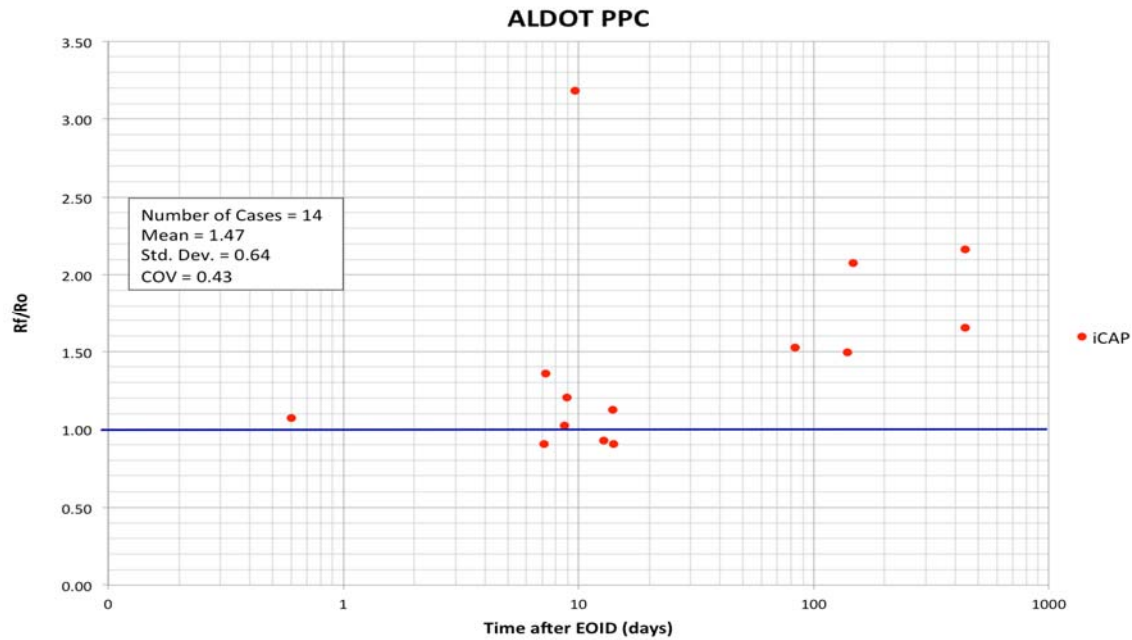


Figure 4.22. Time effect of ALDOT PPC piles using iCAP[®] total pile resistance estimates, including only the time effect on total pile resistance at final restrikes (Rf).

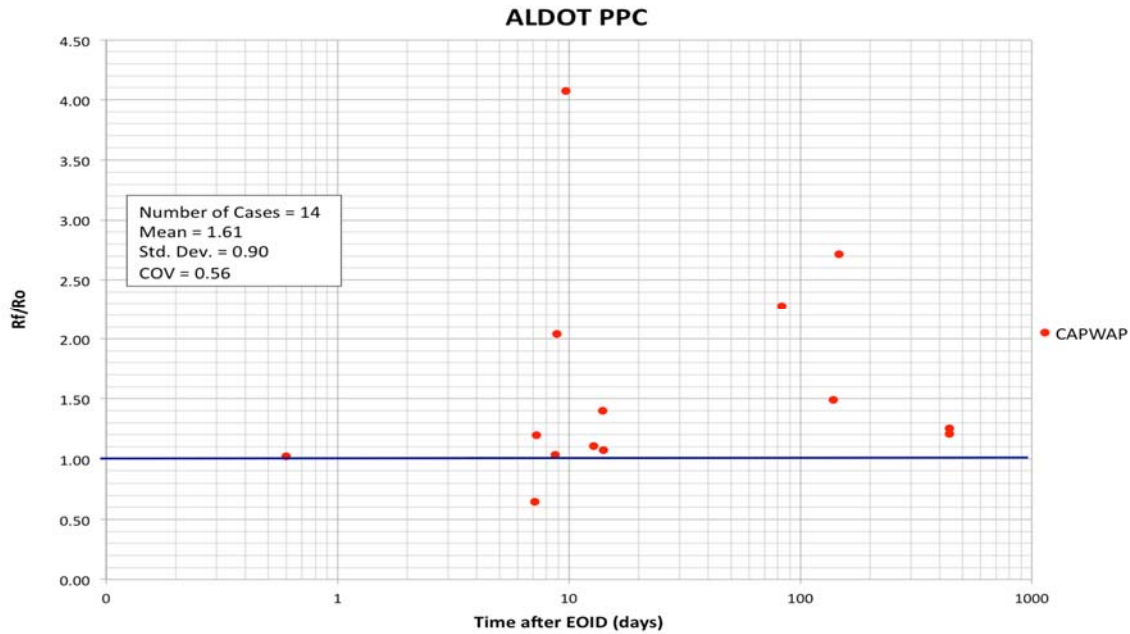


Figure 4.23. Time effect of ALDOT PPC piles using CAPWAP[®] total pile resistance estimates, including only the time effect on total pile resistance at final restrikes (Rf).

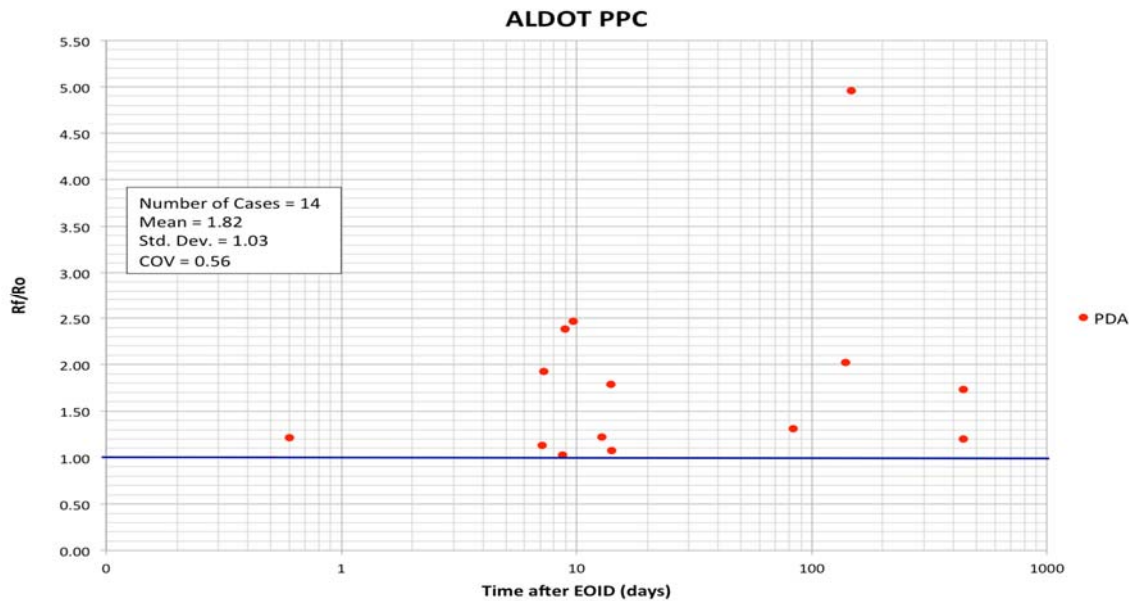


Figure 4.24. Time effect of ALDOT PPC piles using PDA[®] total pile resistance estimates, including only the time effect on total pile resistance at final restrikes (Rf).

Figures 4.25, 4.26, and 4.27 show the time effect of the ALDOT PPC piles using total pile resistance estimates (iCAP[®], CAPWAP[®], and PDA[®], respectively), including only the time effect on total pile resistance at BOR1.

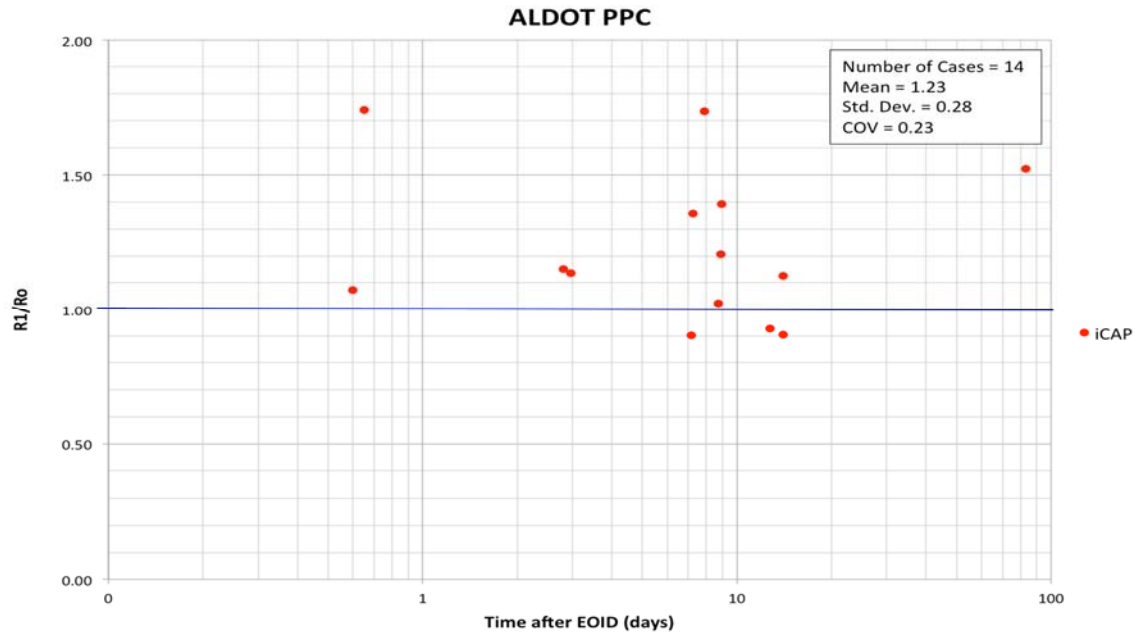


Figure 4.25. Time effect of ALDOT PPC piles using iCAP[®] total pile resistance estimates, including only the time effect on total pile resistance at BOR1 (R1).

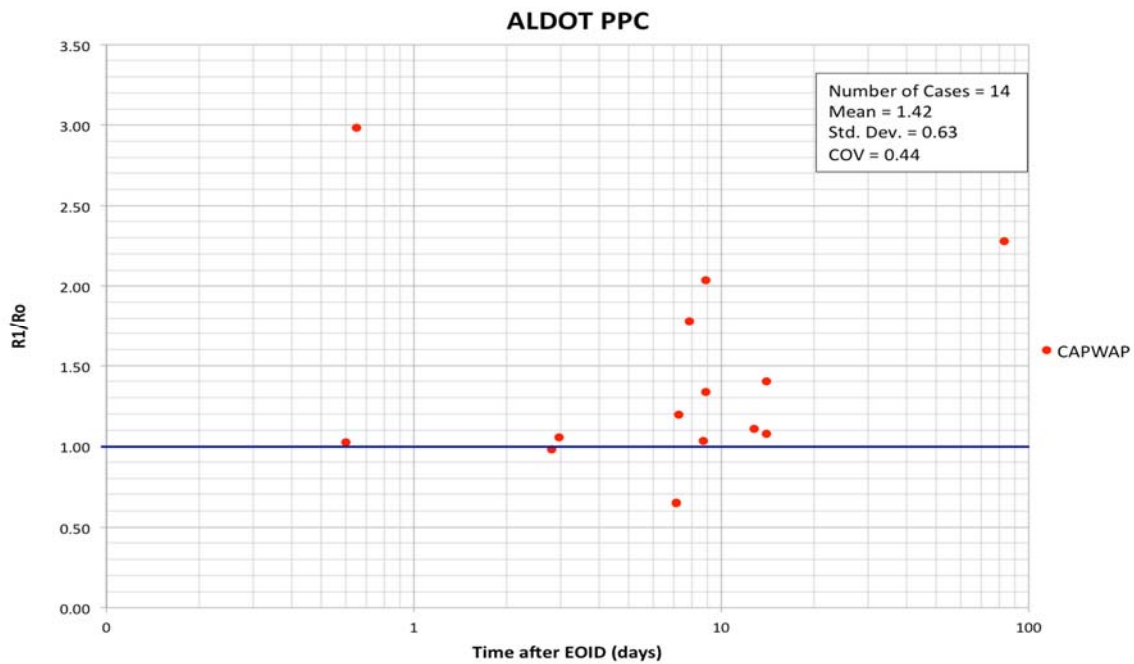


Figure 4.26. Time effect of ALDOT PPC piles using CAPWAP[®] total pile resistance estimates, including only the time effect on total pile resistance at BOR1 (R1).

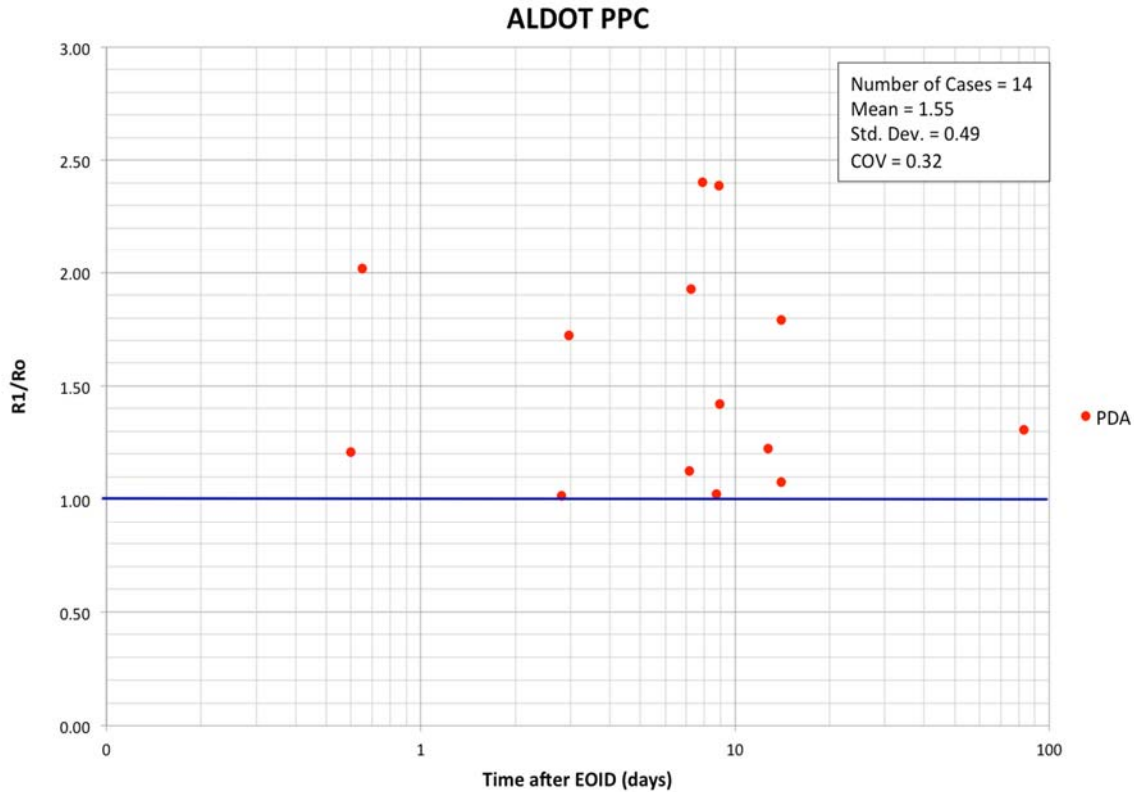


Figure 4.27. Time effect of ALDOT PPC piles using PDA[®] total pile resistance estimates, including only the time effect on total pile resistance at BOR1 (R1).

4.2.4 Load Test Results Comparison of iCAP with CAPWAP and PDA

The total pile resistance estimates using Full iCAP[®] analysis were compared to the CAPWAP[®] and PDA[®] analysis for each test pile (including PPC and H-piles), and these comparisons are plotted for various blow types (EOID, set-check, and BOR) as shown in Figures 4.28 and 4.29, respectively. A set-check is a term used to describe a restrrike that is usually performed within an hour of EOID.

The number of cases, the average (mean) of total pile resistance (R_u / R_u), the standard deviation (Std. Dev.), and coefficient of variation (COV) are also shown in Figures 4.28 to 4.35.

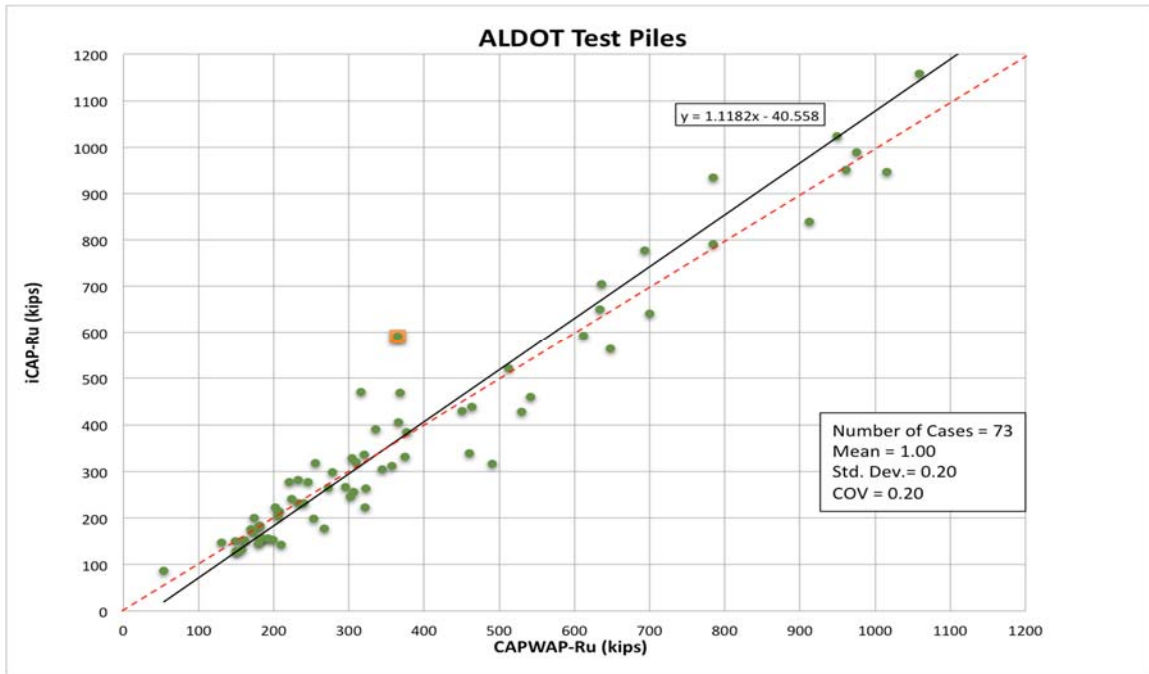


Figure 4.28. Total pile resistance estimation comparison for the ALDOT test piles (PPC and H-piles): Full iCAP[®] vs. CAPWAP[®].

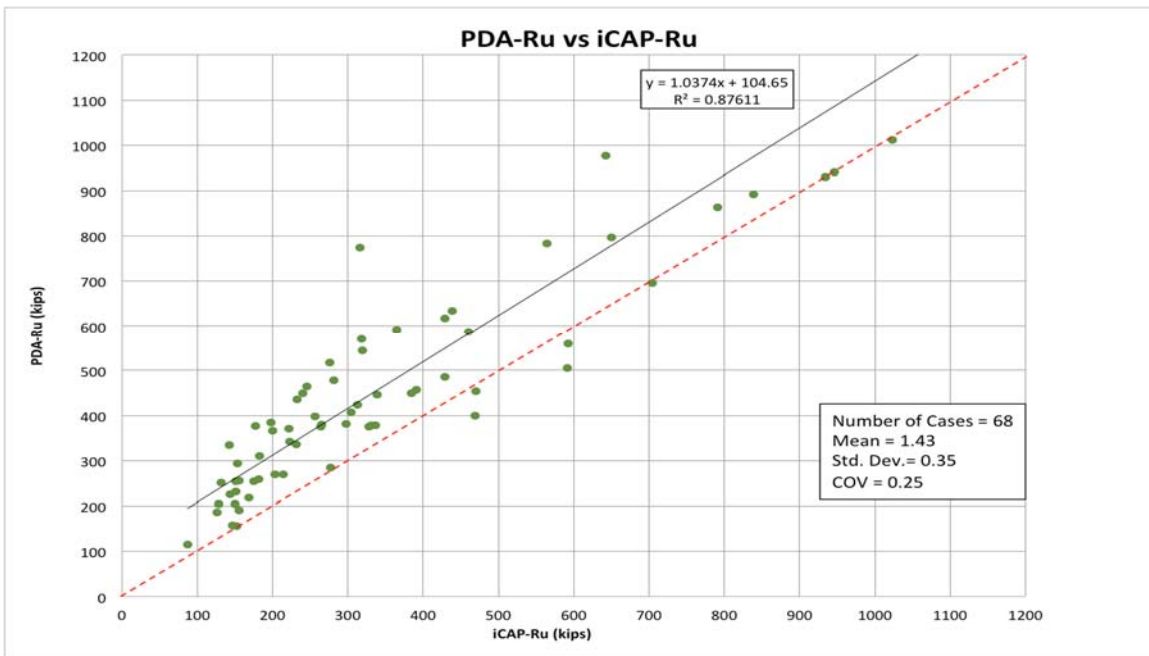


Figure 4.29. Total pile resistance estimation comparison for the ALDOT test piles (PPC and H-piles): PDA[®] vs. Full iCAP[®].

The total pile resistance estimates using Full iCAP[®] analysis were compared to the CAPWAP[®] analysis for each pile type. The comparisons for the H-piles and PPC piles are shown in Figures 4.30 and 4.31, respectively.

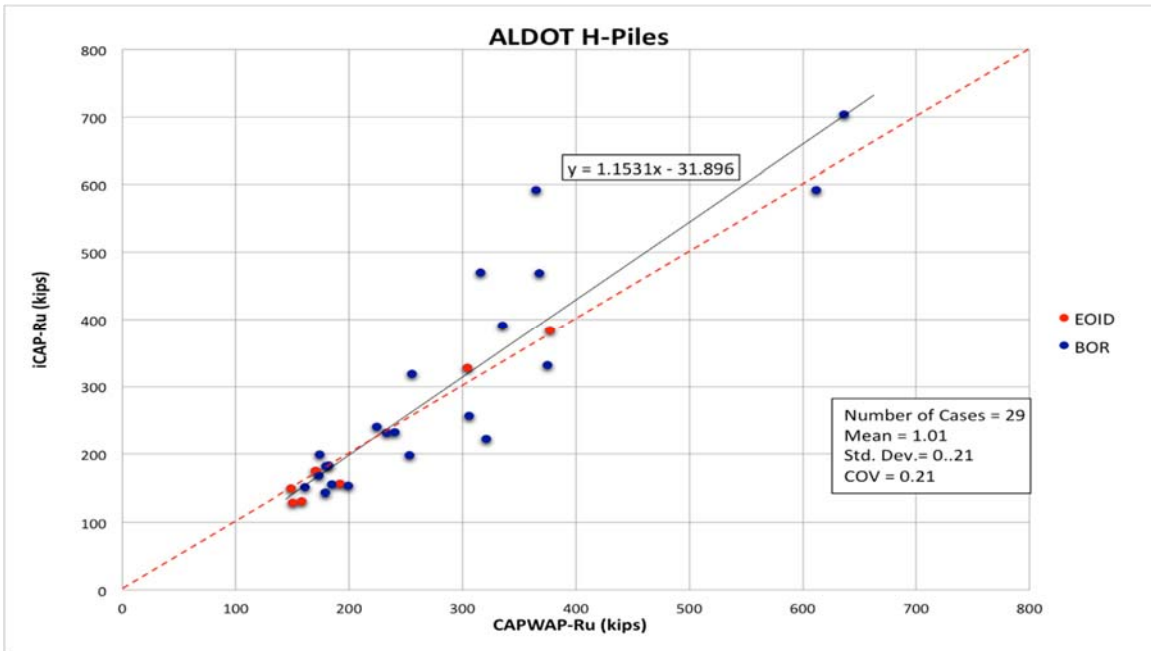


Figure 4.30. Total pile resistance estimation comparison for the ALDOT H-piles: Full iCAP® vs. CAPWAP®.

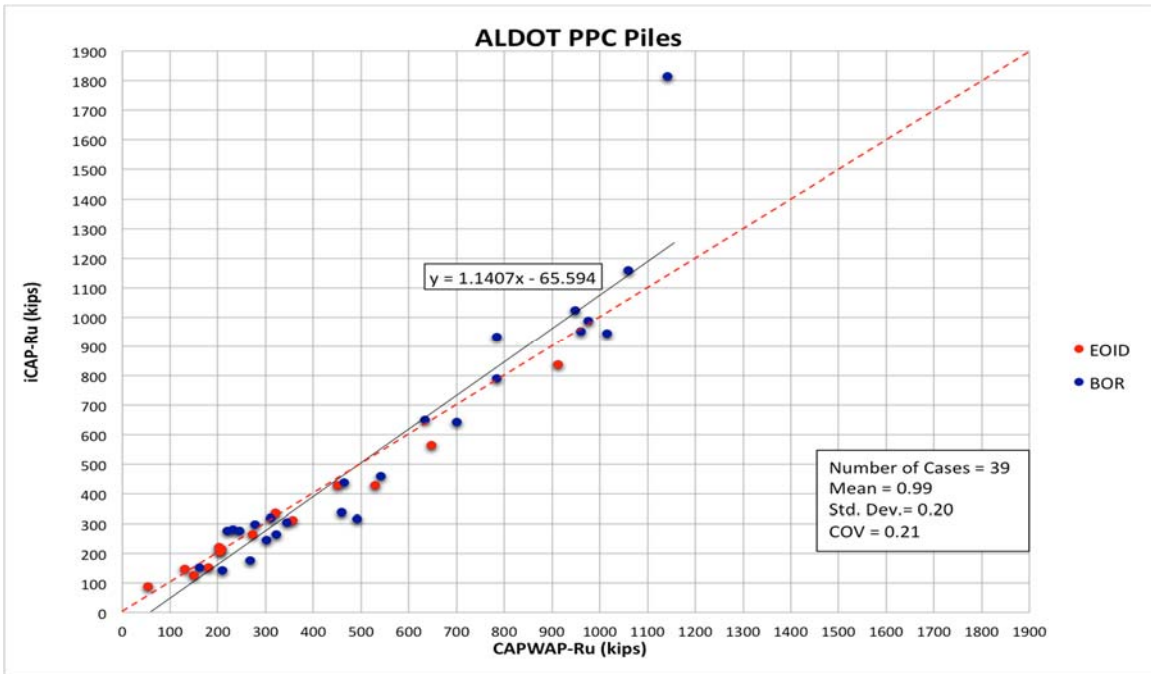


Figure 4.31. Total pile resistance estimation comparison for the ALDOT PPC piles: Full iCAP® vs. CAPWAP®.

The total pile resistance estimates using Full iCAP[®] analysis were compared to the PDA[®] analysis for each pile type. The comparisons for the H-piles and PPC piles are shown in Figures 4.32 and 4.33, respectively.

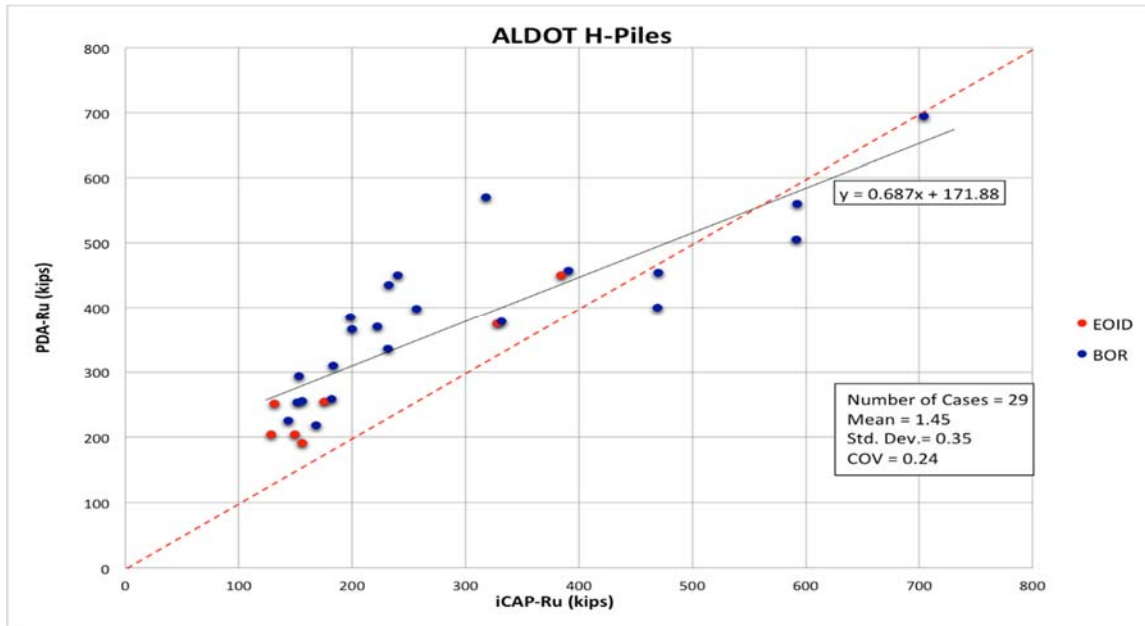


Figure 4.32. Total pile resistance estimation comparison for the ALDOT H-piles: PDA[®] vs. Full iCAP[®].

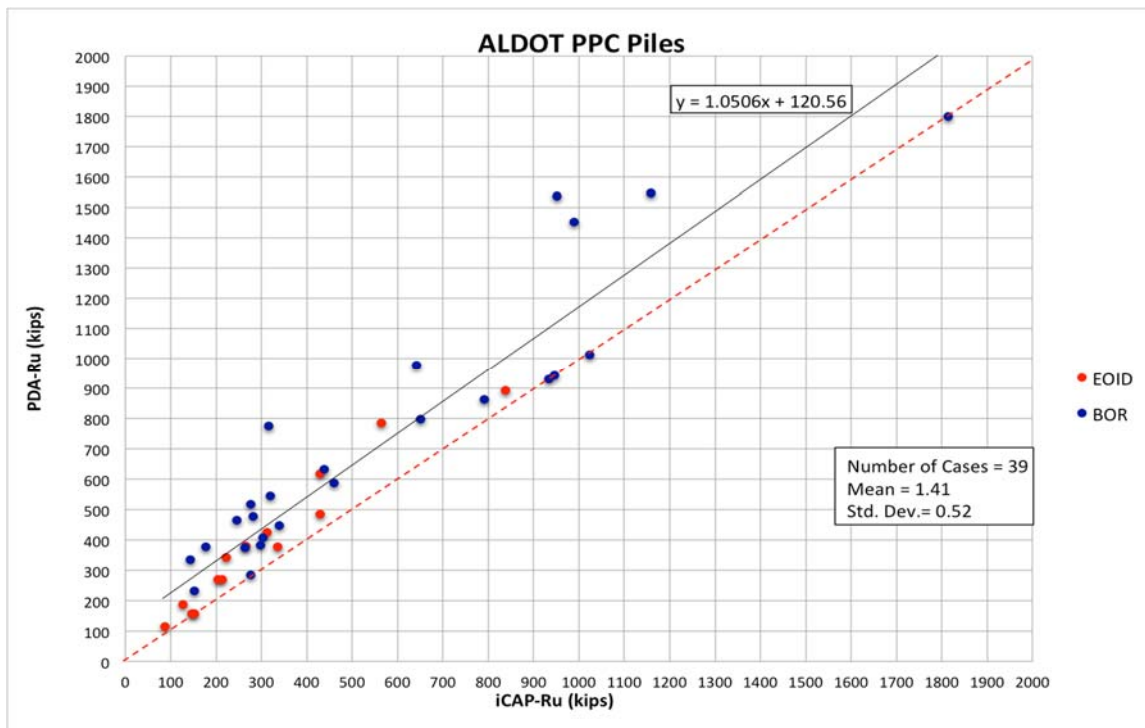


Figure 4.333. Total pile resistance estimation comparison for the ALDOT PPC piles: PDA[®] vs. Full iCAP[®].

The total pile resistance estimates using CAPWAP[®] analysis were compared to the PDA[®] analysis for each pile type. The comparisons for the H-piles and PPC piles are shown in Figures 4.34 and 4.35, respectively.

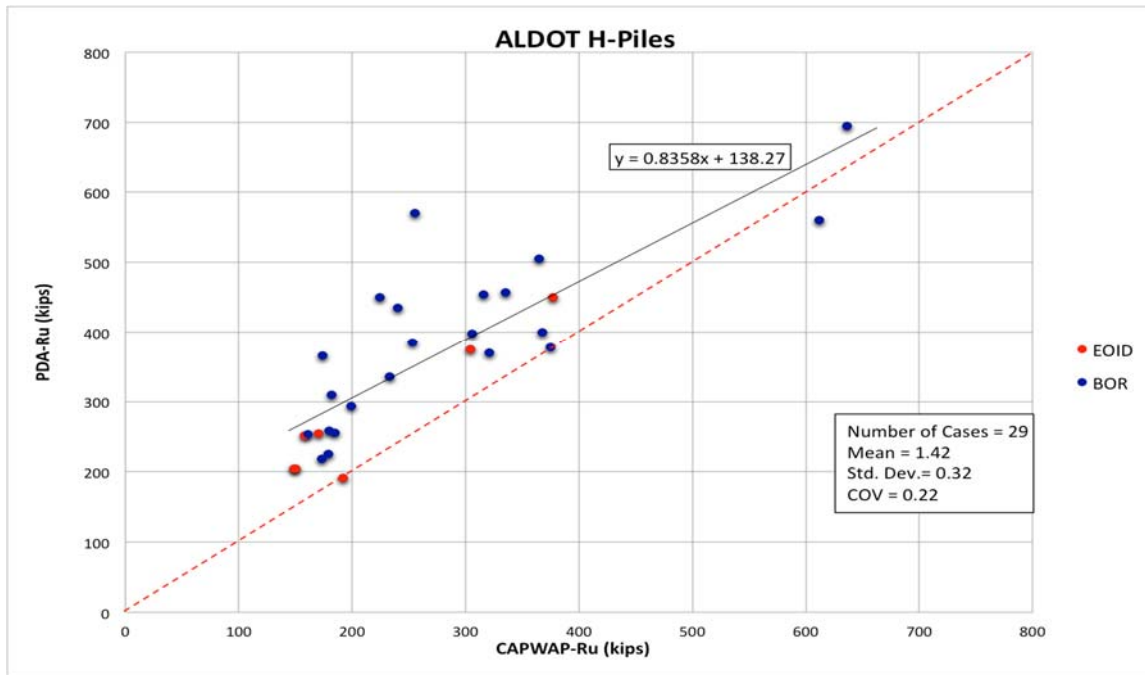


Figure 4.34. Total pile resistance estimation comparison for the ALDOT H-piles: PDA[®] vs. CAPWAP[®].

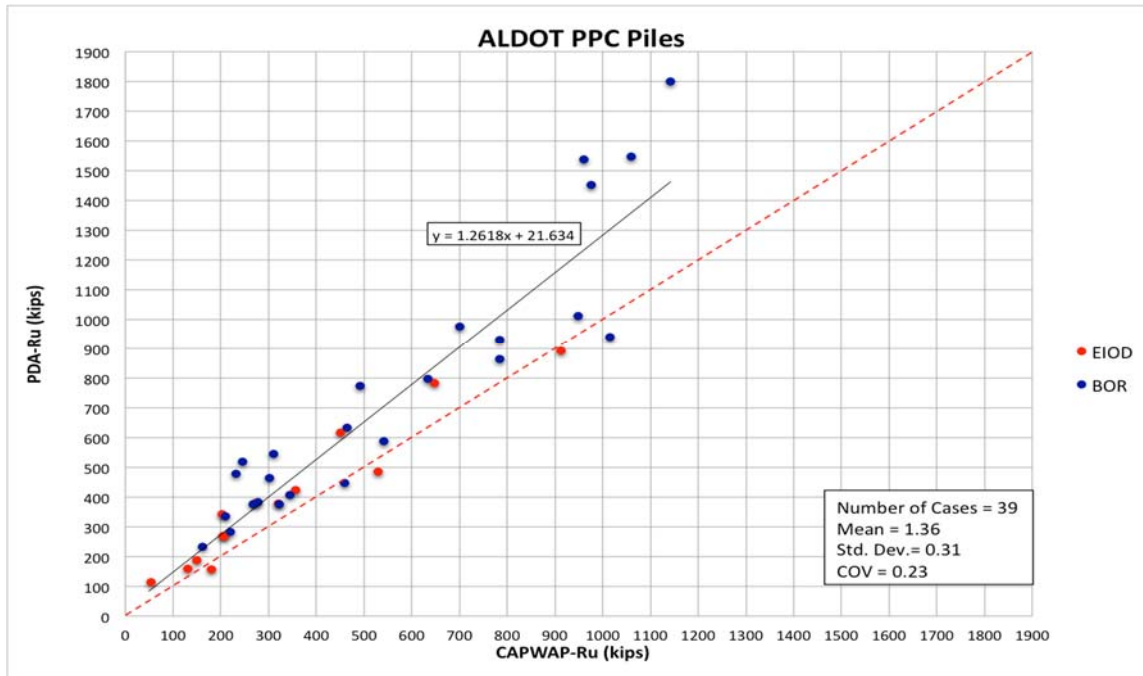


Figure 4.35. Total pile resistance estimation comparison for the ALDOT PPC piles: PDA[®] vs. CAPWAP[®].

The results indicate that the PDA[®] total resistance estimates are larger than the iCAP[®] total resistance estimates by an average of 26% for H-piles and 25% for PPC piles. The PDA[®] total resistance estimates are also larger than the CAPWAP[®] total resistance estimates by an average of 26% for H-piles and 23% for PPC piles. The iCAP[®] total resistance estimates match well with the CAPWAP[®] estimates (see Figures 4.30 to 4.31).

CHAPTER 5– REGIONAL CALIBRATION OF RESISTANCE FACTOR AT THE END OF THE INITIAL PILE DRIVING

In order to develop a LRFD resistance factor utilizing reliability theory, a database of local data is required to be analyzed. Historical data was collected from 27 piles driven and monitored within the state of Alabama between 2009 and 2014. All 27 piles were utilized in the LRFD resistance factor calibration to provide a more accurate statistical analysis. Data will be statistically processed and outliers will be removed, if necessary. Soil borings were also collected for each site, and were used to classify the piles by type of soil encountered. Soil characterization was also utilized for the design of driven piles. The state of Alabama developed a software which uses static capacity analysis as part of pile design known as WBUZPILE. ALDOT also uses dynamic load test analysis to determine the ultimate pile resistance, as well as to monitor the performance of the piles, in the field. Dynamic load test data was collected at end of driving (EOD) and at beginning of restrike (BOR) utilizing Pile Driving Analyzer and then analyzed by signal matching program Case Pile Wave Analysis Program (CAPWAP) to determine pile resistances. The results of the WBUZPILE and CAPWAP analysis are fundamental to the development of LRFD resistance factors utilizing FOSM in the state of Alabama because these results provide the predicted and measured total capacities of each pile.

5.1 Predicted Pile Capacity using WBUZPILE Software

The WBUZPILE software is a computer program developed and utilized by ALDOT to analyze piles under axial loads in the design process. WBUZPILE takes the input of a soil profile, such as SPT corrected blow count, ground water table, pile type, pile dimension, elevation of ground surface, etc, to create a table and plot of the pile capacity throughout various depths. This plot provides ultimate pile capacity (R_u), pile tip resistance (R_t) and shaft resistance (R_s) throughout the depth. The software analysis allows for the utilization of the LRFD approach which is incorporated into factored axial capacities by a resistance factor of 0.71. WBUZPILE uses 0.71 for the LRFD resistance factor which is calculated by calibration by fitting of ASD using DL/LL and FS of 2, based on commonly used values recommended by ALDOT (Ashour, et al. 2012). Based on the pile dimensions and pile type, the foundation designer selects the

maximum factored design load provided for a specific pile dimension and material obtained from the ALDOT Structural Design Manual (ALDOT, 2015). The design capacity is divided by the LRFD resistance factor currently used by ALDOT of 0.71. By knowing the required design pile axial capacity for the determined pile specifications, the required pile embedment length and elevation are selected from the corresponding pile axial capacity provided by the plot. This embedment length is used when installing driven piles. Immediately after installation, at end of driving, a dynamic load test is performed in order to assure and assess that the pile provides the capacity predicted by WBUZPILE at the chosen embedment length. Figure 5.1 shows a sample of a typical plot of pile resistances versus depth.

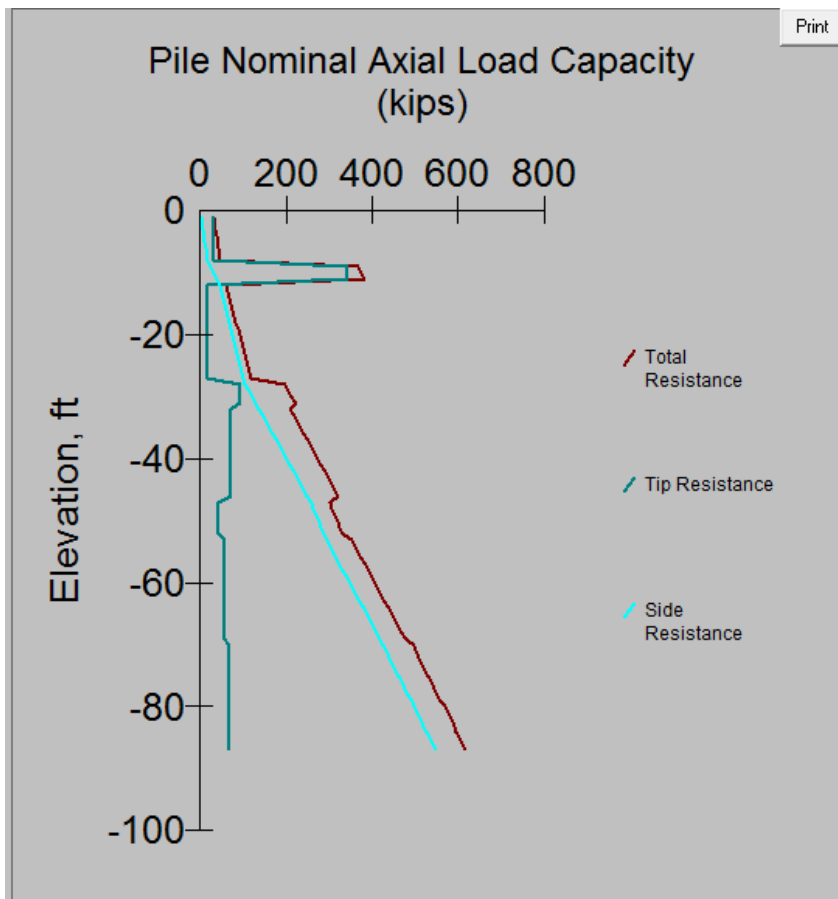


Figure 5.1 Plot of the nominal axial load capacity (Diagram of pile total, tip and side resistance versus depth obtained by WBUZPILE)

WBUZPILE provides an estimate of the ultimate pile capacity or design pile capacity based on embedment length and soil profile. The pile data provided by ALDOT provides the embedment length of a pile and the soil profile. Based on this information, WBUZPILE can be utilized to back estimate the pile axial capacity. The soil and pile information was collected for each of the 27 piles in the ALDOT database to input into the WBUZPILE software. The tip, side, and total resistances of each pile was determined based on the known embedment length and the resistance plot versus depth output of the software. WBUZPILE can be used as a method to predict pile resistance to develop a resistance factor using FOSM reliability theory when incorporated into the calculation of resistance bias factor. While the software can be used with the back-calculated LRFD resistance factor of 0.71, the results can also provide the nominal resistances with no factoring. The FOSM method of determining the resistance bias factors require the unfactored nominal resistances to represent the predicted values. Table 5.1 shows the unfactored tip resistance, shaft resistance, and total resistance of each pile as computed by WBUZPILE.

Table 5.1 Summary of WBUZPILE data for each pile

Pile ID	Pile Type	Pile Dimensions (in)	Embedment Length (ft)	Soil Type	WBUZPILE R-ult (kips)	WBUZPILE R-tip (kips)	WBUZPILE R-Shaft (kips)
1	PSC	30x30	51.8	Mixed	807	541	266
2	PSC	20x20	46	Sand	292	74	219
3	PSC	20x20	61.5	Mixed	423	58	364
4	PSC	20x20	78	Sand	587	47	540
5	HP	10x42	47	Mixed	323	7	316
6	PSC	16x16	50	Sand	341	123	218
7	PSC	20x20	55	Sand	403	85	318
8	PSC	14x14	68	Sand	584	119	465
9	PSC	16x16	55	Mixed	456	140	316
10	PSC	20x20	65	Mixed	856	446	411
11	HP	10x42	53.5	Sand	346	7	339
12	PSC	20x20	66	Mixed	400	75	325
13	PSC	20x20	68	Mixed	489	97	392
14	PSC	20x20	65	Sand	575	148	427
15	PSC	20x20	75	Mixed	422	67	355
16	PSC	14x14	46	Mixed	165	47	117
17	PSC	14x14	65	Mixed	195	11	184
18	HP	12x53	35	Clay	202	22	180

19	HP	14x102	19.8	Clay	113	95	18
20	HP	14x73	25.5	Clay	437	50	387
21	HP	14x73	42	Clay	257	105	152
22	HP	14x73	52	Clay	301	103	198
23	HP	14x73	55	Mixed	383	8	375
24	HP	12x53	62	Sand	351	3	348
25	HP	14x117	102	Mixed	695	18	677
26	PSC	24x24	73.6	Sand	664	88	576
27	PSC	36x37	79.6	Sand	1098	154	944

For each pile recorded in the database, soil borings were analyzed. The pile locations were classified by either sand, clay, or mixed depending on the most predominant soil adjacent to the pile. Adjacent soils that presented 65% or less for either sand or clay were classified as mixed. Those that consisted in 65% and greater of the same soil were considered as the predominant soil.

5.2 Measure Pile Capacity from Processed Load Test Data

Dynamic load test data was collected at EOD and BOR for each restrike time utilizing the results of the Pile Driving Analyzer (PDA). CAPWAP delivered the varying resistances within the pile including ultimate, tip, and unit shaft resistance. Table 5.2 shows the data collected utilizing CAPWAP for measured pile resistances at EOD and BOR in the field. Some of the piles were re-struck more than once and it is shown in Table 5.2 in the column of time by BOR1-BOR5. This data was used to compute the resistance bias factor, which is the ratio of the measured resistance and the predicted (or design) resistance, needed to determine LRFD resistance factor.

Table 5.2 Summary of data collected utilizing CAPWAP

Pile ID	Pile Type	Pile Dimensions (in)	Embedment Length (ft)	Type of Soil	Time	Time from EOD (days)	EOD			BOR		
							R-ult (kips)	R-tip (kips)	R-shaft (kips)	R-ult (kips)	R-tip (kips)	R-shaft (kips)
1	PSC	30x30	51.8	Mixed	BOR1	8	N/A	N/A	N/A	N/A	N/A	N/A
2	PSC	20x20	46.0	Sand	BOR1	1.03	304	130	174	N/A	N/A	N/A
3	PSC	20x20	61.5	Mixed	BOR1	7.1	357	307	51	232	140	92
4	PSC	20x20	78.0	Sand	BOR1	7.9	181	138	43	322	146	175
5	HP	10x42	47.0	Mixed	BOR1	5.9	149	57	92	173	58	115
5	HP	10x42	47.0	Mixed	BOR2	69	149	57	92	179	52	127
6	PSC	16x16	50.0	Sand	BOR1	7.3	205	90	115	245	107	138
7	PSC	20x20	55.0	Sand	BOR1	14	320	219	101	344	229	115
8	PSC	14x14	68.0	Sand	BOR1	6.7	183	62	121	N/A	N/A	N/A
9	PSC	16x16	55.0	Mixed	BOR1	14	150	98	52	210	71	139
10	PSC	20x20	65.0	Mixed	BOR1	8.7	450	370	80	464	302	162
11	HP	10x42	53.5	Sand	BOR1	2.9	150	82	68	180	70	110
12	PSC	20x20	66.0	Mixed	BOR1	83	202	96	106	460	100	460
13	PSC	20x20	68.0	Mixed	BOR1	8.9	208	40	168	278	55	223
13	PSC	20x20	68.0	Mixed	BOR2	139	208	40	168	310	47	263
14	PSC	20x20	65.0	Sand	BOR1	0.6	530	300	230	542	310	232
15	PSC	20x20	75.0	Mixed	BOR1	12.8	273	135	138	302	95	207
16	PSC	14x14	46.0	Mixed	BOR1	8.9	131	65	66	267	65	202
17	PSC	14x14	65.0	Mixed	BOR1	0.7	54	19	35	220	23	133
17	PSC	14x14	65.0	Mixed	BOR1	9.7	54	19	35	161	28	197
18	HP	12x53	35.0	Clay	BOR1	18	170	48	122	161	26	135
19	HP	14x102	19.8	Clay	BOR2	7	158	96	62	182	94	88
19	HP	14x102	19.8	Clay	BOR1	14	158	96	62	185	127	58
19	HP	14x102	19.8	Clay	BOR3	21	158	96	62	174	104	70
19	HP	14x102	19.8	Clay	BOR4	42.3	158	96	62	253	149	104
20	HP	14x73	25.5	Clay	BOR1	0.7	693	499	194	N/A	N/A	N/A
21	HP	14x73	42.0	Clay	BOR1	6.9	377	250	127	636	428	207
22	HP	14x73	52.0	Clay	BOR1	5.9	375	108	267	306	26	280
23	HP	14x73	55	Mixed	BOR1	6.9	304	119	185	335	97	238
24	HP	12x53	62.0	Sand	BOR1	1.5	N/A	N/A	N/A	199	76	123
24	HP	12x53	62.0	Sand	BOR2	7	N/A	N/A	N/A	233	95	137
24	HP	12x53	62.0	Sand	BOR3	30	N/A	N/A	N/A	224	77	147
24	HP	12x53	62.0	Sand	BOR4	123	N/A	N/A	N/A	321	81	240
24	HP	12x53	62.0	Sand	BOR5	420	N/A	N/A	N/A	368	121	247
25	HP	14x117	102.0	Mixed	BOR1	1.5	192	45	147	255	46	209
25	HP	14x117	102.0	Mixed	BOR2	7	192	45	147	612	49	564
25	HP	14x117	102.0	Mixed	BOR3	30	192	45	147	365	45	320
25	HP	14x117	102.0	Mixed	BOR4	123	192	45	147	240	46	194
25	HP	14x117	102.0	Mixed	BOR5	420	192	45	147	316	35	281
26	PSC	24x24	73.6	Sand	BOR1	3	648	330	319	634	240	394
26	PSC	24x24	73.6	Sand	BOR2	7	648	330	319	784	248	536
26	PSC	24x24	73.6	Sand	BOR3	30	648	330	319	1015	321	694
26	PSC	24x24	73.6	Sand	BOR4	123	648	330	319	700	252	448
26	PSC	24x24	73.6	Sand	BOR5	420	648	330	319	785	291	494
27	PSC	36x36	79.6	Sand	BOR1	3	912	309	603	961	341	620
27	PSC	36x36	79.6	Sand	BOR2	7	912	309	603	975	310	665
27	PSC	36x36	79.6	Sand	BOR3	30	912	309	603	949	136	814
27	PSC	36x36	79.6	Sand	BOR4	123	912	309	603	1059	182	877
27	PSC	36x36	79.6	Sand	BOR5	420	912	309	603	1142	233	909

5.3 LRFD Resistance Bias Factors

By utilizing FOSM, resistance bias factors must be computed by comparing predicted and measured pile capacities. The bias factors are utilized in an attempt to eliminate any testing or design bias error that might not be easily identified. Predicted pile capacities were obtained by incorporating current design methods utilized by ALDOT, which includes the WBUZPILE software. The measured data will be the post-processed PDA data acquired in the field and analyzed by the CAPWAP software. Ultimately, the resultant bias factors will provide a dataset that can be used to identify the effectiveness of the current design procedures when compared to the actual measured pile resistances. When the measured capacity is greater than the design or predicted capacity ($R_m > R_p$) by a large amount, the design is considered conservative. However, when the opposite occurs and the design is larger than the measured capacity, ($R_m < R_p$), which creates a resistance bias factor less than one, the safety and integrity of the pile can be a concern.

A resistance bias factor, λ_R , was calculated to accurately utilize the FOSM method in the determination of LRFD resistance factors. The mean, standard deviation and coefficient of variation of the resistance bias factors at EOD were required to be determined to properly utilize the FOSM method of resistance factor calibration. The statistical analysis of the resistance bias factors provides the observation of the performance of pile design method currently used in the state of Alabama with respect to the measured pile capacity data acquired in the field. Because there appears to be a large variation in the performance of piles depending on the type of pile and how these pile materials interact with the encountered soils, multiple resistance bias factors were analyzed.

A resistance bias factor, λ_R , was calculated by dividing the measured ultimate resistance obtained from CAPWAP at EOD by the predicting ultimate resistance or the design resistance obtained from WBUZPILE. It is important to note that the predicted resistance values calculated using the ALDOT design software are unfactored and should not reflect the actual values utilized by ALDOT personnel during the installation of the piles. Table 5.3 shows a summary of resistance bias factors computed at EOD.

Table 5.3 Summary of Resistance Bias Factor

Pile ID	Pile Type	Type of Soil	CAPWAP R-ult (kips) at EOD	WBUZPILE R-ult (kips)	Resistance Bias Factor, λR
1	PSC	Mixed	N/A	807	N/A
2	PSC	Sand	304	292	1.04
3	PSC	Mixed	357	423	0.844
4	PSC	Sand	181	587	0.308
5	HP	Mixed	149	323	0.461
6	PSC	Sand	205	341	0.601
7	PSC	Sand	320	403	0.794
8	PSC	Sand	183	584	0.313
9	PSC	Mixed	150	456	0.329
10	PSC	Mixed	450	856	0.526
11	HP	Sand	150	346	0.434
12	PSC	Mixed	202	400	0.506
13	PSC	Mixed	208	489	0.426
14	PSC	Sand	530	575	0.922
15	PSC	Mixed	273	422	0.647
16	PSC	Mixed	131	165	0.796
17	PSC	Mixed	54	195	0.277
18	HP	Clay	170	202	0.84
19	HP	Clay	158	113	1.402
20	HP	Clay	693	437	1.584
21	HP	Clay	377	257	1.47
22	HP	Clay	375	301	1.246
23	HP	Mixed	304	383	0.794
24	HP	Sand	N/A	351	N/A
25	HP	Sand	192	695	0.276
26	PSC	Sand	648	664	0.976
27	PSC	Sand	912	1098	0.831

A statistical analysis was conducted for the computed resistance bias factors in order to observe any possible outliers within the data. A boxplot was developed for the entire resistance bias factors at EOD. Figure 5.2 shows the boxplot developed for the resistance bias factors at EOD.

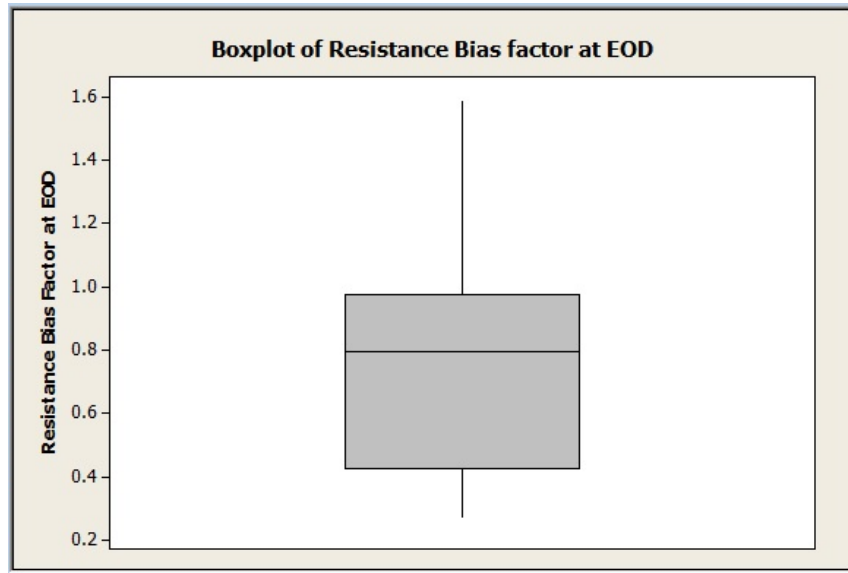


Figure 5.2 Boxplot of Resistance bias factors at EOD calculated by measured/predicted

It can be observed from Figure 5.2 that there was no presence of outliers, and the mean of the resistance bias factor data set is 0.8. It can also be observed that 80% of the resistance bias factors lie below 0.8 and 20% of the resistance bias factor are greater than 0.8. For the statistical analysis of the 25 occurrences of resistance bias factors at EOD required for the determination of the resistance factors, the overall mean is **0.746**, the standard deviation is **0.383**, and the Coefficient of Variation is **0.514**.

Further statistical analysis was conducted to the resistance bias factors based on the type of pile material and the generalized classification of the soils encountered. Piles were classified by pile type and by soil encountered to observe the resistance bias factors with specific conditions and each group's contribution to the overall mean value of resistance bias factors. Table 5.4 shows a summary of the resistance bias factor statistical parameters obtained for each specific pile characterization.

Table 5.4 Summary of Statistical Analysis for resistance bias factor classified by variables

		Mean			S.D.			COV		
		Mixed	Sand	Clay	Mixed	Sand	Clay	Mixed	Sand	Clay
EOD	HP	0.628	0.355	1.308	0.235	0.111	0.289	0.374	0.313	0.221
	PSC	0.544	0.723	-	0.206	0.287	-	0.379	0.397	-

From Table 4.2, the contribution of the different resistance bias factors obtained from classification of the piles by pile type and predominant soil type encountered to the overall resistance bias factor can be observed. Table 4.2 showed that based on pile characterization by pile type and type of soil, only the steel piles installed in clay were higher than the overall resistance bias factor mean value of 0.746. Consequently, the contribution of piles driven in clay affects the overall resistance bias factor to a greater value. At End of Driving, according to Table 4.2, the design capacity is greater than the measured capacity by 37-46% in piles driven into mixed soils, and by 28-65% more for driven piles installed in sands. Also, it was observed that the overall mean value for the entire pile population increased due to the high mean values of steel piles driven into clayey soil, which contributes to the low mean values of other pile characterizations. If the results from clayey soils were to be removed, the mean for sand and mixed soils would be a lower value of 0.61.

5.4 LRFD Resistance Factor Determination

Resistance bias factor and resistance statistical parameters calculated in the previous section are used to compute the LRFD calibrated resistance factors by utilizing First Order Second Moment (FOSM) method. As mentioned in the Literature Review, the FOSM equation is given by

$$\varphi = \frac{\lambda_R(\gamma_{QD}\frac{QD}{QL} + \gamma_{QL}) \sqrt{\frac{1+COV_{QD}^2+COV_{QL}^2}{1+COV_R^2}}}{(\lambda_{QD}\frac{QD}{QL} + \lambda_{QL}) \exp\left\{\beta_T \ln\left(\frac{1+COV_R^2}{1+COV_{QD}^2+COV_{QL}^2}\right)\right\}}, \quad (2.18)$$

where load and resistance uncertainties are incorporated. The load uncertainties to be used were recommended by Paikowsky et al (2004), and the resistance uncertainties are accounted by utilizing FOSM method. Resistance factors were computed for the overall sample population as well as for each pile classification, such as pile type and embedment soils encountered. A value

of 2 was utilized for dead to live load ratio, which is recommended by ALDOT for driven pile design (Ashour et al., 2012). Reliability indices of β 2.33 and 3.0 were used based on recommendations made by Paikowsky et al. (2004), as previously mentioned in chapter 2. The overall resistance factor at EOD by utilizing FOSM method was computed to be **0.38** for $\beta = 2.33$, and **0.30** for $\beta = 3.0$. Table 5.5 shows the calculated resistance factor for each pile material and soil type combination previously described.

Table 5.5 Summary of Resistance Factors classified by pile material type and surrounding soil type

	Resistance Factor $\beta=2.33$			Resistance Factor $\beta=3.0$		
	Mixed	Sand	Clay	Mixed	Sand	Clay
HP	0.29	0.19	0.83	0.22	0.15	0.67
PSC	0.25	0.32	-	0.19	0.24	-

Table 5.5 shows the computed resistance factor based on pile classification for piles driven within the state of Alabama by utilizing WBUZPILE (design capacity) as the prediction capacity and signal matching CAPWAP as the measured data. It is observed from table 5.4 that piles driven in clay presented a major contribution to the overall mean resistance bias factor. As is expected, the clayey soil shows the largest resistance factor of 0.83. For mixed and sandy soils, resistance factor varied from 0.19 to 0.32, which is considerably smaller than the currently utilized back-calculated value of 0.71.

5.5 Effectiveness of Calibrated Resistance Factors

The calibrated resistance factors as determined using the FOSM method were significantly smaller than the current factor of safety back-calculated resistance factor utilized by ALDOT (Ashour et al. 2012). These small values can be related to the discrepancy between the predicted and the measured capacity values used to determine the resistance bias factors. Table 5.6 was developed to show a statistical comparison between the total factored pile capacities

utilizing the a) the back-calculated resistance factor of 0.71 currently used by ALDOT and b) the new calibrated resistance factors calculated in this report based on the variation of the soil and the pile material. Table 5.6 shows the unfactored predicted capacity and the measured capacity obtained originally from WBUZPILE and CAPWAP, respectively. The Factored R-ult using 0.71 column are the results of the unfactored design capacities factored by 0.71 as is customary when designing driven piles using the LRFD Method. The column of factored ultimate resistances (R-ult) are the factored design capacities using the new resistance factors developed in this study.

Table 5.6 Predicted pile resistance utilizing ALDOT current resistance factor, and new calibrated resistance factors by pile classification

Pil ID	Pile Type	Type of Soil	CAPWAP R-ult (kips) at EOD	Unfactored WBUZPILE R-ult (kips)	Factored R-ult (kips) using 0.71	Calculated ϕ based on pile type	Factored R-ult (kips) using calibrated ϕ	Bias Factor Ratio for $\phi = 0.71$	Bias Factor Ratio for Calculated ϕ	
1	PSC	Mixed	N/A	807	573	N/A	N/A	N/A	N/A	
2	PSC	Sand	304	292	207	0.32	93	1.47	3.25	
3	PSC	Mixed	357	423	300	0.25	106	1.19	3.38	
4	PSC	Sand	181	587	417	0.32	188	0.43	0.96	
5	HP	Mixed	149	323	229	0.29	94	0.65	1.59	
6	PSC	Sand	205	341	242	0.32	109	0.85	1.88	
7	PSC	Sand	320	403	286	0.32	129	1.12	2.48	
8	PSC	Sand	183	584	415	0.32	187	0.44	0.98	
9	PSC	Mixed	150	456	324	0.25	114	0.46	1.32	
10	PSC	Mixed	450	856	608	0.25	214	0.74	2.10	
11	HP	Sand	150	346	246	0.19	66	0.61	2.28	
12	PSC	Mixed	202	400	284	0.25	100	0.71	2.02	
13	PSC	Mixed	208	489	347	0.25	122	0.60	1.70	
14	PSC	Sand	530	575	408	0.32	184	1.30	2.88	
15	PSC	Mixed	273	422	300	0.25	106	0.91	2.59	
16	PSC	Mixed	131	165	117	0.25	41	1.12	3.18	
17	PSC	Mixed	54	195	138	0.25	49	0.39	1.11	
18	HP	Clay	170	202	143	0.83	168	1.19	1.01	
19	HP	Clay	158	113	80	0.83	94	1.97	1.68	
20	HP	Clay	693	437	310	0.83	363	2.23	1.91	
21	HP	Clay	377	257	182	0.83	213	2.07	1.77	
22	HP	Clay	375	301	214	0.83	250	1.75	1.50	
23	HP	Mixed	304	383	272	0.29	111	1.12	2.74	
24	HP	Sand	N/A	351	249	N/A	N/A	N/A	N/A	
25	HP	Sand	192	695	493	0.19	132	0.39	1.45	
26	PSC	Sand	648	664	471	0.32	212	1.37	3.05	
27	PSC	Sand	912	1098	780	0.32	351	1.17	2.60	
								Mean	1.05	2.06
								S.D	0.539	0.752
								COV	0.513	0.366

The two far right columns in table 5.6 provide a ratio between the measured capacity and the factored prediction resistances based on the current resistance factor and the newly calculated resistance factors developed in this study. The overall mean value for the ratio of the back-

calculated factored design capacities and the measured capacities is 1.05 with a standard deviation of 0.54. The ratio of the new resistance factored design capacities and the measured capacities is 2.06, with a standard deviation of 0.75. Boxplots were developed to observe the statistical performance of each resistance factored design ratio, as displayed in figure 5.3.

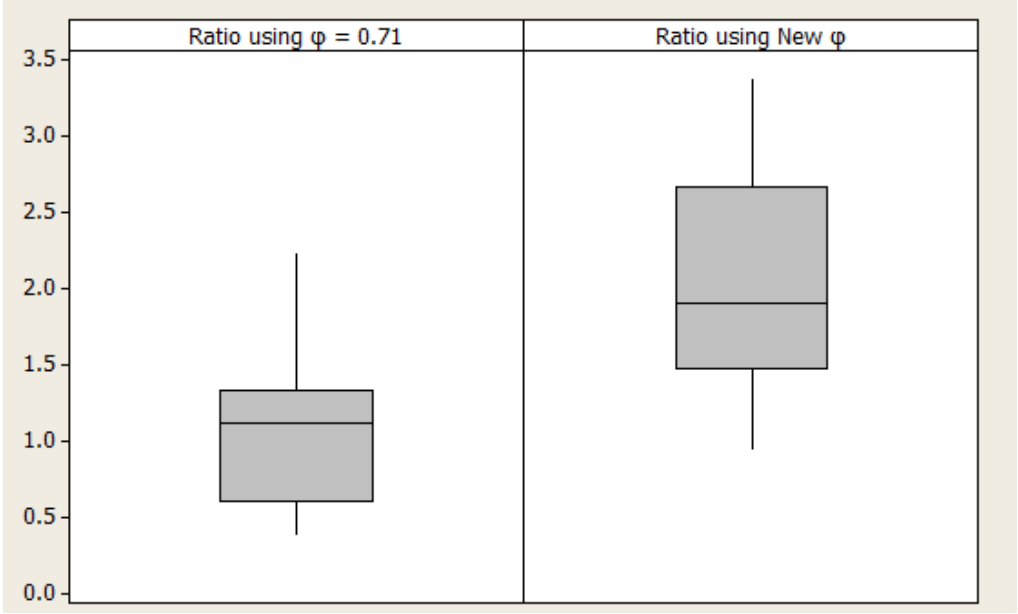


Figure 5.3 Boxplots of the average factored design capacity versus the measured capacity ratios

This combined boxplot shows no outliers within the dataset. Figure 5.3 also indicates that the majority of the ratios are below the average of 1.05 with the current ϕ of 0.71 while the majority of the ratios are larger than the average of 2.06 for the newly generated resistance factored capacities. A comparison between the unfactored design capacities and the measured capacities as provided by figure 5.3 indicate that the measured capacities are lower than design, which is obviously not appropriate. After factoring the design with the current method, the average capacities become very close to equaling the measured loads, however the standard deviation of the ratio comparisons is .054, indicating that half of the allowable design capacities are below the measured loads. Utilizing the new resistance factors generated within this study at first glance shows an overly conservative design approach, the purpose of the LRFD reduction factors is to provide safe design results to a 95% statistical favor.

Additional analysis was conducted to observe the contribution to the newly calculated resistance factors based on pile material type and encountered soils. Table 5.7 through Table 5.11 show the average ratios of each factored capacity versus measured capacities separated into classifications based on pile type and type of soil encountered.

Table 5.7 Comparison between predicted ultimate resistance utilizing 0.71 and new resistance factor for HP piles driven in mixed soils

Pile ID	Pile Type	Type of Soil	CAPWAP R-ult (kips) at EOD	WBUZPILE R-ult (kips)	Factored R-ult (kips) using 0.71	Calculated ϕ depending on pile classification	Factored R-ult (kips)	Bias Resistance factor at 0.71	New Resistance Bias Factor at Calculated ϕ
5	HP	Mixed	149	323	229	0.29	94	0.65	1.59
23	HP	Mixed	304	383	272	0.29	111	1.12	2.74
							Mean	0.884	2.16
							S.D	0.332	0.81
							COV	0.376	0.376

Table 5.8 Comparison between predicted ultimate resistance utilizing 0.71 and new resistance factor for HP piles driven in sandy soils

Pile ID	Pile Type	Type of Soil	CAPWAP R-ult (kips) at EOD	WBUZPILE R-ult (kips)	Factored R-ult (kips) using 0.71	Calculated ϕ depending on pile classification	Factored R-ult (kips)	Bias Resistance factor at 0.71	New Resistance Bias Factor at Calculated ϕ
11	HP	Sand	150	346	246	0.19	66	0.61	2.28
24	HP	Sand	N/A	351	249	N/A	N/A	N/A	N/A
25	HP	Sand	192	695	493	0.19	132	0.39	1.45
							Mean	0.500	1.865
							S.D	0.156	0.59
							COV	0.312	0.315

Table 5.9 Comparison between predicted ultimate resistance utilizing 0.71 and new resistance factor for HP piles driven in clayey soils

Pile ID	Pile Type	Type of Soil	CAPWAP R-ult (kips) at EOD	WBUZPILE R-ult (kips)	Factored R-ult (kips) using 0.71	Calculated ϕ depending on pile classification	Factored R-ult (kips)	Bias Resistance factor at 0.71	New Resistance Bias Factor at Calculated ϕ	
18	HP	Clay	170	202	143	0.83	168	1.19	1.01	
19	HP	Clay	158	113	80	0.83	94	1.97	1.68	
20	HP	Clay	693	437	310	0.83	363	2.23	1.91	
21	HP	Clay	377	257	182	0.83	213	2.07	1.77	
22	HP	Clay	375	301	214	0.83	250	1.75	1.50	
								Mean	1.84	1.58
								S.D	0.404	0.349
								COV	0.219	0.222

Table 5.10 Comparison between predicted ultimate resistance utilizing 0.71 and new resistance factor for PSC piles driven in sandy soils

Pile ID	Pile Type	Type of Soil	CAPWAP R-ult (kips) at EOD	WBUZPILE R-ult (kips)	Factored R-ult (kips) using 0.71	Calculated ϕ depending on pile classification	Factored R-ult (kips)	Bias Resistance factor at 0.71	New Resistance Bias Factor at Calculated ϕ	
2	PSC	Sand	304	292	207	0.32	93	1.47	3.25	
4	PSC	Sand	181	587	417	0.32	188	0.43	0.96	
6	PSC	Sand	205	341	242	0.32	109	0.85	1.88	
7	PSC	Sand	320	403	286	0.32	129	1.12	2.48	
8	PSC	Sand	183	584	415	0.32	187	0.44	0.98	
14	PSC	Sand	530	575	408	0.32	184	1.30	2.88	
26	PSC	Sand	648	664	471	0.32	212	1.37	3.05	
27	PSC	Sand	912	1098	780	0.32	351	1.17	2.60	
								Mean	1.02	2.26
								S.D	0.41	0.90
								COV	0.397	0.396

Table 5.11 Comparison between predicted ultimate resistance utilizing 0.71 and new resistance factor for PSC piles driven in mixed soils

Pile ID	Pile Type	Type of Soil	CAPWAP R-ult (kips) at EOD	WBUZPILE R-ult (kips)	Factored R-ult (kips) using 0.71	Calculated ϕ depending on pile classification	Factored R-ult (kips)	Bias Resistance factor at 0.71	New Resistance Bias Factor at Calculated ϕ
1	PSC	Mixed	N/A	807	573	N/A	N/A	N/A	N/A
3	PSC	Mixed	357	423	300	0.25	106	1.19	3.38
9	PSC	Mixed	150	456	324	0.25	114	0.46	1.32
10	PSC	Mixed	450	856	608	0.25	214	0.74	2.10
12	PSC	Mixed	202	400	284	0.25	100	0.71	2.02
13	PSC	Mixed	208	489	347	0.25	122	0.60	1.70
15	PSC	Mixed	273	422	300	0.25	106	0.91	2.59
16	PSC	Mixed	131	165	117	0.25	41	1.12	3.18
17	PSC	Mixed	54	195	138	0.25	49	0.39	1.11
							Mean	0.77	2.18
							S.D	0.29	0.82
							COV	0.380	0.379

There appears to be a definite trend that the current resistance factor that is back-calculated by ASD Factor of Safety method is producing design capacities that are below the measured data. However, there is not a sufficient amount of data presented to draw significant conclusions from the comparisons of the individual resistance factors developed in this study, as table 5.7 and 5.8 have 2 and 3 data cases, respectively. It is interesting to note that the steel piles embedded into clay have a higher resistance factor than the original design parameters and none of the ratios within this dataset fall below the ratio of 1.

5.6 Discussion of Calibrated LRFD Resistance Factor Results

A statistical analysis has been presented based on the measured resistances obtained by dynamic load test data with predicted resistances developed by WBUZPILE. Using this data, new calibrated resistance factors were developed for driven pile in the state of Alabama. It is important to understand that ALDOT uses WBUZPILE in the design process of driven piles. WBUZPILE is used to select the embedment length of a desired pile based on the varying pile resistances with depth presented by WBUZPILE software. The unfactored and half of the

factored, by currently used resistance factor 0.71, design capacities using the WBUZPILE software tends to be greater than the measured resistances at EOD, as seen in figure 5.4.

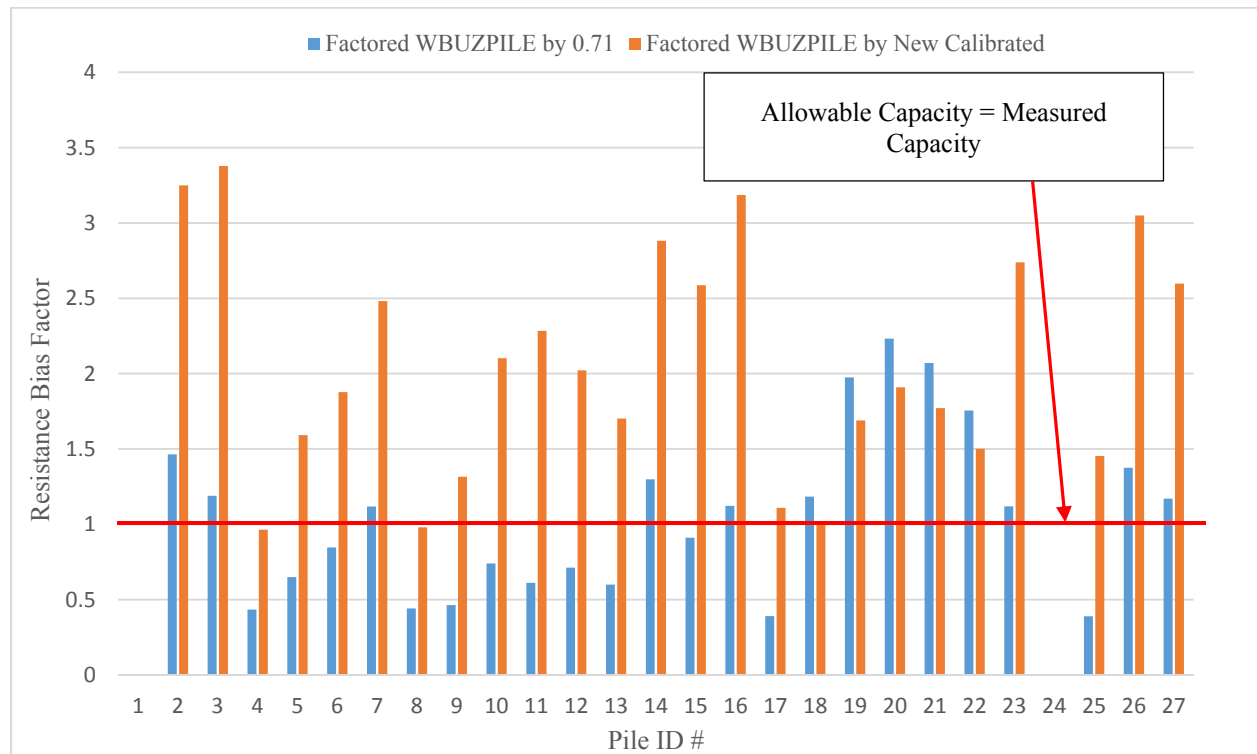


Figure 5.4 Factored design capacity ratios versus the measured capacity ratios

Figure 5.4 shows the ratio of the calculated factored loads for both the current method and the newly acquired method compared with the measured loads. The ratios that are above the horizontal line of 1, are safe because they represent piles that were measured to be larger than the allowable design loads. It is evident that the newly calibrated resistance factors within this study provide a measured pile capacities larger than the factored design loads in all by two case, which is within the statistical parameters of the 95% safe area of the distribution. This occurrence represents an issue since the measured resistance shall always be greater than the design in order to avoid failure. Moreover, it is also known that ALDOT tests various piles during installation. In this report, the predicted capacity is back calculated based on the embedment length of the pile and the soil profile utilizing WBUZPILE. Therefore, since it is know that the piles have not failed, adjustments to the load reduction factors can be made, or an evaluation of the current

design method, including the WBUZPILE software, might be required. Because there are only 25 piles with appropriate data, additional data is needed to provide conclusive recommendations for a change in design. However it should be noted that the current method can produce results where the load tests in the field are less than the design loads and further analysis might be necessary to ensure safe pile installations are achieved. ALDOT procedure currently has these safeguards in place when the initial driving capacity does not reach the factored design loads.

CHAPTER 6 - PRELIMINARY PROCESS TO INCORPORATE PILE SETUP INTO DEVELOPMENT OF RESISTANCE FACTOR

Efforts to regionally calibrate resistance factor for driven piles in the state of Alabama have been conducted. However, there is a lack of incorporation of pile setup in LRFD resistance factor calibration due to the limited amount of data and understanding of the mechanics causing pile setup. In order to use FOSM reliability theory to determine resistance factors, a predicted nominal resistance must be compared with a measured resistance as previously explained and implemented in the standard calibrated performance in Chapter 5. The state of Alabama recorded dynamic load test data for 27 piles within the state at end of driving (EOD) and beginning of restrike (BOR) at different interval times after initial driving was completed. Consequently, when comparing resistances at EOD and at BOR at an interval between 0 to 30 days, it was observed that 19 piles showed an increase of ultimate resistance over time. Also, it is known that setup is mostly related to the increase of shaft capacity on the pile (Ng et al. 2010). A statistical analysis will be performed for piles that showed an increase in shaft resistance for an interval time of 0 to 30 days. This chapter explains the methodology of utilizing pile setup in the computation of resistance factors for the state of Alabama.

6.1 Process of Pile Setup Prediction

In order to incorporate pile setup into LRFD resistance factors calibration by utilizing FOSM, a pile setup capacity prediction needs to be computed. The Skov-Denver setup method is a popular method used to predict pile setup in various soil conditions. This method was proposed by Skov & Denver (1988), and it shows a semi-logarithmic relation between pile capacity and time by the following equation:

$$\frac{Q}{Q_0} = A \log_{10} \left(\frac{t}{t_0} \right) + 1 \quad , \quad (6.1)$$

where A is a dimensionless setup factor and is a function of soil type; Q and Q₀ are the total or the shaft pile capacity (setup) at time t and t₀, respectively; t is the time elapsed after the initial driving; and t₀ is the reference time.

According to Ng (2013), the setup factor A , describes the rate of pile resistance gain. Ng (2013) computed A by analyzing several piles that were re-struck multiple times at different time intervals. A best-fit line was developed utilizing the pile resistance as a function of the different intervals of time after EOD. Best-fit line plots were developed for five HP piles driven into clayey soil that were re-struck during the same intervals of time. Then, an overall average best-fit line was computed utilizing all the piles. Consequently, by calculating a pile setup ratio which compares the pile resistances at EOD and BOR with respect to time, a setup factor, A , can be developed when developing a best-fit line. Moreover, as defined by Skov & Denver (1988), time follows a lognormal distribution. Consequently, in order to compute the best fit line plot between pile setup ratio with respect to time, time needs to be defined as the $\text{Log}_{10}(t/t_0)$. According to Ng. (2013), t_0 is assumed to be 0.1 days, since the lognormal distribution is sensitive to zero values and rearrangement in the soil particles occurs immediately after end of driving. By utilizing a setup factor computed with data collected in the state of Alabama, a pile setup predicted resistance can be computed and incorporated into the FOSM method. Furthermore, statistical analysis in pile setup ratios is needed in order to be confident in the relationship of increase in capacity over time described by the data collected.

6.2 Overview of Required Design Loads at End of Driving and Beginning of Restrike

In order to incorporate pile setup into the calibration of LRFD resistance factors, it is important to observe the performance of the piles by observing the method of design. As it was mentioned before, ALDOT verifies pile resistances at certain intervals of time after the installation of the pile to account for setup to achieve the required design capacity. Moreover, by observing if the required design loads were met whether at end of driving or at beginning of restrike, figure 6.1 was developed. Figure 6.1 shows the pile measured capacities at EOD, the unfactored design capacities and the measured capacities at beginning of restrikes for each pile. Note that some of the piles were re-struck more than once and some of the pile ID # are repeated. Table 6.1 summarizes the occurrences of the cases when a.) pile capacity at EOD was greater than the required design capacity; b.) the required design capacity was not met at EOD but it was met at BOR; c.) the design capacity was greater than capacity at EOD and BOR and it was not met; and d.) none of these cases occurred mostly related to lack of data.

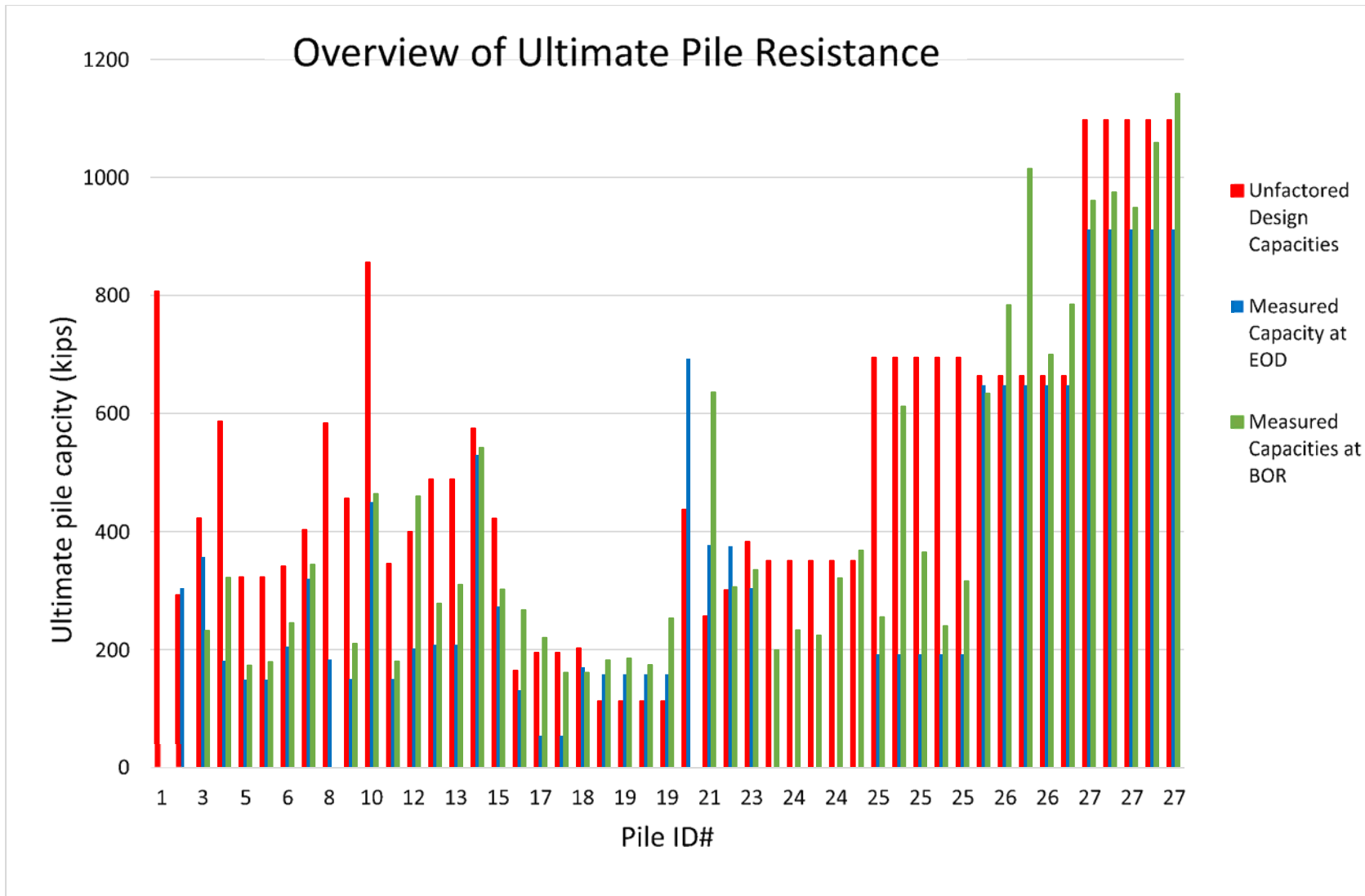


Figure 6.1 Comparison of Pile resistances between the unfactored DesignCapacities and the measured capacities at EOD and restrikes

Table 6.1 Summary of occurrences of comparison among pile capacity at EOD, Design and BOR

	# Occurrences
EOD > Design	3
EOD < Design < BOR	10
EOD, BOR < Design	13
N/A	1
Total	27

From figure 6.1 and Table 6.1 it can be observed that the design capacity of the majority of the piles is greater than the pile resistance at EOD and BOR; thus, the capacity measured at the field by CAPWAP did not meet the required nominal capacity that the pile shall meet. These occurrences represent a major issue in drive pile design. The specific required nominal capacity of driven piles shall be met if not at end of driving, at beginning of restrrike. By not meeting the design capacity, the pile is not capable of supporting the required capacity and it can be exposed to failure. Therefore, based on the analysis of the presented data, there is a major discrepancy between the design capacity calculated by WBUZPILE and the measured capacity computed through CAPWAP. This was expected due to the discrepancy of the resistance bias factor previously calculated. Furthermore, including pile setup into calibration of LRFD resistance factors would improve the design methods since it is an important factor on the verification of design load requirements currently implemented by ALDOT. An analysis of the measured capacities at end of driving and at BOR will be analyzed to account for the increase of capacities on piles in this study. This analysis is conducted by using pile setup ratios.

6.3 Pile Setup Ratio

Dynamic load test data was collected and recorded at end of driving (EOD) and beginning of restrrike (BOR). By analyzing the dynamic load test data of measured resistances recorded by CAPWAP at EOD and BOR, the change in pile capacity was observed over time. A pile setup ratio was computed to determine if there was an increase on the capacity. In order to compute the pile setup ratio, the following equation was utilized:

$$\text{Setup Ratio} = \frac{\text{Measured shaft resistance from CAPWAP at BOR}}{\text{Measured shaft resistance from CAPWAP at EOD}} - 1 \quad (6.2)$$

where only piles that had a setup ratio greater than zero were utilized to account for pile setup. The time of restrike after end of driving varied from 0.6 to 420 days. However, the majority of the piles were re-struck before the 30th day. Moreover, it was more appropriate to compare only pile restrike data within an acceptable time interval such as 0 to 30 days for more accurate calibrated resistance factors. Figure 6.2 shows a histogram of the time of restrike after EOD for all the dynamic load test restrike data collected for driven piles within the state of Alabama. Table 6.2 shows a summary of the computation of the pile setup ratio for the 19 piles that showed an increase in capacity in an interval of 0 to 30 days.

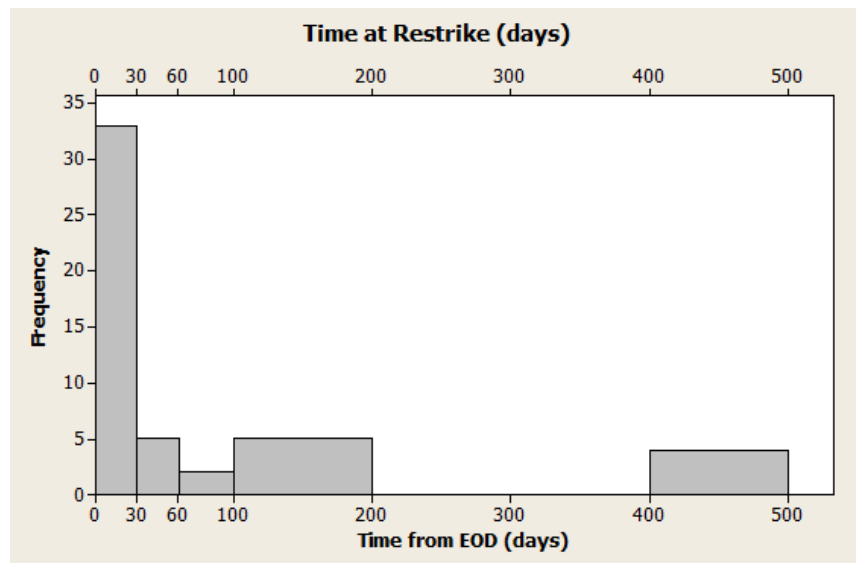


Figure 6.2 Histogram of time at restrike in days for dynamic load test data

Table 6.2 Summary pile setup ratios

Pile ID	Pile Material	Type of Soil	Time from EOD (days)	CAPWAP R-shaft at EOD (kips)	CAPWAP R-shaft at BOR (kips)	Pile Setup Ratio
3	PSC	Mixed	7.1	51	92	0.8
4	PSC	Sand	7.9	43	175	3.1
5	HP	Mixed	5.9	92	115	0.3
6	PSC	Sand	7.3	115	138	0.2
7	PSC	Sand	14.0	101	115	0.1
9	PSC	Mixed	14.0	52	139	1.7
10	PSC	Mixed	8.7	80	162	1.0
11	HP	Sand	2.9	68	110	0.6
13	PSC	Mixed	8.9	168	223	0.3
15	PSC	Mixed	12.8	138	207	0.5
16	PSC	Mixed	8.9	66	202	2.1
17	PSC	Mixed	0.7	35	133	2.8
17	PSC	Mixed	9.7	35	197	4.6
18	HP	Clay	18.0	122	135	0.1
19	HP	Clay	14.0	62	88	0.4
19	HP	Clay	21.0	62	70	0.1
22	HP	Clay	6.9	127	207	0.6
23	HP	Mixed	6.9	185	238	0.3
25	HP	Sand	1.5	147	209	0.4
25	HP	Sand	7.0	147	194	0.3
25	HP	Sand	30.0	147	281	0.9
26	HP	Sand	3.0	319	394	0.2
26	PSC	Sand	7.0	319	448	0.4
26	PSC	Sand	30.0	319	494	0.5
27	PSC	Sand	7.0	603	665	0.1
27	PSC	Sand	30.0	603	814	0.3

6.4 Statistical Analysis of Pile Setup Ratio

Pile setup ratios were statistically analyzed to identify the presence of outliers, compute trendlines, and determine the R-squared of the sample population. Figure 6.3 shows a boxplot for the setup ratios computed. Figure 6.3 shows four outliers are present among the sample population. The pile setup ratio outliers found in the population are highlighted in Table 6.2.

These setup ratio outliers were removed from the population in order to compute more accurate statistical analysis and did not participate on the statistical analysis from this point forward.

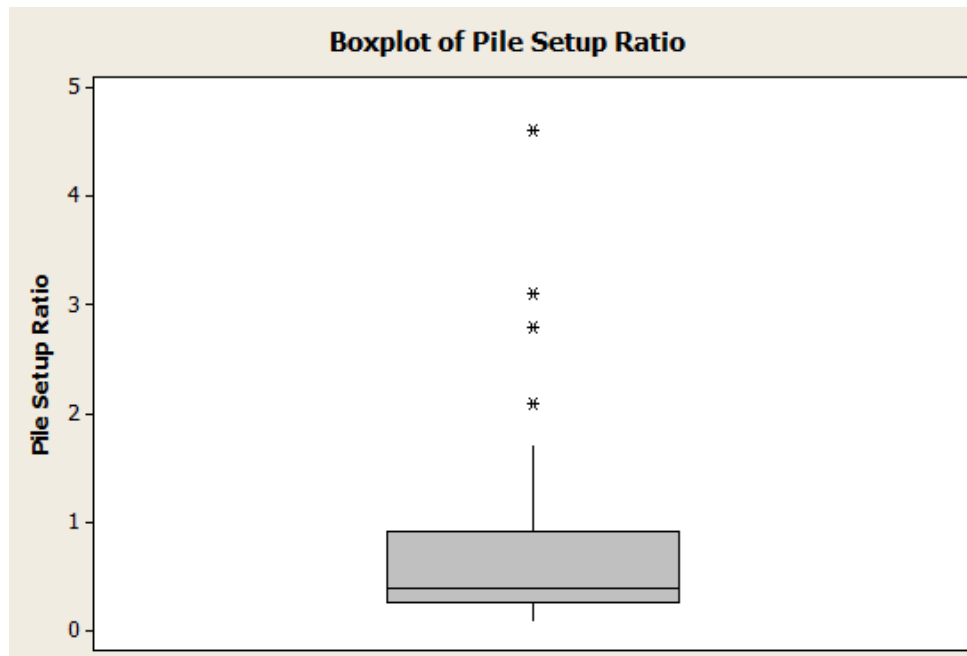


Figure 6.3 Boxplot of pile setup ratios

After removing the outliers, a best fitted line was computed for those pile setup ratio with respect to time in order to observe the R-squared that would define the relationship between sample values and the computed regression. By fitting the best line plot of the pile setup ratios, the setup factor, A , can be determined. Figure 6.4 shows the best-fit line plot and R-squared for pile setup ratios respectively. Figure 6.5 shows the summary of best-fit line plot of pile setup ratios classified by pile type and type of soil; Figure 6.6 through 6.10 shows the fitted line plot of pile setup ratios and R-squared by pile classification.

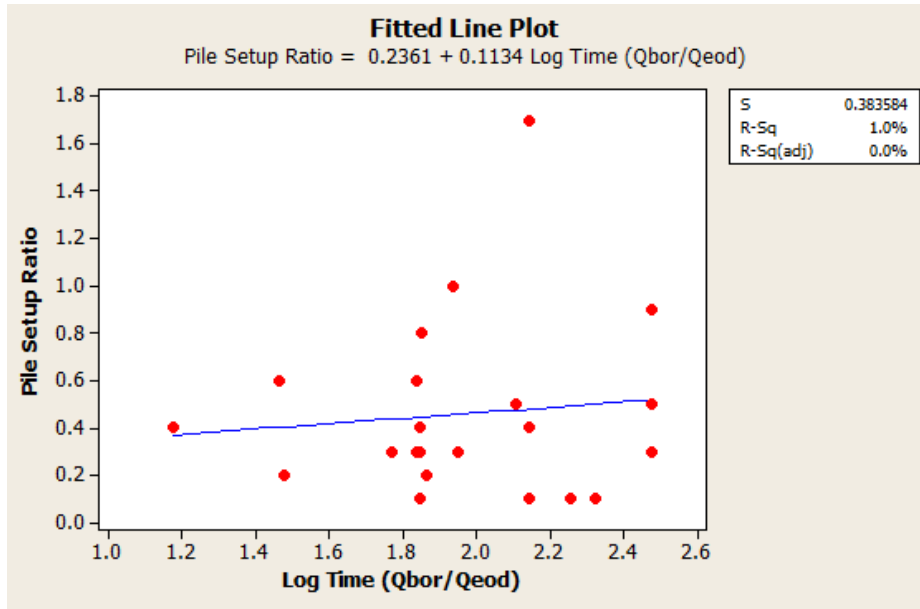


Figure 6.4 Best-fit line plot of pile setup ratio

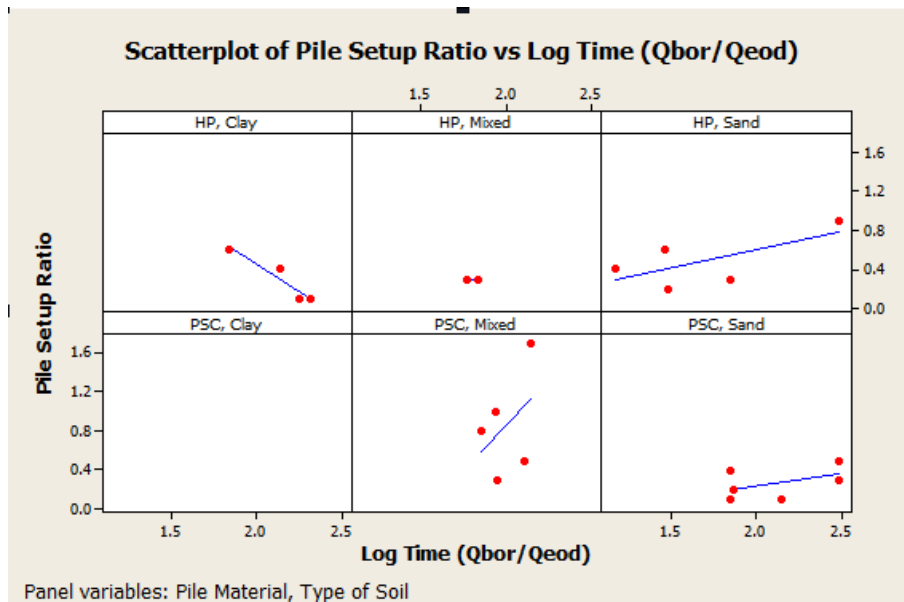


Figure 6.5 Best-fit line plot of pile setup ratio by pile classification

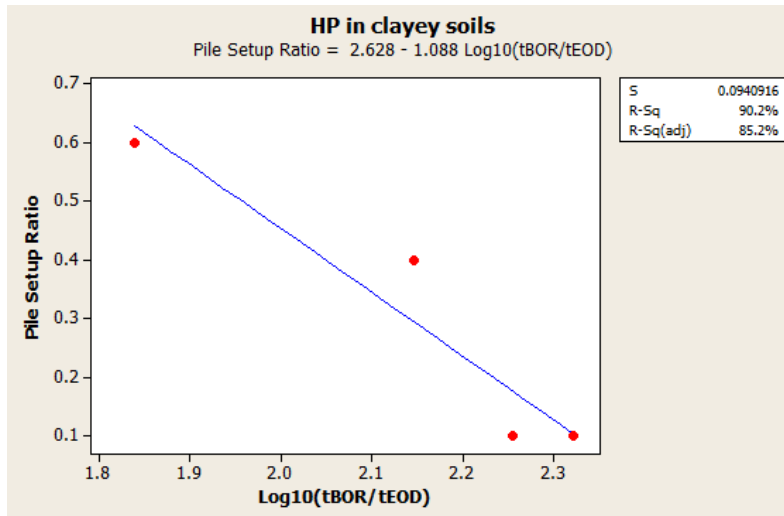


Figure 6.6 Best-fit line plot of pile setup ratio by pile classification

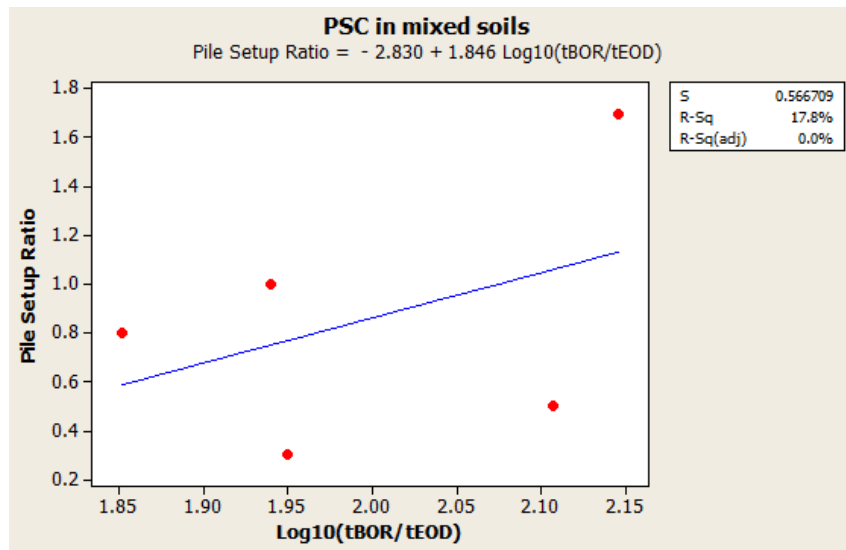


Figure 6.7 Best-fit line plot of pile setup ratio in HP piles driven in clayey soils

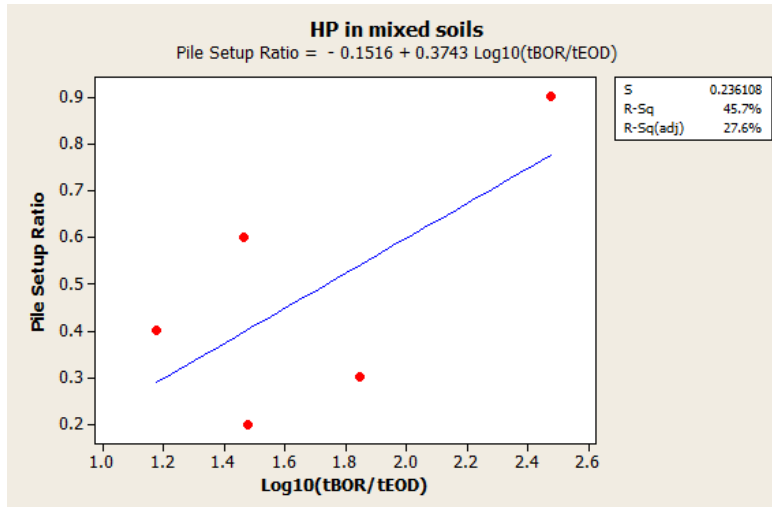


Figure 6.8 Best-fit line plot of pile setup ratio in HP piles driven in mixed soils

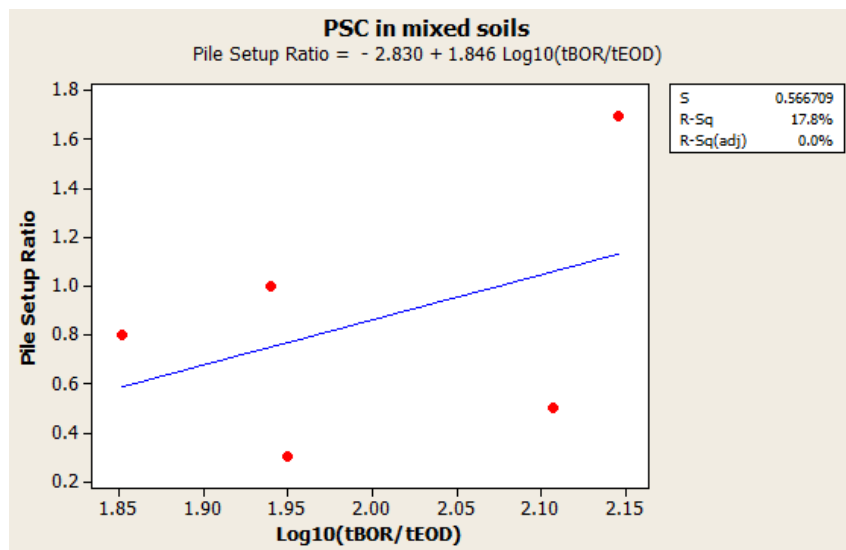


Figure 6.9 Best-fit line plot of pile setup ratio in PSP piles driven in mixed soils

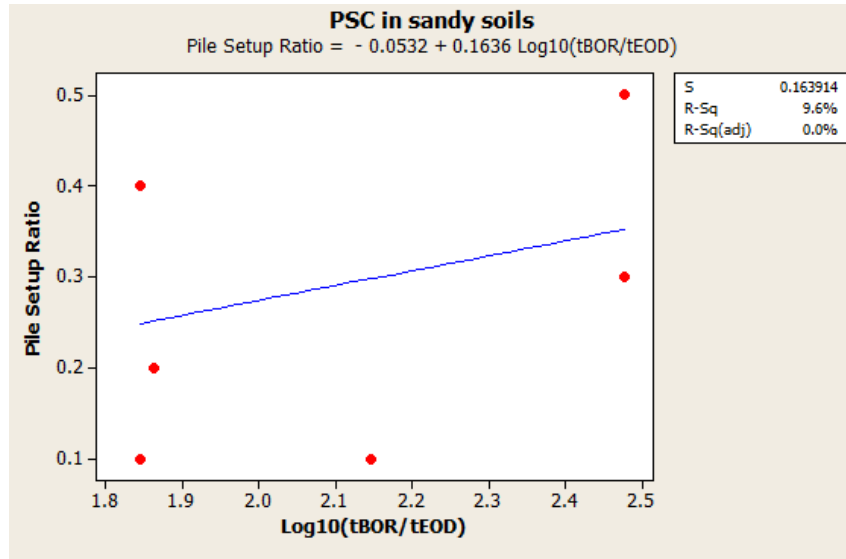


Figure 6.10 Best-fit line plot of pile setup ratio in PSP piles driven in sandy soils

It can be observed from Figure 6.6 through Figure 6.10 that the data did not show any significant trend between increases of pile capacity over time. For the overall best-fit line plot from figure 6.4, the R-squared was 1.0%; which is an extremely poor relationship since a moderate R-squared shall be greater than 50% to conclude a possible trend on the data. Also by analyzing each best-fit line plot based on pile classification, there was also no good trend describing pile setup ratios over time. However, the R-squared for the trend line of the HP piles driven in clayey soil was 90.2%, which was expected since pile setup is a common phenomenon that occurs in clayey soils after EOD. Moreover, only four pile setup ratios were analyzed for HP piles driven into clayey soils. Two of the four pile setup ratios for HP piles in clayey soils were obtained from the same pile at different restrike times. Based on the results of this preliminary analysis, a larger sample population is needed. It can be concluded that analyzing one pile at different restrike times allows the computation of a setup factor (A) since the trend between increases of pile capacity over time in the same pile would better describe the relationship between increases of capacity over time. This type of experimentation would also be required for various types of soils encountered and using the common types of pile materials used within the state.

The data shows that among the 27 piles analyzed in this study, 19 showed setup between 0.6 and 30 days after pile installation. This indicates that the incorporation of pile setup

into the design of driven piles within the state of Alabama can greatly affect the confidence of the safety of the LRFD design, since a large amount of the pile sample population showed an increase in pile resistance over time.

In order to determine resistance factors by utilizing FOSM, predicted and measured resistances must be compared. If restrike data is collected at the same time intervals for similar pile classifications, it is possible to compute a specific setup factor for the state of Alabama to include setup. By determining a setup factor specific for the state of Alabama, Skov-Denver method can be utilized to predict pile resistance that accounts for setup within the state. Consequently, it is fundamental to continue to acquire data of driven piles within the state of Alabama in order to calibrate regional resistance factors that incorporate pile setup in its development. Once there is additional pile test data acquired, further analysis is needed to complete the setup enhancement of the LRFD resistance factor calibration.

CHAPTER 7 – OVERALL CONCLUSIONS AND RECOMMENDATIONS

7.1 Conclusions of Pile Load Testing and Pile Setup Evaluation

One of the main objectives of this research is to organize and analyze pile load testing data collected by the Alabama Department of Transportation to identify set-up potential in Alabama soils and to compare CAPWAP[®], PDA[®], and iCAP[®] estimates for total pile axial resistance. The researchers involved in this project accomplished this objective by organizing and analyzing the ALDOT's historical driven pile test records. Furthermore, they assisted in preparing a database of set-up factors including location (coordinates), pile testing records, pile properties, and soil boring logs for future reference.

The Alabama Department of Transportation provided acquired PDA[®] data for 23 test piles (9 H-piles and 14 PPC piles) installed throughout the central and southern portions of the state to investigate the set-up potential of soils on driven piles. Each of these test piles were analyzed independently and blindly (i.e., without looking at the other dynamic analysis results) by three dynamic analysis methods, iCAP[®], CAPWAP[®] and PDA[®] Methods. Five of these test piles (USA test piles) were installed specifically for research purposes: 4 test piles were installed near the Mobile River (HP 12x53, HP14x117, PPC 24"x24", and PPC 36"x36") and an HP14x102 test pile was installed in Montgomery, AL at the Montgomery Outer Loop Project. The author of this paper analyzed the PDA[®] data with the iCAP[®] software, and thus provided the total pile axial resistance (R_u) estimates using the iCAP[®] Method. A single PDA[®] operator from the ALDOT provided the total pile axial resistance (R_u) estimates using the PDA[®] Method (or Case Method). GRL Engineers, Inc. provided the total pile axial resistance (R_u) estimates using the CAPWAP[®] Method.

The four Mobile River test piles (Pile 8, 9, 22, and 23) were installed mostly in medium sand. However, the bottom 14 feet of Pile 9 (HP14x117) is embedded in a very stiff clay. Each of these test piles were re-struck 5 times over a 14 month period and were also subjected to a static loading test approximately 4 months after EOID. Three of these piles (Pile 8, 9, and 22) achieved the Davisson (1972) failure criterion during the static loading tests, and the iCAP[®] total resistance estimates are reasonably close to each of the SLT results (as shown in Table 4.1). Furthermore, these three piles were the only piles out of the 23 total test piles that achieved the

Davisson (1972) failure criterion. The iCAP[®] results indicate that the Mobile River H-piles (Pile 8 and 9) developed the most set-up from the EOID to the BOR5 (final restrrike). Furthermore, it must be noted that the PDA[®] data at EOID for Pile 8 (HP12x53) was invalid. As a result, the total pile resistance (R_o) estimates at the EOID were replaced by the first restrrike estimates (BOR1) so that set-up potential could be evaluated. The iCAP[®] results indicate that the time effect on Pile 8 (HP12x53) and Pile 9 (HP14x117) at BOR5 is 3.1 and 3.8, respectively. The iCAP[®] results indicate that the time effect on Pile 22 (PPC 24"x24") and Pile 23 (PPC 36"x36") at BOR5 is 1.65 and 2.16, respectively.

Pile 6 (HP14x102) is a relatively short test pile (20 ft) that was installed in clayey sand at the Montgomery Outer Loop Project. It was re-struck 4 times at 7, 14, 21, and 42 days from EOID. The iCAP[®] results indicate that the time effect on Pile 6 at BOR4 is 1.51.

The results indicate that total resistances estimated using the PDA[®] Method are frequently larger than both the iCAP[®] and CAPWAP[®] total resistance estimates, which is likely due to the assumed damping factor (J_c) used in the PDA[®] Method. The results indicate that the PDA[®] total resistance estimates are larger than the iCAP[®] total resistance estimates by an average of 26% for H-piles and 25% for PPC piles. The PDA[®] total resistance estimates are also larger than the CAPWAP[®] total resistance estimates by an average of 26% for H-piles and 23% for PPC piles. However, as shown in Figures 4.28, 4.30, and 4.31, the iCAP[®] total resistance estimates (in most cases) match very well with the CAPWAP[®] total resistance estimates.

The iCAP[®] total resistance results indicate that set-up developed on 74% of the test piles (6 H-piles and 11 PPC piles). The CAPWAP[®] total resistance results indicate that set-up developed on 87% of the test piles (7 H-piles and 13 PPC piles). The PDA[®] total resistance results indicate that set-up developed on 100% of the piles, which is likely due to the assumed damping factor (J_c). The iCAP[®] results indicate that the total axial pile resistance (regardless of pile type or size) increased over time from EOID (set-up) by an average of 70% over a large range of time intervals after EOID if at least 50% of embedment soils surrounding the piles were clays, sandy clays, clayey sands, medium sands, loose sands, medium silty sands, loose silty sands, or Selma chalks. However, the total axial pile resistance decreased over time from EOID (relaxation) by an average of 11% over a large range of time intervals after EOID if at least 50% of embedment soils surrounding the piles were dense sands, firm silty sands, or clay fills.

7.2 Conclusions of LRFD Resistance Factor Calibration by Reliability FOSM Method

This report calculated the LRFD resistance factors for the design of driven piles for soils in the state of Alabama utilizing the First Order Second Moment method. The FOSM method of resistance factor calibration requires a statistical analysis of both predicted and measured driven pile axial resistances. The Alabama Department of Transportation provided historical data of existing driven piles installed throughout the state within the past 5 years. The resistance bias factors were computed for 25 piles with the overall calculated mean of 0.746, with the majority of the resistance bias factors were less than the overall mean. Obtaining resistance bias factors less than 1 shows that the design capacities of the piles were smaller than the measured capacities acquired on the field after installation. This information clearly shows that the design method requires an adjustment to ensure the safety of install piles within the state, which is precisely the purpose of the resistance factors utilized in the LRFD design process.

Utilizing the bias factors generated, the overall resistance factors of 0.38 and 0.30 were calculated with reliability indices of 2.33 and 3.0, respectively. Due to the variation of the soils encountered and the types of pile materials utilized within the State of Alabama, the resistance factors varied from 0.29 to 0.83. A comparison of the design capacities factored by currently used back-calculated resistance factor of 0.71 and the new calibrated resistance factors on this report was conducted. It was obtained that by factoring the design capacities by 0.71, more than half of population was below the measured resistances. However, by utilizing the new calibrated resistance factors over 95% of the piles showed a greater measured capacity than design capacity which represents a greater confidence.

An attempt to incorporate effects of pile setup into the calibration of LRFD resistance factors is also provided. It was shown that based on the data collected, more than half of the pile population did not present a measured capacity greater than allowable design at end of driving or beginning of restrike when using the current design methods. However, the data did show a significant increase in capacity over time for 19 of the 27 piles analyzed. A prediction method was implemented to predict the amount of increased pile capacity at 30 days after EOD. Unfortunately, by analyzing the 19 piles that showed an increase in capacity over a time interval of 30 days, no definitive trend to enhance the current resistance factor model could be performed.

7.3 Recommendations for Future Research

Based on the results of this preliminary analysis, a larger sample population is needed. It can be concluded that analyzing one pile at different restrike times allows the computation of a setup factor (A) since the trend between increases of pile capacity over time in the same pile would better describe the relationship between increases of capacity over time. This type of experimentation would also be required for various types of soils encountered and using the common types of pile materials used within the state.

Based on the results of this study, there are several recommendations to improve the development of resistance factors in the state of Alabama, which can lead to a more confident implementation of the new design methodology. These recommendations include:

Collection of more load test data is needed at end of driving and at beginning of restrike. By utilizing FOSM, the importance of an increased amount of samples is fundamental in order to conduct a more reliable statistical analysis.

It is recommended to not only acquire dynamic load test data at end of driving and beginning of restrike, but to acquire static load test data to fail the pile. According to the AASHTO LRFD Design Specifications, (2012), static load tests to failure of the pile is the most accurate representation of the actual axial capacity of the piles.

The bias factor of 0.746 indicates a need for additional analysis of the WBUZPILE software and the current methods of driven piles design. It is recommended that a thorough analysis of the WBUZPILE outputs be compared with the current FHWA procedures for axial capacity calculations.

Incorporating pile setup into the driven pile design specifically for the state of Alabama due to the geologic soil conditions would provide a more efficient foundation system for state structures. By the incorporation of pile setup, it is also recommended the development of a pile setup factor that can be computed by analyzing multiple piles at different time intervals. This setup factor can be used for the prediction of pile resistances incorporating setup, and a new resistance factor can be developed that accounts for the increase of pile capacity over time. This implementation would require a significant amount of testing and experimentation as a more robust database is required.

This research prepared a database of set-up factors for future references. It is

recommended to continue to add to this database to develop a more reliable assessment of set-up through the entire State of Alabama. This database should be increased especially in soils (such as clays, sandy clays, clayey sands, medium sands, loose sands, medium silty sands, loose silty sands, or Selma chalks) that are most likely to develop set-up. The results contained in this database may eventually be used to establish a recommended set-up protocol to incorporate into the design of driven piles for a more economical foundation system.

REFERENCES

- AbdelSalam, S. S., Ng, K. W., Sritharan, S., Suleiman, M. T., & Roling, M. (2012). Development of LRFD Procedures for Bridge Pile Foundations in Iowa. Volume III: Recommended Resistance Factors with Consideration of Construction Control and Setup. Final Report No. IHRB Projects TR-584. Ames, IA,
- ALDOT Bridge Bureau (2015). Structural Design Manual.
- "Alabama Department of Transportation Standard Specifications for Highway Construction." (2012). Montgomery, AL.
- ALDOT. (2011). "Alabama Department of Transportation One-Hundredth Annual Report Centennial Edition." Montgomery, AL.
- ALDOT. (2012). "Alabama Department of Transportation One Hundred First Annual Report." Montgomery, AL.
- Allen, T. M., Nowak, A. S., & Bathurst, R. J. (2005). Calibration to determine load and resistance factors for geotechnical and structural design. Transportation Research Circular Number E-C079, TRB, Washington, D.C., 83 p.
- American Association of State Highway and Transportation Officials (1994). LRFD Bridge Design Specifications. Washington, D.C., 1st Ed.
- American Association of State Highway and Transportation Officials (1995). Standard Specifications for Highway Bridges, Division I. Washington, DC, 15th ed. (with Interim Specifications)
- American Association of State Highway and Transportation Officials (2012). LRFD Bridge Design Specifications. Washington, D.C., Customary. U.S. Units, 6th edition
- Ashour Mohamed, Helal Amr, & Ardalan Hamed (2012). Upgrade of Axially Loaded Pile-Soil Modeling with the Implementation of LRFD Design Procedure. Contract No. 930-769. Final report submitted to State of Alabama Department of Transportation (ALDOT). Hunstville, AL
- Barker, R.M., J.M. Duncan, K.B. Rojiani, P.S.K. Ooi, C.K. Tan & S.G. Kim (1991). Manuals for the Design of Bridge Foundations. National Cooperative Highway Research Program Report 343. *Transportation Research Board*, Washington, D.C., 308p.
- Basu, P., Salgado, R., Prezzi, M., and Chakraborty, T. (2009). A Method for Accounting for Pile Setup and Relaxation in Pile Design and Quality Assurance. Joint Transportation Research Program (JTRP) Report No. FHWA/IN/JTRP-2009/24.

- Bradshaw, A., Baxter, C., and Osborn, P. (2004). "Lessons Learned from Pile Driving on the Central Artery/ Tunnel Project." *Advances in Deep Foundations*, Geotechnical Special Publication No. 132, ASCE.
- Budge, A. S. (2009). "Study of Pile Setup Evaluation Methods." *Rep. No. MN/RC 2009-38*, Minnesota Department of Transportation Research Services Section, St. Paul, MN.
- Bullock, P. J. (1999). "Pile Friction Freeze: A Field and Laboratory Study". Ph.D. Dissertation. University of Florida, Florida.
- Chow, F.C., Jardine, R.J., Bruzy, F., and Nauroy, J.F. (1998). "Effects of Time on Axial resistance of Pipe Piles in Dense Marine Sand." *Journal Geotechnical and Geoenvironmental Engineering*, 124(3), 254-264.
- Das, B. M. (2010). *Geotechnical Engineering Handbook*. J. Ross Publishing Inc., Ft. Lauderdale, FL.
- Fellenius, B. H., (1980). The Analysis of results from routine pile load tests. *Ground Engineering*, London, 13(6) 19-31.
- Goble, G. G., Rausche Frank, & Likins, G. E., Jr (1980). The analysis of pile driving. A state of Art. *Intl. Seminar on the Application of Stress-Wave Theory on Piles*. Boulder, CO.
- Hannigan, P.J., Goble, G.G., Likins, G.E., Rausche F. (2006). *Design and Construction of Driven Pile Foundations - Reference Manual Volumes I and II*. Federal Highway Administration, Pub. No. FHWA NHI-05-043, April, 2006.
- Kehoe, S.P., (1989). An analysis of time effect on the bearing capacity of driven piles. Master's report, Department of Civil Engineering, University of Florida, Gainesville, Florida.
- Kiseok, K., Jae, H.P., & Kim, K. J., (2007). Evaluation of Resistance Bias Factors for Load and Resistance Factor Design of Driven Steel Pipe Piles. *Contemporary Issues in Deep Foundations* (GSP 158), pp. 149-158.
- Komurka, V.E. (2011). *Driven Pile Test Program Report – Lafayette Bridge Replacement*, submitted to Minnesota Department of Transportation, Wagner Komurka Geotechnical Group, INC., St. Paul, Minnesota.
- Komurka, V.E., and Wagner, A.B., and Edil, T.B. (2003). *Wisconsin Highway Research Program #0092-00-14: Estimating Soil/pile Set-up, Final Report*, submitted to the Wisconsin Department of Transportation, Wagner Komurka Geotechnical Group, Inc., St. Paul, Minnesota.
- Lee, W., Kim, D., Salgado, R., and Zaheer, M. (2010). "Setup Of Driven Piles In Layered Soil." *Japanese Geotechnical Society*, Vol. 50(No. 5), 585-598.

- Likins, G.E., Liang, L., and Hyatt, T. (2012). "Development of Automatic Signal Matching Procedure - iCAP®". *Proceedings from Testing and Design Methods for Deep Foundations*. IS-Kanazawa: Kanazawa, Japan, 97-104 and 363-370.
- Long, J.H., Kerrigan, J.A., and Wysockey, M.H., (1999). Measured Time Effects for Axial Capacity of Driven Piling. *Transportation Research Record* 1663, Paper No. 99-1183, pp. 8-15
- Long, J.H., Hendrix J., & Baratta, A. (2009a). Evaluation/Modification of IDOT Foundation Piling Design and Construction Policy Illinois Center for Transportation. Report No. FHWA-ICT-09-037. Report submitted to Illinois Dept. of Transportation, Urbana, IL.
- Long, J. H., Hendrix, J., & Jaromin, D. (2009b). Comparison of Five Different Methods for Determining Pile Bearing Capacities. Report No. WHRP 08-07. Wisconsin Highway Research Program, Wisconsin Dept. Of Transportation, Urbana, IL.
- Luna, Ronaldo (2014). Evaluation of Pile Load Tests for Use in Missouri LRFD Guidelines. Project TRyy1226. Missouri Department of Transportation. Jefferson City, MO.
- Mc Vay, C.M., Birgisson, B., Zhang, L., Perez,A., & Putcha, S., (2000). Load and Resistance Factor Design for Driven Piles using Dynamic Methods-A Florida Perspective. *Geotechnical Testing Journal*, Vol 23 (1), pp 55-66.
- Mitchell, Charles C. Jr. & J. Cameron Loerch (2008). *Soil Areas in Alabama. United States Department of Agriculture. Natural Resources Conservation Service Soils Website*.
- Ng, C. W. W., Simons, N., and Menzies, B. (2004). *A Short Course in Soil-structure Engineering of Deep Foundations, Excavations and Tunnels* . Thomas Telford, London.
- Ng, K. W. (2011). "Pile Setup, Dynamic Construction Control, and Load and Resistance Factor Design of Vertically-Loaded Steel H-Piles ". Doctor of Philosophy. Iowa State University, Ames, Iowa.
- Ng, K.W., Suleiman, M.T., & Sritharan, S. (2010). LRFD Resistance Factors Including the Influence of Pile Setup for Design of Steel H-Pile Using WEAP. Geotechnical Special Publication No. 199, *Advances in Analysis, Modeling & Design, Proc. of the Annual Geo-Congress of the Geo-Institute*, ASCE, Feb 20-24, Fratta, D., Puppala, A.J., and Muhunthan, B., ed., West Palm Beach, FL, pp. 2153–2161
- Nowak, A. S., (1999). Calibration of LRFD Bridge Design Code, NCHRP Report 368, Transportation Research Board, National Research Council, Washington, D.C.
- Paikowsy, S.G., Nguyen, T.C. Kuo, Baecher, G., Ayyub, B., Stenersen, K., O'Malley, L. Chernauskas, & O'Neill, M., (2004). Load and Resistance Factor Design (LRFD) for Deep Foundations, NCHRP Report 507, Transportation Research Board, Washington, D. C.
- PDA®-W Manual* (2001). Pile Dynamics, Inc., Cleveland, OH.

- Peck, R.B., (1958). A study of the comparative behavior of friction piles. HRB, Special Report 36, HRB. National Research Council, Washington, D.C.
- Prakash, S. (1990). *Pile Foundations In Engineering Practice*. John Wiley & Son, Inc., New Jersey.
- Preim, M.J., March, R., Hussein, M.H. (1989). *Bearing Axial resistance of Piles in Soils with Time Dependent Characteristics*. Proceedings of the International Conference on Piling and Deep Foundations: London.
- Rahman M.S., Gabr M.A., Sarica R.Z. & Hossain M.S., (2002). Load and Resistance Factor (LRF) for Analysis/Design of Piles Axial Capacity. Final Report. Raleigh, North Carolina.
- Rausche, F., and Klesney, A. (2007). "Hammer Types, Efficiencies and Models in GRLWEAP." *PDCA 11th Annual International Conference and Exposition*, Nashville, TN, 97-118.
- Rausche, F., Goble, G., and Likins, G. (1985). "Dynamic Determination of Pile Capacity." *J.Geotech.Engrg.*, 111(3), 367-383.
- Rausche, F., Likins, G., Liang, L., and Hussein, M. (2010). "Static and Dynamic Models for CAPWAP® Signal Matching." American Society of Civil Engineers, 534-553.
- Rausche, F., Robinson, B., & Liang, L. (2000). Automatic signal matching with CAPWAP. Application of Stress-Wave Theory to Piles. Cleveland, Ohio
- Reddy, S. C. (2014). "Ultimate and Serviceability Limit State Reliability-based Axial Capacity of Deep Foundations ". Ph.D. Dissertation. Oregon State University, Corvallis, OR.
- Rosenblueth, E. & L. Esteva (1972). Reliability basis for some Mexico codes. Special Pub. SP-31, American Concrete Institute, 141-155.
- Schmertmann, J. (1991). "The Mechanical Aging of Soils." *J.Geotech.Engrg.*, 117(9), 1288-1330.
- Seed, H.B., and Reese, L.C. (1955). "The Action of Soft Clay along Friction Piles." *Proceedings of the American Society of Civil Engineers* 81, Paper No. 2882, 731-765.
- Seward, N. J., and Curtin, W. G. (2006). *Structural Foundation Designers' Manual*. Blackwell Pub, Oxford.
- Skov, R., and Denver, H. (1988). "Time-dependence of Bearing Capacity of Piles." *Proceedings of the Third International Conference on Application of Stress-Wave Theory to Piles*. Fellenius, B.G., editor, BiTech Publishers, Vancouver, BC, 717-723.

Smith Trevor D., Banas Andrew, Gummer Max & Jin Jaesup (2011). Recalibration of the GRLWEAP LRFD Resistance Factor for Oregon DOT. Final Report SPR 683. Oregon Department of Transportation Research Section.

Svinkin, M. (2002). "Engineering Judgement in Determination of Pile Capacity by Dynamic Methods." American Society of Civil Engineers, 898-914.

Tomlinson, M. J., and Woodward, J. (2008). *Pile Design and Construction Practice Fifth Edition*. Taylor & Francis, London and New York.

Verma, Neha B.E., (2010). Implementation of LRFD Pile Setup in Clayey Soil in Louisiana. Thesis, submitted to Louisiana Tech University. Baton Rouge, LA

Vesic, A.S. (1977). *Synthesis of Highway Practice 42: Design of Pile Foundations*, TRB, National Research Council, Washington, D.C., 1977.

Warrington, D.C, (2007). *Pile Driving by Pile Buck*. Pile Buck International. Vero Beach, FL.

Withiam, J.L, E.P. Voytko, J.M. Duncan, R.M. Barker, B.C. Kelly, S.C. Musser & V. Elias (1998). NHI Course No. 132068, Load and Resistance Factor Design (LRFD) for Highway Bridge Substructures, Reference Manual and Participant Workbook. Prepared for FHWA, Office of Technology Applications, Washington, DC, 735p. (Manual and Workbook, 2001)

Wang, X., Verma, Neha., & Steward, Eric., (2009). Estimating setup of piles driven into Louisiana clayey soils. Final draft report, submitted to Louisiana Transportation Research Center, Baton Rouge, Louisiana, pp. 1-174

Yang Luo & Liang Robert (2007). Incorporating Long-term set-up into Load and Resistance Factor Design of Driven Piles in Sand. Final Report. TRB 86th Annual Meeting Committee (AFS30) technical session Soil Set-up and Relaxation Effects on Bearing Capacity of Driven Piles. Houston, TX

Yoon, S., Ching, T., & Melton, M. (2011). Pile Load Test and Implementation of Specifications of Load and Resistance Factor Design. *Journal of the Transportation Research Board*. Vol. 2212. pp. 22-33. Louisiana

Zhang, L., Tang, W. H., & Ng, C. W. (2001). Reliability of Axially Loaded Driven Pile Groups. Final Report. *Journal of Geotechnical and Geoenvironmental Engineering*. Vol. 127, No. 12.

ADDENDUM REPORT: PILE DRIVING VIBRATION MONITORING OF THE
FUTURE MOBILE RIVER BRIDGE PROJECT

Final Report on Vibrations Due to Pile Driving at the Mobile River Bridge Site

Research Project 930-839R

INVESTIGATION OF PILE SETUP (FREEZE) IN ALABAMA

Development of a Setup Prediction Method and Implementation into LRFD Driven Pile Design

Addendum: Pile Driving Vibration Monitoring of the Future Mobile River Bridge Project



John Cleary, Ph.D., P.E. (P.I. for Vibration Monitoring)

Eric Steward, Ph.D. (Co. P.I. for Vibration Monitoring)

Andrew Gillis (Graduate Student)

Department of Civil Engineering

University of South Alabama

Mobile, AL 36688

June 12, 2015

ACKNOWLEDGEMENT

The Alabama Department of Transportation sponsored this project. Their support for this study is greatly appreciated.

DISCLAIMER

The contents of this report reflect the views of the authors who are responsible for the facts and accuracy of the data presented herein. The contents do not necessarily reflect the official views or policies of the Alabama DOT or the University of South Alabama. This report does not constitute a standard, specification, or regulation. Comments contained in this paper related to specific testing equipment and materials should not be considered an endorsement of any commercial product or service; no such endorsement is intended or implied.

TABLE OF CONTENTS

LIST OF TABLES	iv
LIST OF FIGURES	iv
ABSTRACT.....	v
INTRODUCTION	1
Background.....	1
Objective.....	1
Scope.....	2
Report Organization.....	2
LITERATURE REVIEW	3
Construction Vibrations	3
Damage Thresholds	4
Dynamic Settlement.....	6
Vibration Prediction.....	7
EXPERIMENTAL DESIGN	9
Overview.....	9
Project Site.....	9
Vibration Monitoring.....	11
RESULTS	13
Vibration Levels.....	13
Prediction Equation.....	16
CONCLUSIONS.....	18
Recommendations for Future Research	18
REFERENCES	19
Appendix A: Soil Reports.....	21
Appendix B: Pile Driving Hammer Information	33

LIST OF TABLES

Table 1: Typical ground vibrations from construction equipment (Hanson, Towes and Lance 2006)	3
Table 2: Continuous vibration levels and effects (Hendriks 2002)	4
Table 3: AASHTO and FTA criteria for construction vibrations	5
Table 4: State criteria for construction vibrations.....	6
Table 5: Suggested “n” values based on soil class: Adopted from (Jones & Stokes 2004)	8
Table 6: Soil profile at site location.....	9
Table 7: Pile descriptions.....	10
Table 8: Geophone location during testing.....	12
Table 9: Maximum PPV (in/sec) during pile driving operations.....	13

LIST OF FIGURES

Figure 1: Location of project site, Mobile, AL (Google 2013)	1
Figure 2: Vibration limits from the USBM (Siskind, et al. 1980)	5
Figure 3: Plan view of Mobile River Bridge Project Site.....	10
Figure 4: Maximum recorded vibration levels during pile installation	14
Figure 5: Bar chart of restrikes on precast concrete piles (PCP).....	15
Figure 6: Data plot of restrikes on precast concrete piles (PCP)	15
Figure 7: Peak particle velocity versus distance	17

ABSTRACT

All projects have some amount of inherent risk; one such risk associated with construction projects is the potential for ground vibrations that could damage nearby structures. Research has been conducted on the effects of vibrations on structures; however, the expected levels of vibration are dependent on several factors including the soil conditions at the construction site. Therefore, site-specific investigations are often recommended.

After concerns were raised by the Alabama Department of Transportation (ALDOT) about damage potential at a project site in South Alabama, an addendum was added to a research project related to investigating pile setup in Alabama soils. The purpose of the addendum was to investigate ground vibrations from pile driving at a project site near the Mobile River in Mobile, Alabama.

An investigation and vibration monitoring program was developed for four pile sizes that are often used by the Alabama Department of Transportation (ALDOT). The piles included thirty-six inch square and twenty-four inch square concrete piles, as well as, two steel H-Piles. The piles were driven using typical installation techniques and the vibration levels at various distances from the piles were monitored.

The investigation found that the largest vibrations were observed while driving the thirty-six inch concrete pile. The maximum vibrations observed had a magnitude of 0.82 inches per second at fifty feet from the pile. The vibrations at 150 feet from the pile had dissipated to 0.15 inches per second. The results of the monitoring program and a literature review determined that an allowable vibration level of 0.5 inches per second for modern structures and 0.1 inches per second for potentially sensitive structures should be established for construction activity at or near the location of the project site. Additionally, a survey distance of 150 feet for modern structures and 250 feet for potentially sensitive structures is recommended.

INTRODUCTION

Background

The following report contains the analysis of ground vibrations generated during a pile driving research study located at the Mobile River Bridge Project Site. The project site, owned by the Alabama Department of Transportation (ALDOT), is located on the Mobile River just south of the Alabama Cruise Terminal, Figure 1. The study consisted of monitoring ground vibrations during the installation of four driven piles; two precast concrete piles and two steel H-piles. The study was conducted in response to concerns raised by ALDOT related to possible damage of nearby structures from ground-borne vibrations. The primary objective of this project was to determine the distance that pile driving operations can be conducted with minimal risk to nearby structures. To accomplish this, the vibration levels at various distances from the driven piles were determined and a prediction equation for other distances was developed. This study was conducted by researchers from the Department of Civil Engineering at the University of South Alabama between August 15, 2013 and August 27, 2013.

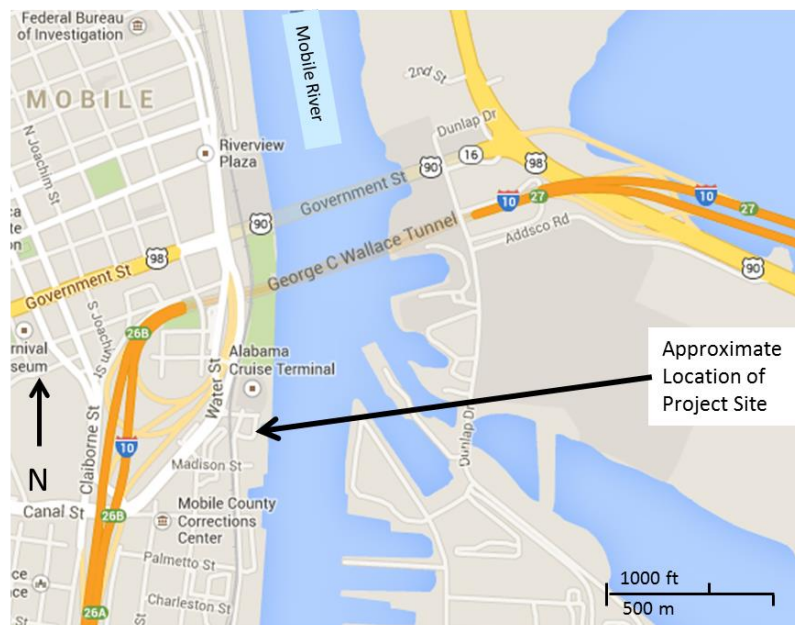


Figure 1: Location of project site, Mobile, AL (Google 2013)

Objective

This project consisted of several objectives. The first was to determine the vibration levels from typical piles used by ALDOT. The second objective was to develop a methodology to predict vibrations at any distance from the pile. The third and final objective of the project was to develop guidelines on allowable vibrations for the project site.

Scope

The scope of this report is limited to the vibrations portion of the larger project: *Investigation of Pile Setup (Freeze) In Alabama: Development of a Setup Prediction Method and Implementation into LRFD Driven Pile Design; Addendum: Pile Driving Vibration Monitoring of the Future Mobile River Bridge Project* (Research Project 930-839R).

The vibrations portion of the project was limited to the aforementioned location near the Mobile River. The project included monitoring vibrations during pile installation and restrikes, analysis of vibration data, development of vibration prediction methodology, and vibration limit recommendations.

Report Organization

The report is organized into five main sections: Introduction, Literature Review, Experimental Design, Results, and Conclusions. Each section contains sub sections as needed.

LITERATURE REVIEW

Construction Vibrations

Ground vibrations are commonly generated from several sources including roadway traffic, railroad traffic, and construction activity. Vibrations can be measured and quantified using several different parameters including: displacement, velocity, and acceleration. Ground vibrations are typically measured by the velocity of the ground surface and reported as Peak Particle Velocity or PPV. Typical units of PPV are inches per second (in/sec) in the US system or millimeters per second (mm/sec) in the SI system of units. Typical construction activity that generates vibrations includes: pile driving, heavy equipment operation, concrete breaking (jackhammers), and truck/equipment traffic. Although the level of vibrations generated from these sources can vary widely, some typical vibration levels have been included in Table 1.

Table 1: Typical ground vibrations from construction equipment (Hanson, Towes and Lance 2006)

Equipment		PPV (in/sec) (Distance = 25 ft.)
Pile Driver (impact)	upper range	1.518
	typical	0.644
Pile Driver (vibratory)	upper range	0.734
	typical	0.170
Bulldozer	large	0.089
	small	0.003
Caisson Drilling		0.089
Loaded Trucks		0.076
Jackhammer		0.035

Table 1 shows that under typical conditions, pile driving has the potential to create large vibration levels, relative to other construction activity. The pile installation method, however, can affect the level of vibrations. High displacement piles are typically driven using an impact hammer and low displacement piles are sometimes driven using a vibratory hammer. Research has shown that the vibration magnitudes from vibratory hammers are typically smaller than from impact hammers. Additionally, installation techniques such as pre-boring and jetting can reduce vibration levels from impact pile driving (Woods 1997).

The mechanism of vibration formation is the transfer of energy from the pile driving hammer to the pile and then to the surrounding soil. The transfer of energy comes from two main sources. The first is the skin friction that is developed along the surface of the pile and the second is the displacement of the soil at the pile tip. For high displacement piles, the main source of energy transfer is at the pile tip. Several factors can affect the magnitude of vibrations including pile size, pile type, soil type, and the hammer energy. The most important factor in determining vibration levels is the distance from the pile, since vibrations will mitigate or dampen with distance from the source (Dowding 1996).

Damage Thresholds

Vibrations generated from construction activity can cause several concerns at adjacent structures that range from annoyance to structural damage. Several studies have been conducted to determine the relationship between vibration levels, human perception, and structural damage. Table 2 contains a summary of a study reported by Hendriks (2002) for continuous vibrations. The study concluded that vibration levels that are large enough to “annoy people” are at threshold levels for architectural damage to structures that contain plaster walls or ceilings. Since these levels are below levels of even minor structural damage, the perception of building occupants can sometimes lead to discrepancies in the effects of vibrations. The values listed in Table 2 are generally conservative when compared to pile driving vibrations since they were developed for continuous vibrations. Pile driving operations develop discontinuous vibrations that can reduce the damage potential (Hendriks 2002).

Table 2: Continuous vibration levels and effects (Hendriks 2002)

Vibration Level (Peak Particle Velocity)	Human Reaction	Building Effects
0.006-0.019 in/sec	Threshold of perception;	Vibrations unlikely to cause damage
0.08 in/sec	Vibration readily perceptible	Recommended upper level for ruins and ancient monuments
0.1 in/sec	Continuous vibrations begin to annoy people	Virtually no risk of “architectural” damage to normal buildings
0.2 in/sec	Vibrations annoying to people in buildings	Threshold at which there is a risk of “architectural” damage to normal dwelling- houses with plaster wall and ceilings
0.4-0.6 in/sec	Vibrations considered unpleasant by people subjected to continuous vibrations	Vibrations at a greater level than normally expected from traffic, but would cause “architectural” damage and possible minor structural damage

In addition to the many studies to determine the effect of vibrations on structures, several State and Federal Agencies, as well as, International Organizations have developed guidelines on permissible vibration levels due to construction activity. Much of the early work related to vibrations was performed by the United States Bureau of Mines (USBM) in the 1970’s and 80’s (Siskind, et al. 1980). This research focused on vibrations from blasting operations. Figure 2 shows the recommended vibration limits for blasting as a function of frequency. The limits range from 0.2 to 2.0 inches per second (in/sec).

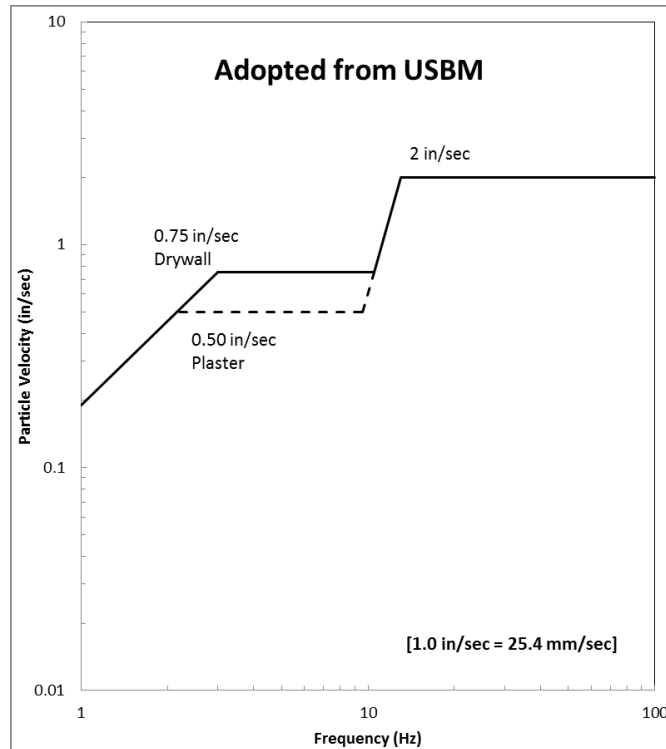


Figure 2: Vibration limits from the USBM (Siskind, et al. 1980)

The American Association of State Highway and Transportation Officials (AASHTO) and the Federal Transit Administration (FTA) have developed guidelines for vibration limits that range from 0.1 to 1.5 in/sec depending on the structure type as shown in Table 3.

Table 3: AASHTO and FTA criteria for construction vibrations

Organization/Jurisdiction	Comments	PPV (in/sec)
American Association of State Highway and Transportation Officials (AASHTO 1990)	Residential buildings, plastered walls	0.2-0.3
	Residential buildings in good repair with gypsum board walls	0.4-0.5
	Engineered structures, without plaster	1.0-1.5
	Historic sites or other critical locations	0.1
Federal Transit Administration (FTA 2006)	Reinforced-concrete, steel or timber	0.5
	Engineered concrete and masonry	0.3
	Non-engineered timber and masonry	0.2
	Buildings extremely susceptible to vibration damage	0.12

The vibration criteria developed by the various states also have a wide range of values as shown in Table 4. If the table is carefully analyzed, the vibration limits can be divided into several categories including: modern structures, sensitive structures, and miscellaneous structures. The range of vibration limits for modern structures is from 0.4 to 1.0 in/sec and sensitive structures have a range of 0.08 to 0.2 in/sec. These vibration limits correlate well to the AASHTO and FTA limits. A thorough review of construction vibration limits can be found in several reports including: (Tao and Zhang 2012), (Wilson Ihrig & Associates 2012), and (Cleary 2013).

Table 4: State criteria for construction vibrations

Organization/Jurisdiction	Comments	PPV (in/sec)
California Department of Transportation (Caltrans 2002)	Upper level for possible damage	0.4-0.6
	Threshold for damage to plaster	0.20
	Ruins and ancient monuments	0.08
Florida DOT (FDOT 2010)	All construction	0.5
	Fresh concrete	1.5
Iowa DOT (Iowa DOT n.d.)	Project specific specification	0.2
Louisiana Department of Transportation and Development (Tao and Zhang 2012)	General scenario	
	- New requirements	0.5
	- Old requirements	0.2
	Historic structures or loose sandy soil	0.1
New Hampshire DOT (NH DOT 2010)	Modern Homes	0.75
	Older Homes	0.50
New York City DOT (New York City DOT 2009)	Piles driven adjacent to subway structures (may be lowered)	0.5
Rhode Island DOT (RIDOT 2010)	Lower limits may be applied by engineer	1.0

Dynamic Settlement

In addition to structural damage and human perception, dynamic settlement can occur due to construction vibrations. Research has shown that if loose cohesionless soils (loose sands) are present, relatively low vibration levels can cause densification (Dowding 1996). This densification can lead to settlement related damage in adjacent structures. Loose sands are typically defined as having a relative density less than 40% (Tao and Zhang 2012). Dynamic settlement has occurred in some soils at vibration levels as low as 0.1 in/sec. If loose sands are located on or near a project site, then special considerations for construction vibrations need to be considered.

Vibration Prediction

Since it is typically unrealistic for most construction projects to conduct full scale testing to determine the expected levels of vibrations and since only a discrete number of locations are measured during testing, several methods have been developed to predict vibration levels. The first prediction equations were developed as early as 1912 by Golitsin who developed a simple equation to predict the peak particle displacement of ground vibrations from earthquakes. The equation, as reported by (Bayraktar, et al. 2013) is as follows,

$$A_2 = A_1 \sqrt{r_1/r_2} e^{-\gamma(r_2-r_1)}, \quad (1)$$

where A_1 is the peak particle displacement of ground vibrations at a distance r_1 from the source, A_2 is the peak particle displacement of ground vibrations at a distance r_2 from the source, and γ is a vibration attenuation coefficient.

More recently, several methods have been developed to predict the peak particle velocity (PPV) from construction activity, pile driving in particular. Hendriks (2002) reported several equations to predict the propagation of construction vibrations. The first equation presented by Hendriks was first reported by Richart, et.al. (1970), who cited Bornitz (1931),

$$V = V_o (D_o/D)^{0.5} e^{\alpha(D_o-D)} \quad (2)$$

where V is the peak particle velocity at distance D , V_o is the peak particle velocity at reference distance D_o , and α is a vibration attenuation parameter that must be determined experimentally.

Hendriks (2002) also reported a simplified equation for pile driving vibrations that is similar to an equation reported by Woods (1997) as follows,

$$V = V_o (D_o/D)^k \quad (3)$$

where V is the peak particle velocity at distance D , V_o is the peak particle velocity at reference distance D_o , and k is a vibration attenuation parameter that must be determined experimentally.

Several researchers have found that a better correlation with predicted and measured vibrations could be determined by including the energy of the pile driving hammer in the equation. This approach is often referred to as the “scaled-distance” approach. One commonly used equation was developed by Wiss and reported by Bayraktar, et al. (2013),

$$v = k [D/\sqrt{W_t}]^{-n} \quad (4)$$

where W_t is the energy of the source, v is the peak particle velocity at distance D , k is the intercept value of the peak particle velocity at a scaled distance of $D/(W_t)^{1/2}$ equal to one, and n is a vibration attenuation parameter that must be determined experimentally.

The previous equations are relatively accurate at predicting ground vibrations when compared to experimental data, however, they all require testing to determine the soil parameters. Jones & Stokes (2004) performed an extensive literature review and determined that the following equation, with the assumed values shown, could be used to predict pile driving vibrations without experimental evaluations:

$$PPV_{Impact\ Pile\ Driver} = PPV_{Ref}(25/D)^n(E_{equip}/E_{ref})^{0.5} \quad (5)$$

where $PPV_{Impact\ Pile\ Driver}$ is the peak particle velocity at distance D in feet, PPV_{Ref} is equal to 0.65 in/sec for a reference pile driver at 25 feet, E_{ref} is equal to 36,000 ft-lb (rated energy of reference pile driver), E_{equip} is the rated energy of impact pile driver in foot-pounds, and n is a vibration attenuation parameter with a recommended value of 1.1.

Jones and Stokes also provided a table, Table 5, with suggested “n” values based on the soil type.

Table 5: Suggested “n” values based on soil class: Adopted from (Jones & Stokes 2004)

Soil Class	Description of Soil	Suggested Value of “n”
I	Weak or soft soils: loose soils, dry or partially saturated peat and muck, mud, loose beach sand, and dune sand, recently plowed ground, soft spongy forest or jungle floor, organic soils, top soil. (shovel penetrates easily)	1.4
II	Competent soils: most sands, sandy clays, silty clays, gravel, silts, weathered rock. (can dig with shovel)	1.3
III	Hard soils: dense compacted sand, dry consolidated clay, consolidated glacial till, some exposed rock. (cannot dig with shovel, need pick to break up)	1.1
IV	Hard, competent rock: bedrock, freshly exposed hard rock. (difficult to break with hammer)	1.0

EXPERIMENTAL DESIGN

Overview

The main objective of this research was to determine the distance from nearby structures that pile driving operations can be conducted with minimal risk to those structures. It is important to note that these guidelines were developed for typical piles used by ALDOT at the project site. The project was divided into two phases, collecting data during pile driving and analyzing the data. The information related to the project site, the test piles, the pile driving equipment, and the data collection equipment is located below.

Project Site

The project site is located on the west bank of the Mobile River, just south of the Alabama Cruise Terminal. The soil profile at the site consists primarily of sandy soils to a depth of 90 feet below the ground surface with a clay layer located at an approximate depth of 90 to 110 feet. Table 6 contains a summary of the soil layers that were defined by a standard penetration test (SPT) conducted at the project site. Appendix A contains the details of the soil investigations conducted by an ALDOT drill crew and Southern Earth Sciences.

Table 6: Soil profile at site location

Depth (ft.)	Basic Material	Average Blow Count	Consistency
0-23.5	Sand	12	Loose to Medium
23.5-89.5	Sand	31	Medium to Dense
89.5-108.5	Clay	28	Stiff to Very Stiff
108.5-115	Sand	27	Medium

Figure 3 contains a plan view of the project site. The dashed line in the figure represents the approximate property boundary. Note that the pile locations are approximate and the drawing is not to scale. The arc lines shown in the drawing represent the approximate distance from the piles to where the monitoring equipment was located.

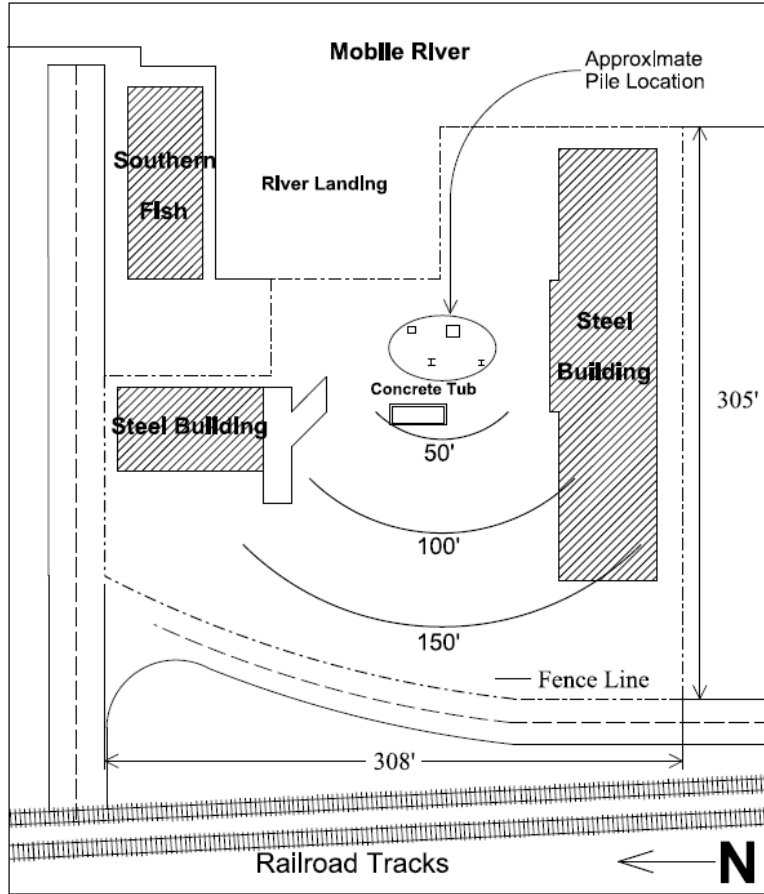


Figure 3: Plan view of Mobile River Bridge Project Site

Four test piles were driven for this project, two prestressed precast concrete piles (PPC) and two steel H-Piles. Table 7 contains descriptions of the piles and Appendix B contains the details of the two pile driving hammers utilized on this project. The piles were installed using typical techniques including pile jetting or vibration followed by driving with a diesel hammer. The concrete piles were jetted to a depth of approximately 30 feet and driven to the final elevation using a Delmag Model D-62-22 diesel hammer. A vibratory driver was used to drive the steel HP 14 to 55 feet and the HP 12 to 15 feet. The steel piles were then driven to the final elevation using an APE Model D30-42 diesel hammer.

Table 7: Pile descriptions

Pile	Cross Section	Material	Length
#1	24" Square	Precast Concrete	81 ft
#2	36" Square	Precast Concrete	89 ft
#3	HP14x117	Steel	106 ft
#4	HP12x53	Steel	70 ft

Vibration Monitoring

Data collectors were placed at various locations throughout the pile installation and testing process. The data collectors utilized for this project were Minimate Plus tri-axial geophones manufactured by Instatel. Each tri-axial geophone unit contains three geophones oriented on three mutually perpendicular axes. The units come with software allowing data collection and analysis in several configurations. For this research, the units were configured to collect histogram data during two-second intervals. When configured in this way the data collector measures all vibrations over the interval, but only records the maximum PPV and the frequency that it occurred at for each geophone over the two second interval.

The geophones were placed at predetermined distances from each pile during installation. Three of the data collectors were located at approximately 50, 100, and 150 feet. A fourth data collector, which had two geophone units attached to it, was located at various distances throughout testing to collect additional information. Table 8 contains a detailed account of the location of each data collector during testing.

During the initial driving of the 36-inch PPC pile, geophone number three was located at the edge of the project site near Southern Fish and Oyster, an adjacent property owner. The fourth data collector had one geophone unit placed at 100 feet from the pile and the other geophone unit was attached to the brick façade of a building that was located on the project site. Please note that the 30-day restrike was at 32-days for the 36-inch concrete pile and 31-days for the 24-inch concrete pile.

Table 8: Geophone location during testing

Initial Drive	Pile Type	Geophone Unit					#4b
		#1	#2	#3	#4a		
Aug. 19, 2013	36" PCP	50 ft	150 ft	69 ft	100 ft	Building	
Aug. 20, 2013	24" PCP	99.5 ft	142 ft	n/a	n/a	n/a	
Aug. 21, 2013	HP 12	53 ft	101 ft	144 ft	n/a	n/a	
Aug. 21, 2013	HP 14	58 ft	106 ft	146 ft	n/a	n/a	
24 Hour Restrike							
Aug. 22, 2013	HP 12	50 ft	150 ft	100 ft	n/a	n/a	
Aug. 22, 2013	HP 14	50 ft	150 ft	100 ft	n/a	n/a	
3-Day Restrike							
Aug. 22, 2013	36" PCP	50 ft	n/a	100 ft	n/a	n/a	
Aug. 23, 2013	24" PCP	50 ft	150 ft	100 ft	n/a	n/a	
7-Day Restrike							
Aug. 26, 2013	36" PCP	50 ft	150 ft	100 ft	75 ft	125 ft	
Aug. 27, 2013	24" PCP	50 ft	150 ft	100 ft	75 ft	125 ft	
30-Day Restrike							
Sept. 20, 2013	36" PCP	50 ft	150 ft	100 ft	n/a	n/a	
Sept. 20, 2013	24" PCP	55 ft	155 ft	105 ft	n/a	n/a	
Sept. 20, 2013	HP 12	50 ft	150 ft	100 ft	n/a	n/a	
Sept. 20, 2013	HP 14	50 ft	150 ft	100 ft	n/a	n/a	

RESULTS

Vibration Levels

Vibrations were monitored during installation and restrikes on the 36-inch concrete pile at three, seven, and thirty days. A communication error occurred between the ALDOT personnel, the pile driving contractor, and the research team during the installation of the 24-inch concrete pile which resulted in the start of driving prior to the installation of the vibration monitors. Due to this error, the 24-inch concrete pile only had vibrations monitored during the final stage of driving and at all restrikes. The steel piles were monitored during installation and during the one day and thirty day restrikes.

Baseline vibration data was collected at the project site by monitoring vibration levels due to railroad activity from a pair of railroad tracks located adjacent to the project site, Figure 3. The approximate distance from the tracks to the data collectors was determined and the vibration levels from train activity were evaluated. Due to the relatively low vibration levels recorded during train activity, baseline data was not collected for truck traffic.

The vibration data collected from the project site was analyzed and the peak particle velocity (PPV) from each pile was recorded. Table 9 contains a summary of the results. The largest recorded vibration during this study occurred while driving the 36-inch concrete pile and resulted in a PPV of 0.82 inches per second at a distance of 50 feet.

Table 9: Maximum PPV (in/sec) during pile driving operations

Vibration Source	Horizontal Distance from Pile		
	50 feet	100 feet	150 feet
36" Concrete Pile	0.82	0.28	0.15
HP14x117	0.18	0.09	0.11
HP12x53	0.23	0.07	0.08
Railroad Activity	0.03 ¹	0.02 ¹	0.02 ¹

¹The approximate distances were 60, 110, and 160 feet

Figure 4 shows the maximum PPV for the 36-inch concrete pile, the H-Piles, and railroad activity observed during testing. Since the maximum vibrations occurred during the beginning of the driving process, the 24-inch concrete pile was not included in this figure. The figure confirms that the largest vibrations recorded were associated with the installation of the 36-inch concrete pile.

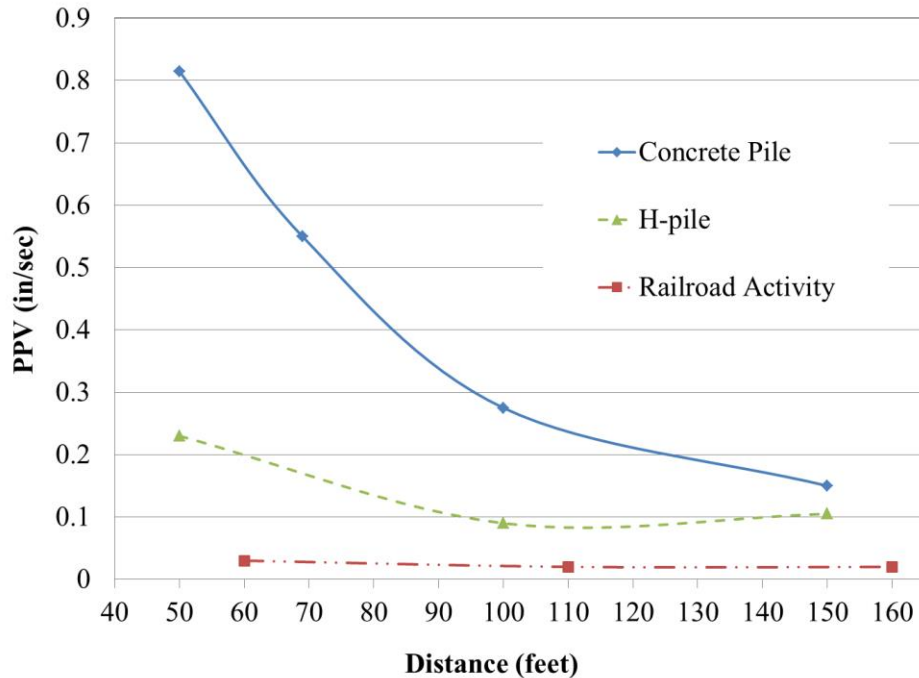


Figure 4: Maximum recorded vibration levels during pile installation

During the driving of the 36-inch concrete pile, one of the geophones was attached to the brick façade of a building that was located on the project site. The building was located to the south of the piles, Figure 3, and was approximately 90 feet from the 36-inch concrete pile. The brick façade was located on the west end of the building and was approximately 140 feet from the pile. The data from this geophone was analyzed and it was determined that the vibration levels were below the threshold for detection, 0.005 in/sec. This indicates that the ground vibrations did not have enough energy to cause vibrations in the building. Additionally, crack width monitors were installed on the outside wall of the building. The crack widths and lengths were monitored throughout the project and it was determined that there were no changes in any of the cracks.

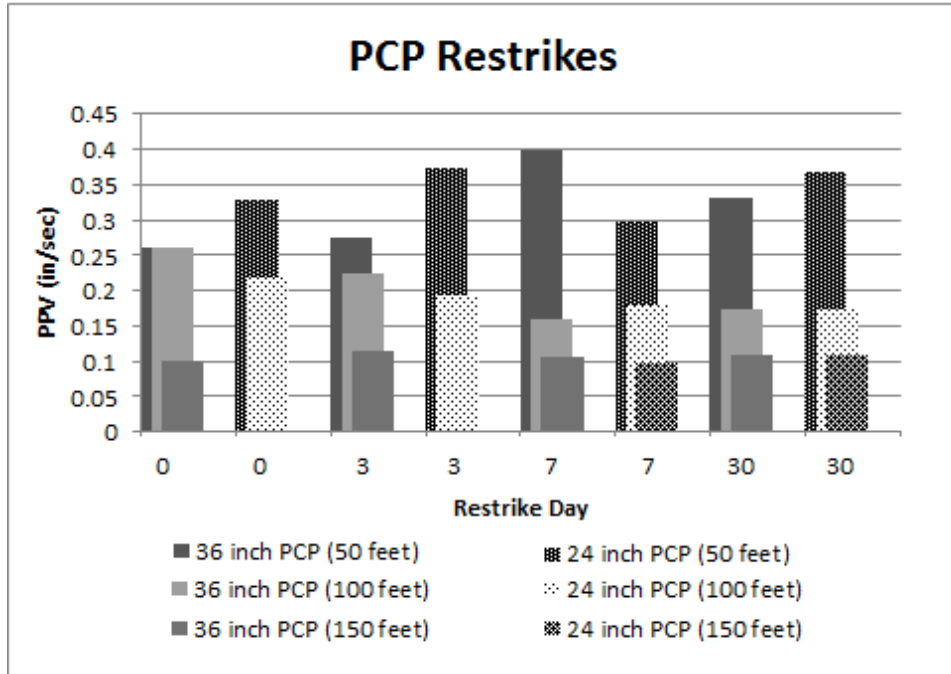


Figure 5: Bar chart of restrikes on precast concrete piles (PCP)

An analysis was performed to compare the vibrations between the 24- and 36-inch concrete piles since data was not collected throughout the driving of the 24-inch pile. Figure 5 shows a bar chart of the vibration levels for each of the concrete piles during the restrikes, note that day zero is at the end of drive. Figure 6 shows the same data in the form of a data plot. The data indicates that the vibration levels for the 24- and 36-inch concrete piles are similar and that the maximum vibrations, near the start of driving, would be expected to be approximately equal for each concrete pile.

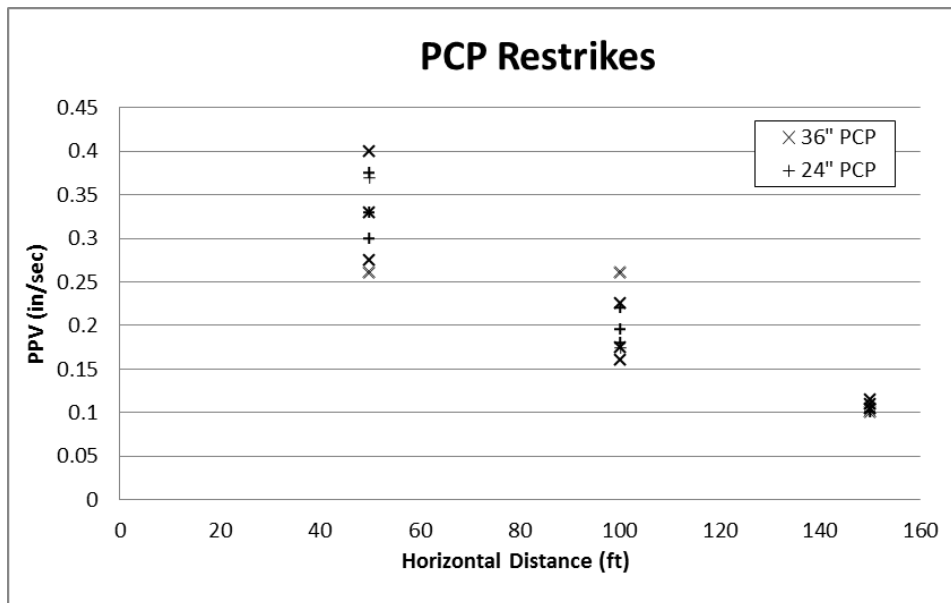


Figure 6: Data plot of restrikes on precast concrete piles (PCP)

Prediction Equation

The second major objective of this project was to develop a methodology to predict the vibration level at various distances from the pile location. Since the primary use of this research is for determining the vibration levels for piles typically used by ALDOT located at or near the project site, two prediction equations were developed. The equations are based on the maximum peak particle velocities while driving the 36-inch concrete pile and the H-piles. Both equations are based on Equation 3, as presented by Hendriks (2002), where the vibration attenuation parameter (k) was determined with the experimental data. Equation 6 was developed to predict vibrations for 36 inch concrete pile,

$$PPV = 0.15 \left(\frac{150}{d} \right)^{1.6}, \quad (6)$$

and Equation 7 was developed to predict vibrations for the H-piles,

$$PPV = 0.23 \left(\frac{50}{d} \right)^{1.6}, \quad (7)$$

where, in both equations, PPV is the peak particle velocity at distance (d) in inches per second and d is the distance from the pile in feet.

Figure 7 shows a plot of the experimental data and the peak particle velocities based on the prediction equation. The results indicate that the prediction equation model fit the experimental data well. However, due to the unusual increase in vibration magnitude at 150 feet for the H-piles, the prediction equation under-predicts the vibration magnitude at 150 feet. It was also noted that the soil attenuation parameter (k) for both equations was determined to be 1.6. This was expected since the parameter is primarily dependent on the soil properties and less dependent on the pile type or hammer energy.

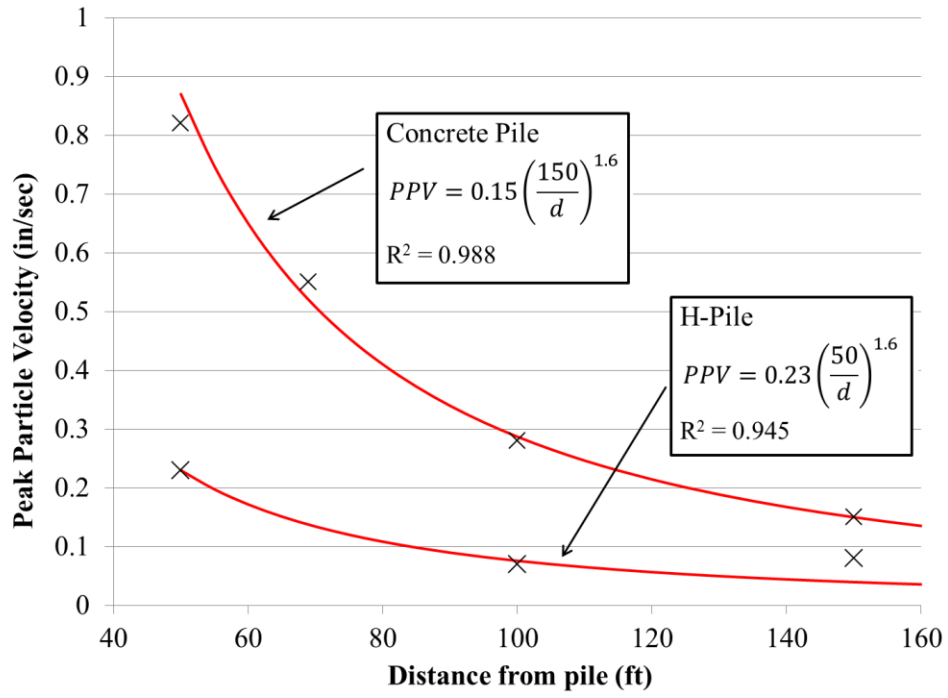


Figure 7: Peak particle velocity versus distance

CONCLUSIONS

The experimental data shows that the largest vibrations occurred during the installation of the 36-inch concrete pile, which was recorded as 0.82 inches per second. According to the research presented in Table 2 (Hendriks 2002), a vibration level of 0.82 inches per second has the potential to cause structural damage to an adjacent structure. However, this vibration was recorded at a distance of 50 feet from the pile; the vibration level at 100 feet from the pile was reduced to 0.275 inches per second. This vibration level could cause potential architectural damage to buildings constructed with plaster, but would not likely cause structural damage. At 150 feet the vibration levels were reduced to 0.15 inches per second, a level that would have little to no risk of damage to adjacent structures.

Based on the experimental data and a thorough review of the literature, it is recommend that a maximum vibration level of 0.5 inches per second for modern structures and 0.1 inches per second for potentially sensitive structures be allowed for construction activity at or near the location of the project site. These vibration levels are the allowable levels at the location of the structure. To determine if any structures should be surveyed and monitored for potential vibration damage, a survey distance of 150 feet for modern structures and 250 feet for potentially sensitive structures should be established. The monitoring distances should be measured from the source of the vibration. The ground vibration prediction equation that was developed would estimate a peak particle velocity of 0.15 inches per second at 150 feet and 0.07 inches per second at 250 feet. The survey distances are well beyond the distance where the prediction equation would estimate vibration levels of 0.5 and 0.1 inches per second and therefore would represent conservative survey distances to ensure adjacent structures are not damaged.

Recommendations for Future Research

The research presented in this report contains detailed analysis for a particular location in the state of Alabama; however, data has not been collected and analyzed for other regions of the state with differing soil conditions. A state wide research project should be initiated to determine vibration propagation and attenuation criteria for soil conditions located throughout the state. This data could be used to develop prediction equations that could be used in project planning. Additionally, the results of this research could be used to develop model vibration specifications for the state of Alabama.

In addition to the research mentioned above, it is recommended that a vibration monitoring program be developed for any large scale construction projects in urban environments. These programs could be used not only to ensure the construction activity is not damaging nearby structures, but to ensure the public that the DOT is proactive in preventing damage.

REFERENCES

- AASHTO. *Standard recommended practice for evaluation of transportation-related earthborne vibrations*. Washington, DC: Designation R8-81, American Association of State Highway and Transportation Officials, 1990.
- Bayraktar, Mehmet Emre, Youngcheol Kang, Mark Svinkin, and Farrukh Arif. *Evaluation of Vibration Limits and Mitigation Techniques for Urban Construction*. Final Report (FDOT Contract No.: BDK80 977-22), Tallahassee, FL: Florida Department of Transportation, 2013.
- Board, Transportation Research. *NCHRP Synthesis of Highway Practice: Dynamic Effects of Pile Installation on Adjacent Structures*. Engineering, Washington, D.C: National Research Council, 1997.
- Caltrans. *Transportation Related Earthborne Vibrations*. Technical Advisory, TAV-02-01-R9601, California Department of Transportation, 2002.
- Cleary, John. "Synopsis on State Requirements for Vibrations During Pile Driving." *ASCE Texas Section Fall Conference and ASCE Construction Institute Summit*. Dallas, Texas, 2013.
- Dowding, Charles H. *Construction Vibrations*. Upper Saddle River, NJ: Prentice Hall, 1996.
- FDOT. *Standard Specifications for Road and Bridge Construction*. Florida Department of Transportation, 2010.
- FTA. *Transit Noise and Vibration Impact Assessment*. Washington, DC: Federal Transit Administration, Prepared by C.E. Hanson, D.A. Towers, and L.D. Meister, Prepared for the Office of Planning and Environment, 2006.
- Google, Google Maps. "*Mobile, AL.*" Map. November 1, 2013.
- Hanson, Carl, David Towes, and Meister Lance. *Transit Noise and Vibration Impact Assessment*. Washington D.C.: United States of America Department of Transportation, Federal Transit Administration, 2006.
- Hendriks, Rudy. *Transportation Related Earthborne Vibrations*. Engineering, Sacramento: California Department of Transportation, 2002.
- Iowa DOT. *Special Provisions for Vibration Monitoring (Multiple)*. Iowa Department of Transportation, n.d.
- Jones & Stokes. *Transportation- and construction-induced vibration guidance manual*. June. (J&S 02-039.) Sacramento, CA. Prepared for California Department of Transportation, Noise, Vibration, and Hazardous Waste Management Office, 2004.

- New York City DOT. *Standard Highway Specifications*. New York City Department of Transportation, 2009.
- NHDOT. *Standard Specifications for Road and Bridge Construction*. New Hampshire Department of Transportation, 2010.
- Richart, F. E., R. D. Woods, and J. R. Hall. *Vibrations of Soils and Foundations*. Englewood Cliffs, New Jersey: Prentice-Hall, 1970.
- RIDOT. *Standard Specifications for Road and Bridge Construction*. Rhode Island Department of Transportation, 2010.
- Siskind, D E, M S Stagg, J W Kopp, and C H Dowding. *Structure Response and Damage Produced by Ground Vibration From Surface Mine Blasting*. Washington, D.C.: Report of Investigations 8507, U.S. Bureau of Mines, 1980.
- Tao, Mingjiang, and Mo Zhang. *Update LADOTD Policy on Pile Driving Vibration Management*. FHWA/LA.11/483: Louisiana Department of Transportation and Development, 2012.
- Wilson Ihrig & Associates, ICF International, and Simpson Gumpertz & Heger. *Current Practices to Address Construction Vibration and Potential Effects to Historic Buildings Adjacent to Transportation Projects: NCHRP 25-25/Task 72*. National Cooperative Highway Research Program, 2012.
- Woods, R D. *Dymanic Effects of Pile Installations on Adjacent Structures, NCHRP Synthesis 253*. Washington, D.C.: Transportation Research Board, National Research Council, 1997.

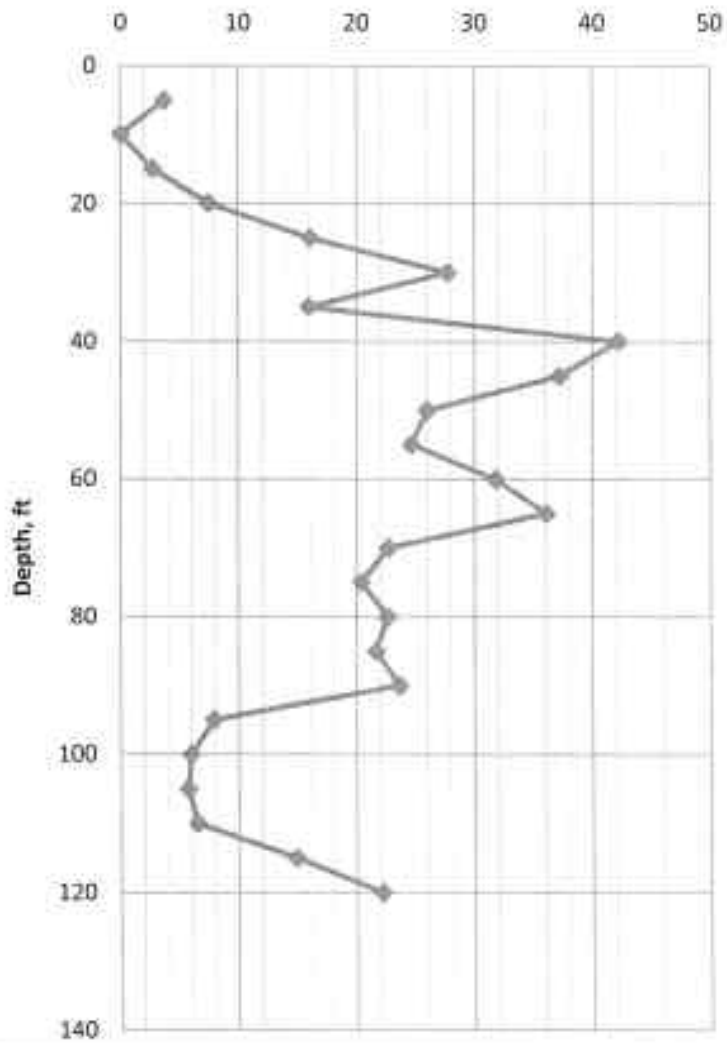
Appendix A: Soil Reports

Two soil investigations were performed at the site. The first was a Standard Penetration Test (SPT), which was performed at two locations. The first location, labeled B-1 in the documents that follow, was located at a property owned by ALDOT that is several hundred feet to the west of the project site. This location was an alternate location for testing. The second location, labeled B-2, was at the project site in the vicinity of where the test piles were installed. The SPT test was performed by an ALDOT drill crew.

The second soil investigation performed was a Seismic Cone Penetration Test (SCPT). Two locations were also investigated, both on the project site. The first test was performed at the location of the test piles and the second was located at 100 to 120 feet from the test piles. The results of both investigations are included here. The SCPT was conducted by Southern Earth Sciences.

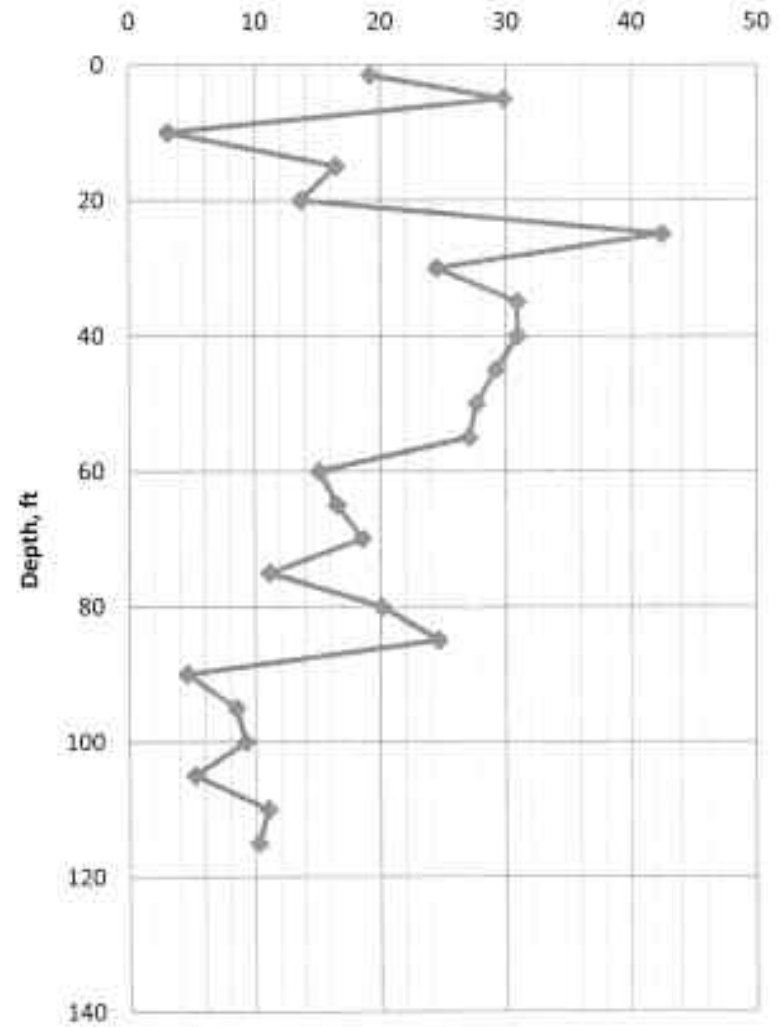
B-1

N_{160} Corrected Blow Count



B-2

N_{160} Corrected Blow Count



Project# DPI-0030 (005) Division 9th

Station _____ Offset _____ Ft _____

Ground Elev. 0.0 Water Elev. in Hole _____

Depth of Strata BOR# B-1 Visual BOR Loc. _____

From	To	Consistency or Density	Approx. Moisture	Color	Basic Matl.
0.0	0.3	Asphalt			
0.3	18.5	v. loose	Moist	Br	br sand
18.5	23.5	Loose	Moist	Br	SAND
23.5	38.5	Med	Moist	TAN	SAND
38.5	63.5	Dense	Moist	TAN	sand
63.5	68.5	Very Dense	Moist	TAN	sand
68.5	93.5	Dense	Moist	Tan	sand
93.5	108.5	stiff	Moist	Gray	Clay
108.5	118.5	HARD	Moist	Gray	Clay
118.5	120.0	DENSE	Moist	Gray	SAND

Remarks by Driller Installed well monitor
 GPS Cord. 42' 1"
 LAT. Water - 10' 3" 24Has
 LONG. _____

County Mobile Date 8-8-12

C/L Driller Young/Evans

Type Drill Used SE 9050 Total Hole Depth 120.0

Identification CME 550x 2 25 Hollow Steels

Other Pertinent Components	Sample No.	Penetration or Sample Elev.		"N" Blow			"N" Value
		From	To	5	1.0	1.5	
	* 1-A	3.5	5.0	1	1	1	2
w/ clay	* 1-B	8.5	10.0	W	0	H	UGH
	* 1-C	13.5	15.0	W	1	1	2
	1-D	18.5	20.0	1	2	4	6
	1-E	23.5	25.0	5	5	9	14
	1-F	28.5	30.0	10	12	14	26
	1-G	33.5	35.0	9	7	9	16
w/ sand	* 1-H	38.5	40.0	26	23	22	45
w/ sand	* 1-I	43.5	45.5	23	23	19	42
large matl	1-J	48.5	50.0	11	14	17	31
	1-K	53.5	55.0	9	16	15	31
	1-L	58.5	60.0	18	20	22	42
	* 1-M	63.5	65.0	20	23	27	50
	* 1-N	68.5	70.0	14	16	17	33
	1-O	73.5	75.0	7	15	16	31

* Samples in JARS

Project# DP1-0030 (005) Division 9th

Station _____ Offset _____ Ft _____

Ground Elev. 0.0 Water Elev. in Hole _____

Depth of Strata BOR# B-2 Visual BOR Loc. _____

From	To	Consistency or Density	Approx. Moisture	Color	Basic Matl.
0.0	0.2	Topsoil	---		
0.2	3.5	Loose	Moist	Br	SAND
3.5	8.5	Med	Moist	Br	SAND
8.5	13.5	✓ Loose	Moist	Br	SAND
13.5	23.5	Med	Moist	Gray	SAND
23.5	28.5	Dense	Moist	Tan	SAND
28.5	33.5	Med	Moist	Tan	SAND
33.5	58.5	Dense	Moist	Tan	SAND
58.5	78.5	Med	Moist	Tan	SAND
78.5	89.5	Dense	Moist	Tan	SAND
89.5	93.5	Stiff	Moist	Gray	Clay
93.5	103.5	✓ Stiff	Moist	Gray	Clay
103.5	108.5	Stiff	Moist	Gray	Clay
108.5	115.0	Med	Moist	Gray	SAND

Remarks by Driller _____

GPS Cord. _____

LAT. _____

LONG. _____

County Mobile Date 8-9-12

C/L Driller Turner/Evans

Type Drill Used SE 9050 Total Hole Depth 115.0

Identification CME 550X 2.25 Hollow Steels

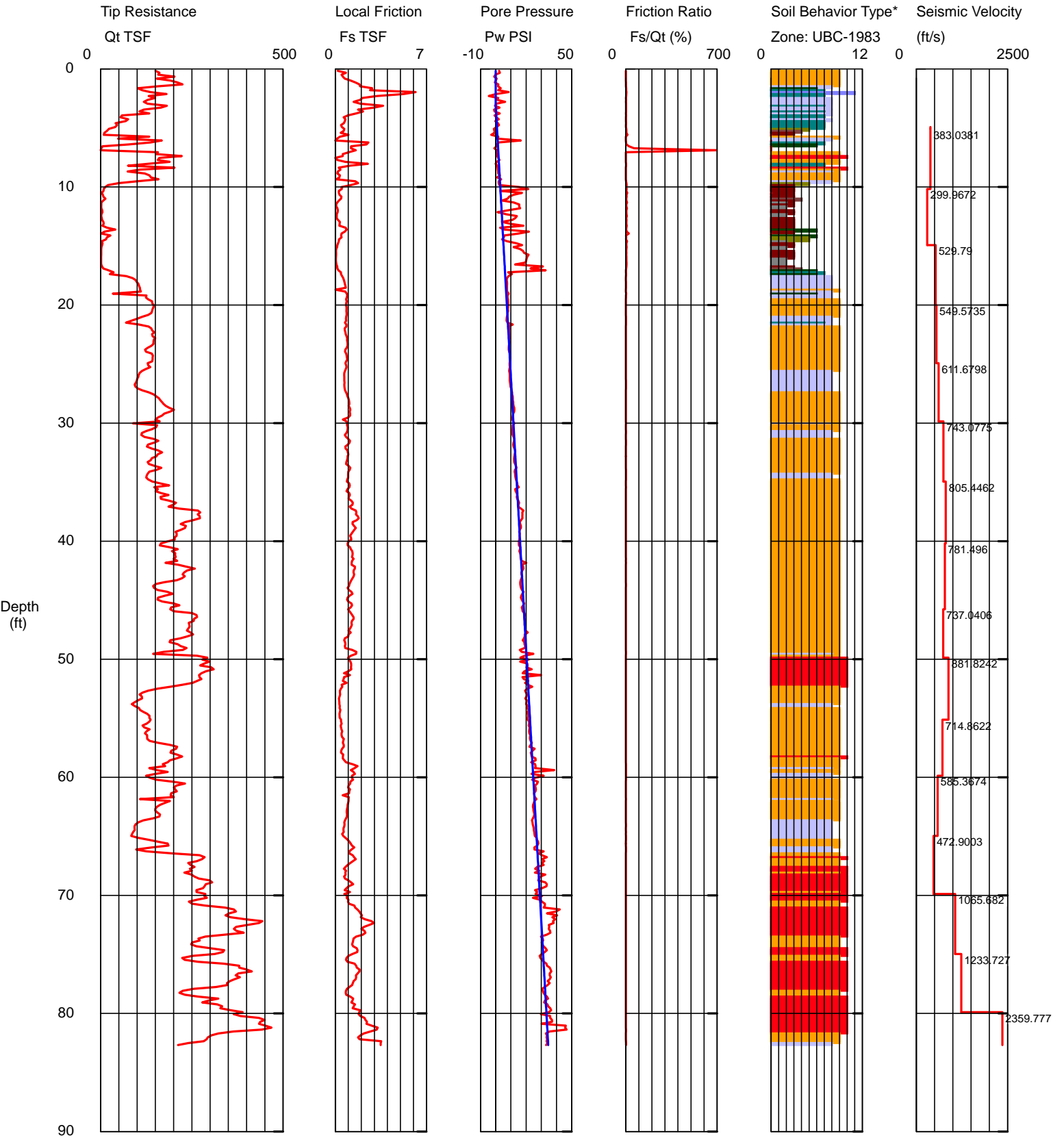
Other Pertinent Components	Sample No.	Penetration or Sample Elev.		"N" Blow			"N" Value
		From	To	5	1.0	1.5	
	* 2-A	0.0	1.5	9	4	4	8
w/Gravel	* 2-B	3.5	5.0	5	7	9	16
w/orig. mat'l	* 2-C	8.5	10.0	1	1	1	2
	* 2-D	13.5	15.0	2	5	7	12
	2-E	18.5	20.0	5	4	7	11
	* 2-F	23.5	25.0	16	14	19	37
	2-G	28.5	30.0	10	11	12	23
	* 2-H	33.5	35.0	7	15	16	31
	2-I	39.5	40.0	7	13	20	33
	2-J	43.5	45.0	9	14	19	33
w/SAND & orig mat'l	2-K	49.5	50.0	7	15	18	33
	2-L	53.5	55.0	10	16	18	34
	* 2-M	58.5	60.0	10	10	10	20
	2-N	63.5	65.0	6	12	11	23
	2-O	68.5	70.0	12	17	10	27

* JAR Sample

Southern Earth Sciences

Operator: Mike Wright
 Sounding: SCPT-1
 Cone Used: DDG0892

CPT Date/Time: 8/14/2013 9:08:56 AM
 Location: Test Pile Evaluation
 Job Number: 13-000



Maximum Depth = 82.68 feet

Depth Increment = 0.164 feet

- 1 sensitive fine grained
 - 2 organic material
 - 3 clay
- Groundwater measured at 3.1'

- 4 silty clay to clay
- 5 clayey silt to silty clay
- 6 sandy silt to clayey silt

- 7 silty sand to sandy silt
- 8 sand to silty sand
- 9 sand

- 10 gravelly sand to sand
- 11 very stiff fine grained (*)
- 12 sand to clayey sand (*)

N30.68546 W88.03791

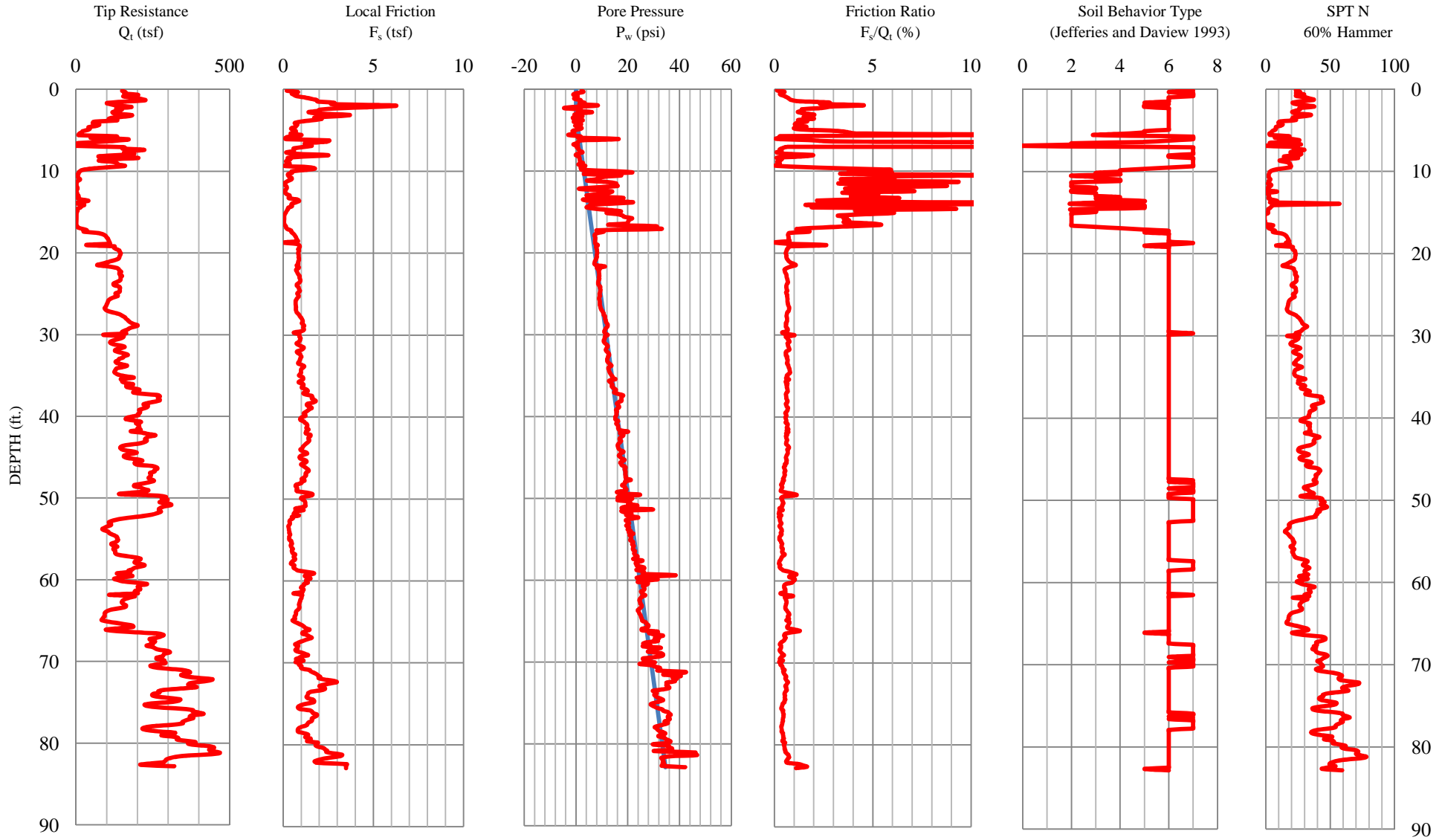
*Soil behavior type and SPT based on data from UBC-1983

CONE PENETRATION TEST LOG

Project Name: Test Pile Evaluation
Project No.: 13-000
Sounding: SCPT-1

Cone Used: DDG0892
Operator: Mike Wright
CPT Date: 8/14/2013

Groundwater Level: 3.1 feet
Elevation: Unknown
Lat/Long: N30.68546 W88.03791



Baseline Data:

	Q_t (tsf)	F_s (tsf)	P_w (psi)
Initial Baseline:	0	0	0
Final Baseline:	-0.602	0.002	-0.172

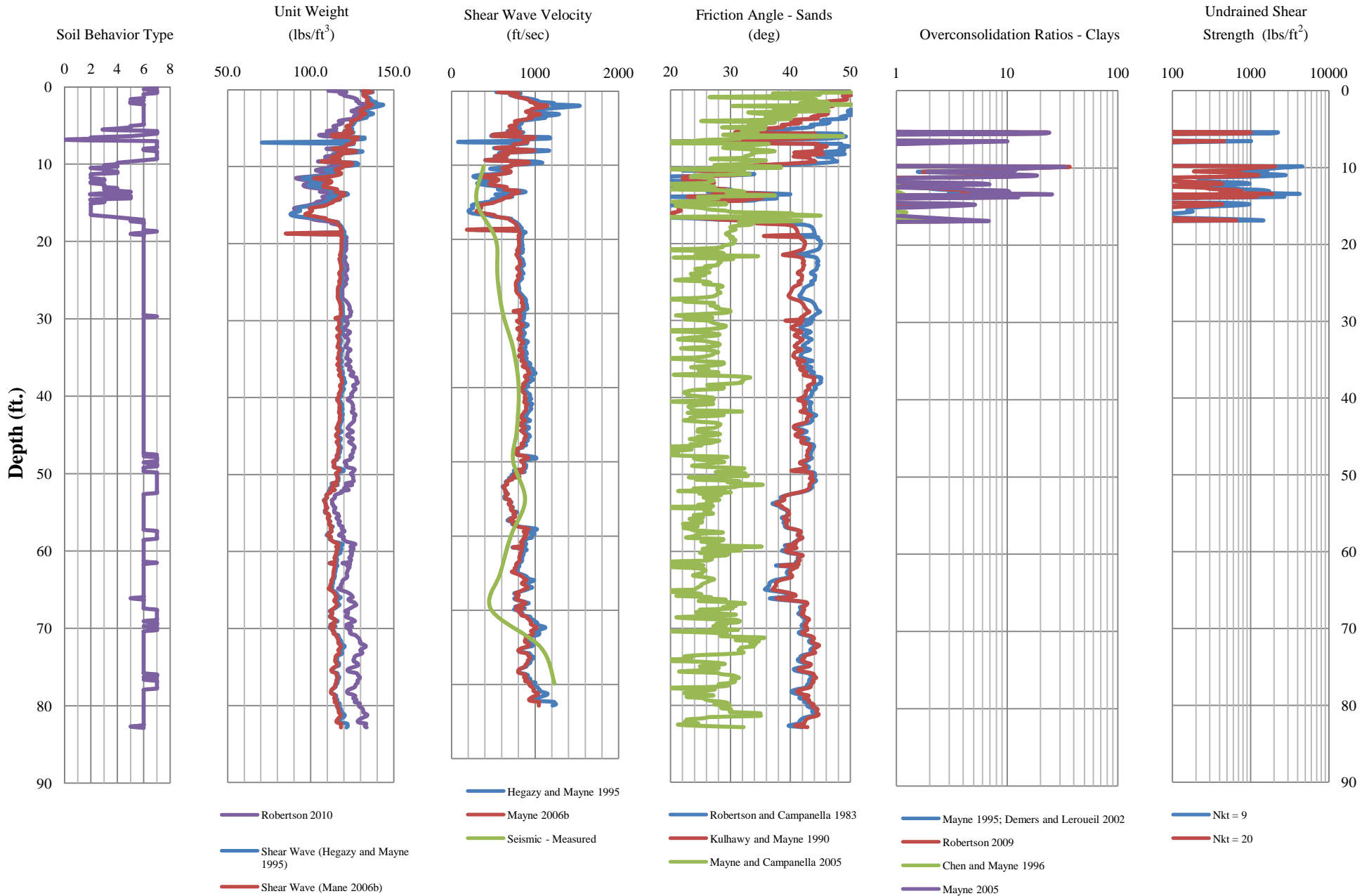
SPT N, SOIL BEHAVIOR TYPE, OR ZONE NUMBER FROM CPT CLASSIFICATION INDEX, I_c
 Organic Clay Soils = 2, Clays = 3, Silt Mixtures = 4, Sand Mixtures = 5, Sands = 6, Gravelly Sands = 7

CONE PENETRATION TEST LOG

Project Name: Test Pile Evaluation
Project No.: 13-000
Sounding: SCPT-1

Cone Used: DDG0892
Operator: Mike Wright
CPT Date: 8/14/2013

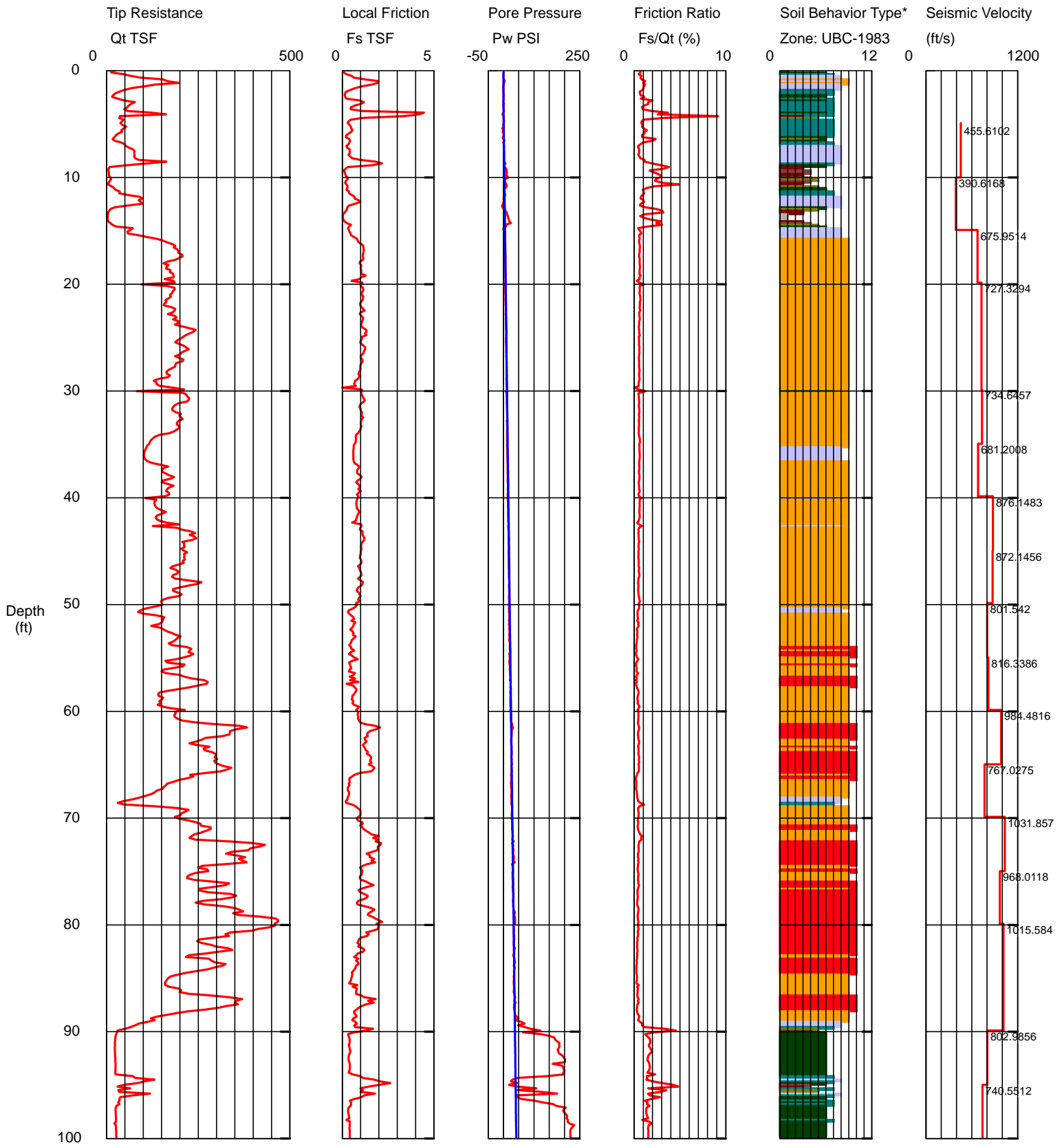
Groundwater Level: 3.1 feet
Elevation: Unknown
Lat/Long: N30.68546 W88.03791



Southern Earth Sciences

Operator: Mike Wright
 Sounding: SCPT-2
 Cone Used: DDG0892

CPT Date/Time: 8/14/2013 10:35:15 AM
 Location: Test Pile Evaluation
 Job Number: 13-000



Maximum Depth = 99.90 feet

Depth Increment = 0.164 feet

- 1 sensitive fine grained
 - 2 organic material
 - 3 clay
- Groundwater measured at 3.2'

- 4 silty clay to clay
- 5 clayey silt to silty clay
- 6 sandy silt to clayey silt

- 7 silty sand to sandy silt
- 8 sand to silty sand
- 9 sand

- 10 gravelly sand to sand
- 11 very stiff fine grained (*)
- 12 sand to clayey sand (*)

N30.68541 W88.03821

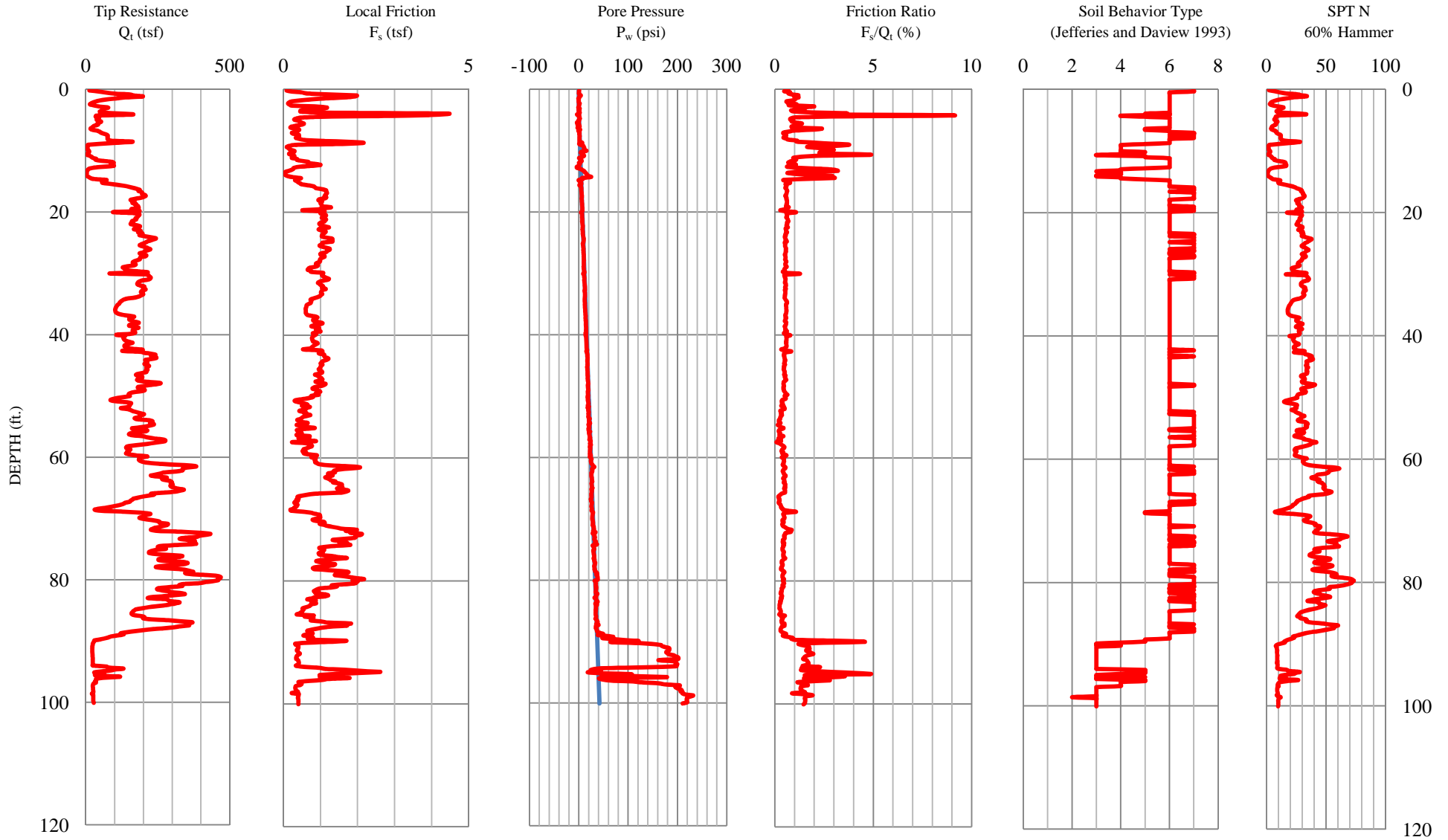
*Soil behavior type and SPT based on data from UBC-1983

CONE PENETRATION TEST LOG

Project Name: Test Pile Evaluation
Project No.: 13-000
Sounding: SCPT-2

Cone Used: DDG0892
Operator: Mike Wright
CPT Date: 8/14/2013

Groundwater Level: 3.2 feet
Elevation: Unknown
Lat/Long: N30.68541 W88.03821



Baseline Data:

	Q_t (tsf)	F_s (tsf)	P_w (psi)
Initial Baseline:	0	0	0
Final Baseline:	0.357	0.012	0.210

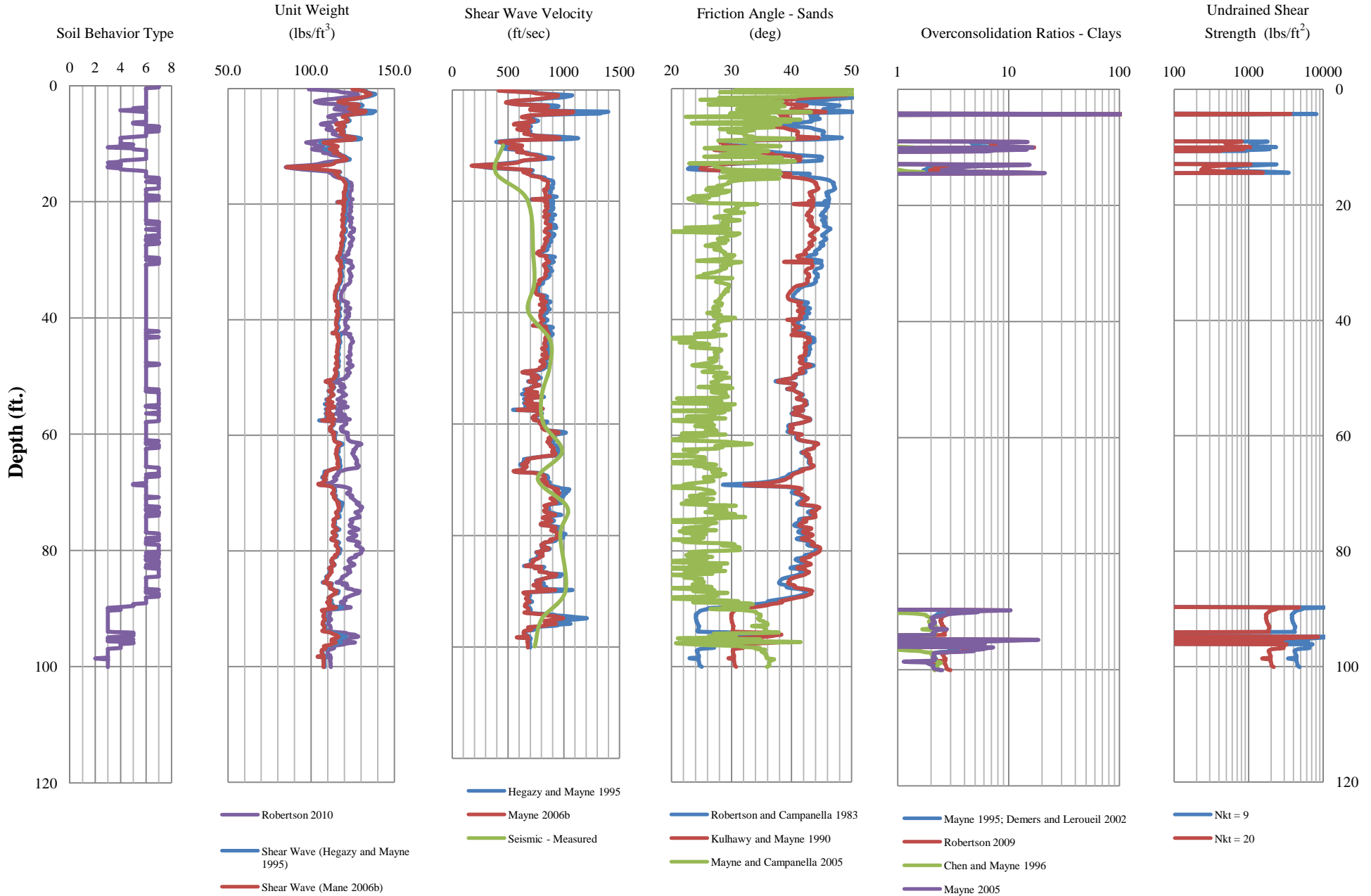
SPT N, SOIL BEHAVIOR TYPE, OR ZONE NUMBER FROM CPT CLASSIFICATION INDEX, I_c
 Organic Clay Soils = 2, Clays = 3, Silt Mixtures = 4, Sand Mixtures = 5, Sands = 6, Gravelly Sands = 7

CONE PENETRATION TEST LOG

Project Name: Test Pile Evaluation
Project No.: 13-000
Sounding: SCPT-2

Cone Used: DDG0892
Operator: Mike Wright
CPT Date: 8/14/2013

Groundwater Level: 3.2 feet
Elevation: Unknown
Lat/Long: N30.68541 W88.03821



Appendix B: Pile Driving Hammer Information

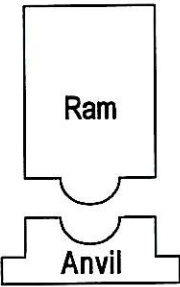
	Fuel Setting #1	Fuel Setting #2	Fuel Setting #3	Fuel Setting #4
Concrete Piles used Delmag Model D-62-22 Single Acting Diesel Hammer				
<u>36 in PCP</u>				
Setting Usage	Down to 43 feet	43 to 45 feet	45 to 48 feet	48 feet to end Restrikes
Rated Energy	78,960 ft. lbs.	109,725 ft. lbs.	138,960 ft. lbs.	165,000 ft. lbs
<u>24 in PCP</u>				
Setting Usage	Down to 61 feet	61 feet to end Restrikes	N/A	N/A
Rated Energy	78,960 ft. lbs.	109,725 ft. lbs.		
Steel Piles used APE Model D30-42 Single Acting Diesel Hammer				
<u>HP 14</u>				
Setting Usage	N/A	N/A	Entire depth Restrikes	N/A
Rated Energy			66,977 ft. lbs.	
<u>HP 12</u>				
Setting Usage	N/A	Entire depth Restrikes	N/A	N/A
Rated Energy		55,070 ft. lbs		

FORM C-14 **ALABAMA DEPARTMENT OF TRANSPORTATION**
 Revised 08-07-95 **PILE AND DRIVING EQUIPMENT DATA FORM**

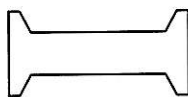
Project Number USA Test Pile & Vibration	County Mobile	Division 9th
---	------------------	-----------------

Pile Driving Contractor or Subcontractor Jordan Pile Driving Inc.	Bridge Identification Number N/A
--	-------------------------------------

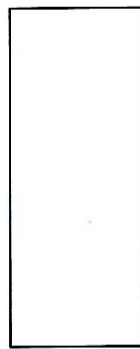
Details of access method to pile top for dynamic testing are: Attached Not Applicable

Hammer Components		Hammer	Manufacturer: <u>Delmag</u> Model: <u>D-62-22</u> Type: <u>S.A. Diesel</u> Serial No.: <u>238</u> Rated Energy: <u>165,000</u> (ft.-lbs.) at <u>11.3</u> (ft.) Length of Stroke Modifications: <u>Adjustable Fuel Pump</u> <table border="1"> <tr><td>Pump Setting 1</td><td>78,960 ft. lbs.</td></tr> <tr><td>Pump Setting 2</td><td>109,725 ft. lbs.</td></tr> <tr><td>Pump Setting 3</td><td>136,950 ft. lbs.</td></tr> <tr><td>Pump Setting 4</td><td>165,000 ft. lbs.</td></tr> </table>	Pump Setting 1	78,960 ft. lbs.	Pump Setting 2	109,725 ft. lbs.	Pump Setting 3	136,950 ft. lbs.	Pump Setting 4	165,000 ft. lbs.
	Pump Setting 1	78,960 ft. lbs.									
Pump Setting 2	109,725 ft. lbs.										
Pump Setting 3	136,950 ft. lbs.										
Pump Setting 4	165,000 ft. lbs.										

	Capblock (Hammer Cushion)	Material: <u>Aluminum & Micarta Alternating</u> Thickness: <u>6</u> (in.) Area: <u>381</u> (in. ²) Modulus of Elasticity - E : <u>450 KSI</u> (P.S.I.) Coefficient of Restitution - e : <u>0.8</u>
---	----------------------------------	---

	Pile Cap	<table border="1"> <tr><td>Helmet</td><td><input checked="" type="checkbox"/></td></tr> <tr><td>Bonnet</td><td><input type="checkbox"/></td></tr> <tr><td>Anvil Block</td><td><input type="checkbox"/></td></tr> <tr><td>Drivehead</td><td><input type="checkbox"/></td></tr> </table> Weight : <u>10,000</u> (lbs.) Note: Should include weight of striker plate.	Helmet	<input checked="" type="checkbox"/>	Bonnet	<input type="checkbox"/>	Anvil Block	<input type="checkbox"/>	Drivehead	<input type="checkbox"/>
Helmet	<input checked="" type="checkbox"/>									
Bonnet	<input type="checkbox"/>									
Anvil Block	<input type="checkbox"/>									
Drivehead	<input type="checkbox"/>									

	Pile Cushion	Cushion Material: <u>Plywood</u> Thickness: <u>10</u> (in.) Area: <u>576</u> (in. ²) Modulus of Elasticity - E : <u>45 KSI</u> (P.S.I.) Coefficient of Restitution - e : <u>0.5</u>
---	---------------------	--

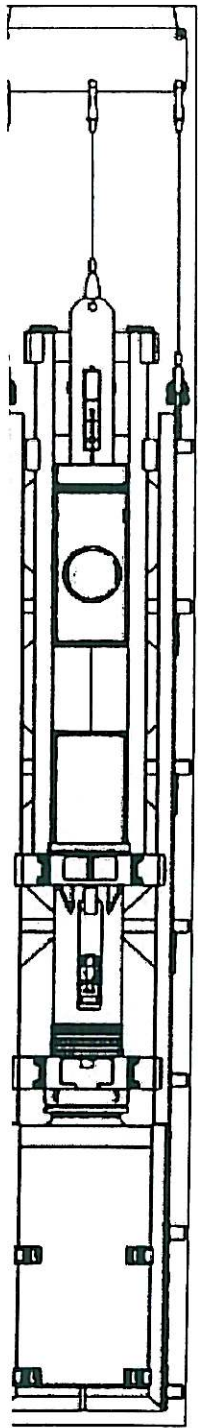
	Pile	Pile Type: <u>36" x 36" & 24" x 24" Prestressed Concrete Test Pile</u> Length (in Leads): <u>89' & 81'</u> (ft.) Weight / Ft: <u>936 & 510</u> (lbs./ft.) Wall Thickness: <u>NA</u> (in.) Taper: <u>NA</u> Cross Sectional Area: <u>489 & 898</u> (in. ²) Design Pile Capacity: _____ (Tons) Description of Splice: <u>N/A</u> Tip Treatment Description: <u>N/A</u>
---	-------------	---

Note: If mandrel is used to drive this pile, attach separate manufacturer's detail sheet(s) including weight and dimensions.

Submitted By: Davis Daniel Date: _____

Model D62-22 Diesel Hammer

Maximum obtainable energy	203,216 ft-lbs
Maximum obtainable stroke	178 inches
Pump setting 1: (minimum)	78,956 ft-lbs
Pump setting 2:	109,749 ft-lbs
Pump setting 3:	137,186 ft-lbs
Pump setting 4: (maximum)	164,250 ft-lbs
Stroke at rated energy	135 inches
Energy at rated stroke	165,000 ft-lbs
Speed (blows per minute)	36-50
Ram	13,700 lbs
Anvil	2,833 lbs
Hammer weight (includes trip device)	29,491 lbs
Typical operating (weight with drive cap)	32,963 lbs
Fuel tank (runs on diesel or bio-diesel)	25.86 gal
Oil tank	8.32 gal
Weight	1100 lbs
Diameter	25 inches
Thickness	8 inches
Type	Monocast MC 901
Diameter	25 inches
Thickness	2 inches
Elastic-modulus	285 kips per square inch
Coeff. of restitution	0.8
Weight (fits 8 by 26 inch leads)	1,350 lbs
Diesel or Bio-diesel fuel	5.28 gal/hr
Lubrication oil	0.84 gal/hr
**Grease twice per day	
Length overall	232.6 inches
Length over cylinder extension	272.0 inches
Impact block diameter	27.9 inches
Width over bolts	32.6 inches
Hammer width overall	31.5 inches
Width for guiding- face to face	22.0 inches
Hammer center to pump guard	19.3 inches
Hammer center to bolt center	15.0 inches
Hammer depth overall	38.2 inches
Minimum clearance for leads	19.7 inches



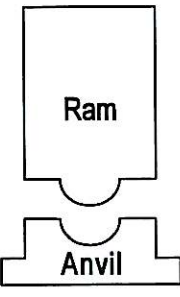
FORM C-14 **ALABAMA DEPARTMENT OF TRANSPORTATION**
 Revised 08-07-95 **PILE AND DRIVING EQUIPMENT DATA FORM**

Project Number: USA Test Pile & Vibration
 County: Mobile
 Division: 9th

Pile Driving Contractor or Subcontractor: Jordan Pile Driving Inc.
 Bridge Identification Number: N/A

Details of access method to pile top for dynamic testing are: Attached Not Applicable

Hammer Components



Hammer

Manufacturer: APE Model: D30-42
 Type: S.A. Diesel Serial No.:
 Rated Energy: 74,419 (ft.-lbs.) at 11.25 (ft.) Length of Stroke

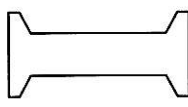
Modifications: Adjustable Fuel Pump

Pump Setting 1	37,209 ft. lbs.
Pump Setting 2	55,070 ft. lbs.
Pump Setting 3	66,977 ft. lbs.
Pump Setting 4	74,419 ft. lbs.



Capblock (Hammer Cushion)

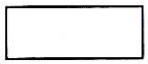
Material: Aluminum & Micarta Alternating
 Thickness: 4 (in.) Area: 398 (in.²)
 Modulus of Elasticity - E : 285 (P.S.I.)
 Coefficient of Restitution - e : 0.8



Pile Cap

Helmet
 Bonnet
 Anvil Block
 Drivehead

Weight : 1,704 (lbs.)
 Note: Should include weight of striker plate.



Pile Cushion

Cushion Material: N/A
 Thickness: N/A (in.) Area: N/A (in.²)
 Modulus of Elasticity - E : N/A (P.S.I.)
 Coefficient of Restitution - e : N/A



Pile

Pile Type: HP 12 x 53 & HP 14 x117
 Length (in Leads): 70' & 106' (ft.)
 Weight / Ft: 53 & 117 (lbs./ft.)
 Wall Thickness: N/A (in.) Taper: NA
 Cross Sectional Area: (in.²)
 Design Pile Capacity: (Tons)
 Description of Splice: Mechanical

Tip Treatment Description:

Note: If mandrel is used to drive this pile, attach separate manufacturer's detail sheet(s) including weight and dimensions.

Submitted By: Davis Daniel Date: _____

APE Model D30-42 Single Acting Diesel Impact Hammer

D30-42 Finishing Dolphin Piles.



MODEL D30-42 (3.0 metric ton ram)

SPECIFICATIONS

Stroke at maximum rated energy	135 in (343 cm)
Maximum rated energy (Setting 4)	74,419 ft-lbs (100.47 kNm)
Setting 3	66,977 ft-lbs (90.42 kNm)
Setting 2	55,070 ft-lbs (74.34 kNm)
Minimum rated energy (Setting 1)	37,209 ft-lbs (50.23 kNm)

(Variable throttle allows for infinite fuel settings)

Maximum obtainable stroke	157 in (381 cm)
Maximum obtainable energy	86,546 ft-lbs (117 kNm)
Speed (blows per minute)	34-53

WEIGHTS

Ram	6,615 lbs (3,000 kg)
Anvil	1,358 lbs (616 kg)
Anvil cross sectional area	367.94 in ² (2373.80 cm ²)
Hammer weight (includes trip device)	13,571 lbs (6,154 kg)
Typical operating (weight with DB26 and H-beam insert)	16,223 lbs (7,357 kg)

CAPACITIES

Fuel tank (runs on diesel or bio-diesel)	17.4 gal (65 liters)
Oil tank	5 gal (19 liters)

CONSUMPTION

Diesel or Bio-diesel fuel	2.6 gal/hr (9.84 liters/hr)
Lubrication	0.26 gal/hr (1 liters/hr)
Grease	8 to 10 pumps every 45 minutes of operation time.

Optional Variable Throttle Control.



STRIKER PLATE FOR DB 26

Weight	628 lbs (284 kg)
Diameter	22.5 in (57.15 cm)
Area	398 in ² (2567.74 cm ²)
Thickness	6 in (15.24 cm)

CUSHION MATERIAL

Type/Qty	Micarta / 2 each
Diameter-DB26	22.5 in (57.15 cm)
Thickness	1 in (25.4 mm)

Drive Base Assembly.



Type/Qty	Aluminum / 3 each
Thickness	1/2 in (12.7 mm)
Diameter	22.5 in (57.15 cm)
Total Combined Thickness	3.5 in (8.89 cm)
Area	398 in ² (2567.74 cm ²)
Elastic-modulus	285 ksi (1,965 mpa)
Coeff. of restitution	0.8

DRIVE CAP

DB 26:	1,076 lbs (488 kg)
--------	--------------------

INSERT WEIGHT

H-Beam insert for 12" (305 mm) and 14" (355 mm):	948 lbs (430 kg)
Large pipe insert for sizes 12" to 24" diameter:	1,830 lbs (830 kg)

MINIMUM BOX LEAD SIZE/OPERATING LENGTH

Minimum box leader size	8 in x 26 in (20.32 cm x 66 cm)
Operating length as described above	354 in (900 cm)



Corporate Offices
7032 South 196th
Kent, Washington 98032 USA
(800) 248-8498 & (253) 872-0141
(253) 872-8710 Fax

Visit our WEB site:
www.apexibro.com
e-mail: ape@apexibro.com